1-1-2006

Model organic-inorganic hybrid copolymers based on polyhedral oligomeric silsesquioxane.

Gregoire Cardoen
University of Massachusetts Amherst

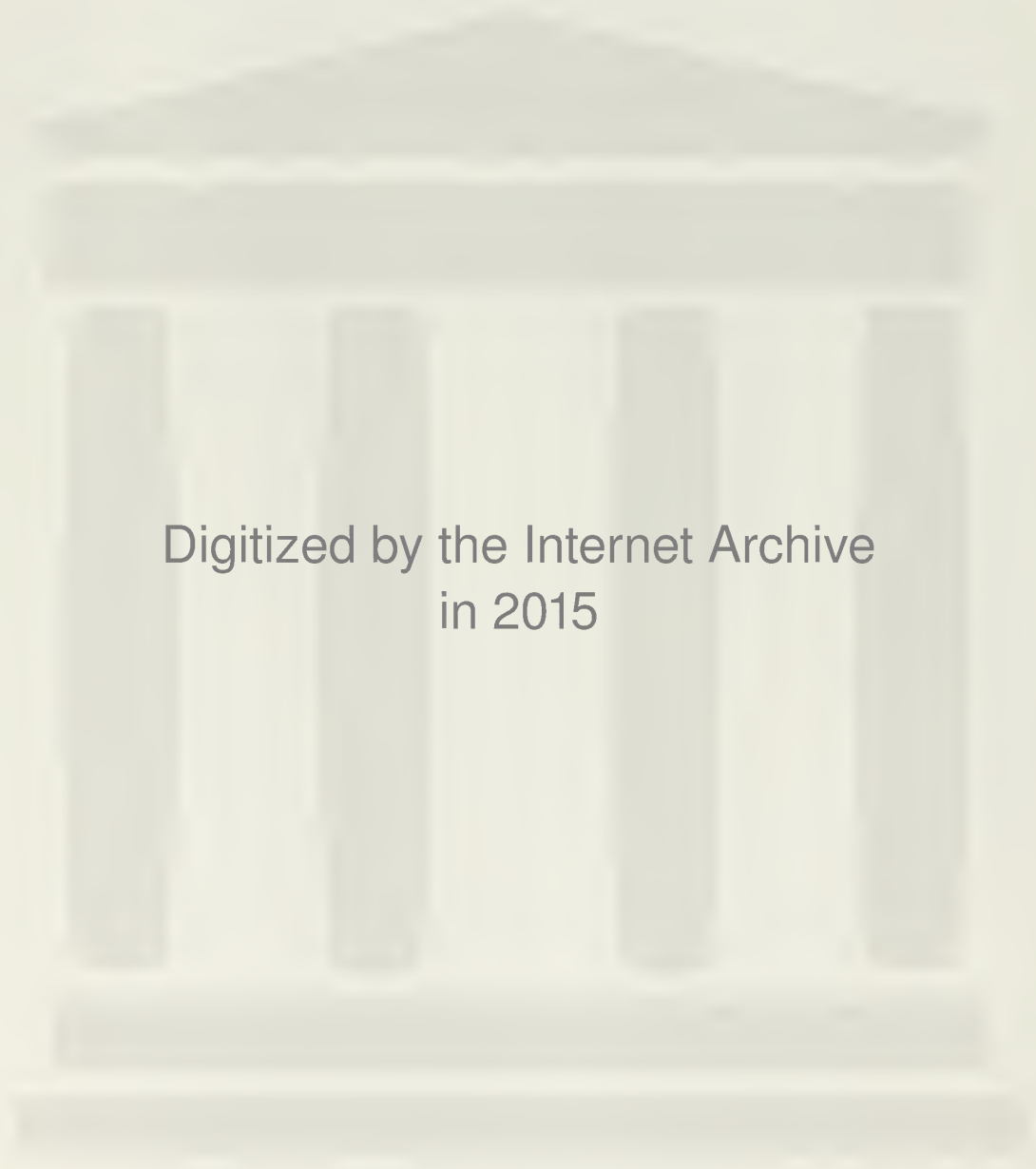

MODEL ORGANIC-INORGANIC HYBRID COPOLYMERS BASED ON POLYHEDRAL OLIGOMERIC SILSESQUIOXANE

A Dissertation Presented

by

GREGOIRE CARDOEN

Submitted to the Graduate School of the
University of Massachusetts Amherst in partial fulfillment
of the requirements for the degree of

DOCTOR OF PHILOSOPHY

September 2006

Polymer Science and Engineering

MODEL ORGANIC-INORGANIC HYBRID COPOLYMERS BASED ON POLYHEDRAL OLIGOMERIC SILSESQUIOXANE

Dissertation Presented

by

GREGOIRE CARDOEN

Approved as to style and content by:

_____

E. Bryan Coughlin, Chair

_____

Thomas J. McCarthy, Member

_____

Vincent M. Rotello, Member

_____

Shaw Ling Hsu, Department Head
Polymer Science and Engineering

MODEL ORGANIC-INORGANIC HYBRID COPOLYMERS BASED ON POLYHEDRAL OLIGOMERIC SILSESQUIOXANE

Dissertation Presented

by

GREGOIRE CARDOEN

Approved as to style and content by:

E. Bryan Coughlin, Chair

Thomas J. McCarthy, Member

Vincent M. Rotello, Member

Shaw Ling Hsu, Department Head
Polymer Science and Engineering

DEDICATION

To my parents Agnès and Jean-Marie

ACKNOWLEDGEMENTS

I would like to express my profound gratitude to my advisor Prof. Bryan Coughlin for his help and constant support over the last five years. We decided to tackle a very challenging research topic both technically and theoretically and this would not have been possible without his advice and understanding. I really appreciate the fact that he always gave me a lot of freedom to pick a research project and that really made a difference in the final outcome of this work. I am also very grateful to Prof. Tom McCarthy and Prof. Vince Rotello for being on my committee and providing me with of insight into the research I was conducting.

In the course of my Ph.D. research, I had the chance to work in Prof. Jimmy Mays' laboratory at the University of Tennessee, Knoxville, TN. Jimmy has been incredibly helpful and supportive for all the work I had to do. He made all the logistic aspects of that trip very simple (with a lot of help from Trish, his wife!). I will keep an excellent memory of the wine-tasting nights at his place. In this laboratory, I met many really nice people like Ravi, Brandon, Helen, George, and Wade. Special thanks to Baskaran who helped me a lot. His talent and patience were a source of inspiration to me.

The work environment in the Coughlin group has always been great. All the past and current members have been very helpful to me. I want to thank especially Gunjan for having the patience to listen to me for hours and for being willing to work with me on a couple of projects. Thank you to Yoan, the other French fellow, for his support at all times and for setting up a French quarter in the Coughlin office with me. Tarik, a late arrival in the lab, was a lot of fun to discuss things with.

Throughout these five years, I received constant support from many friends. I am very fortunate that all my friends from France stayed on my side at all times, even though they were five thousand miles away. In UMass, I met many wonderful people. I will especially remember the good times I shared with Roberto, Maja, Juan Camillo, Frieder, Maria Claudia, Maria, Tanya, Arnaud, Grégoire, Séverine, Keumyea, Dimitris, Peter S., Peter K., Joe, Jake and Alenka.

Last but not least, I will always be thankful to my family, especially my parents, my brother and my sister for being so supportive and for giving to courage to continue and finish this adventure.

ABSTRACT

MODEL ORGANIC-INORGANIC HYBRID COPOLYMERS BASED ON POLYHEDRAL OLIGOMERIC SILSESQUIOXANE

SEPTEMBER 2006

GREGOIRE CARDOEN

M.Sc., ECOLE NATIONALE SUPERIEURE DE CHIMIE DE MONTPELLIER, FRANCE

Ph.D., UNIVERSITY OF MASSACHUSETTS, AMHERST

Directed by: Professor E. Bryan Coughlin

Hybrid organic-inorganic materials is a new class of materials having important technological potential. In this thesis, Polyhedral Oligomeric Silsesquioxane (POSS) is used as an inorganic building block which is tethered to an organic polymer. The influence of POSS on the thermal properties as well as the morphology of the final hybrid is the main focus of this work. Different polymerization chemistries were utilized to incorporate POSS into an organic polymer.

Cyclooctadiene was copolymerized with CpPOSS norbornene via Ring-Opening Metathesis Polymerization. The poly(butadiene-*r*-POSS) series showed lamellae formation after film casting for POSS loading higher than 30 wt%. IbuPOSS-NCO was then attached to a series of well-defined alcohol-terminated polystyrene (PSOH). The alcohol-terminated polystyrene were synthesized by the anionic polymerization of styrene, terminating the reaction with the endcapping of the living polymer by ethylene oxide, which enabled precise control over the molecular weight and the polydispersity (PDI<1.1). Increased thermal resistance was observed upon POSS addition to the

PSOH series. Block copolymers of polystyrene and poly(HEMA-POSS) were then synthesized. A series of poly(styrene-*b*-HEMA) were first synthesized by anionic polymerization under high vacuum and POSS-NCO was reacted with the pendant alcohol of the HEMA block. By varying the volume fraction of each block, lamellar and cylindrical morphologies could be obtained. Long range order was observed by Small Angle X-ray Scattering in the samples having a lamellar morphology. Film casting provided orientation of the lamellae parallel to the surface of the beaker.

A manifold for the safe polymerization of ethylene oxide and butadiene was designed. A diblock copolymer of poly(butadiene-*b*-ethylene oxide) was synthesized to show the versatility of the manifold.

TABLE OF CONTENTS

LIST OF TABLES

LIST OF FIGURES

LIST OF ABBREVIATIONS

AIBN	2,2′-Azobis(2-methylpropionitrile)
ATRP	Atom Transfer Radical Polymerization
BCC and *bcc*-	Body-Centered Cubic packing
BSA	4,4′-[1,3 phenylenebis-(1-methylethylidene)]BiS(Aniline)
cLam	Crystalline lamellae
CpPOSS-NCO	1-[isocyanotopropyldimethylsilyl]-3,5,7,9,11,13,15-hepacyclopentylpentacyclo [9.5.1.1^{3,9}.1^{5,15}.1^{7,13}] octasiloxane
Cu(I)Br	Copper (I) Bromide
D	Diorganosiloxane ($R_2SiO_{2/2}$) unit
d	Lamellae spacing
DBTDL	Dibutyltin dilaurate
DGEBA	Diglycidyl Ether of Bisphenol A
DPE	Diphenylethylene
DSC	Differential Scanning Calorimetry
f	Volume fraction
FCC and *fcc*-	Face-Centered Cubic packing
FFT	Fast Fourier Transform
FTIR	Fourier Transform Infrared Spectroscopy
GLYMO	3-(glycidyloxypropyl)trimethoxysilane
GPC	Gel Permeation Chromatography
GTP	Group Transfer Polymerization
Gyr	Bicontinuous cubic structure
HPLC	High Pressure Liquid Chromatography
HEMA	2-hydroxyethyl methacrylate
HEX and *Hex*	Hexagonally packed cylinders
IbuPOSS-NCO	1-[isocyanotopropyldimethylsilyl]-3,5,7,9,11,13,15-hepacyclopentylpentacyclo [9.5.1.1^{3,9}.1^{5,15}.1^{7,13}] octasiloxane
LAM and *Lam*	Simple lamellae
LEO	Low Earth Orbit
M	Triorganosiloxy ($R_3SiO_{1/2}$) unit
M_n	Number average molecular weight
M_w	Weight average molecular weight
MAO	Methylaluminoxane
MLAM	Modulated lamellae
N	Degree of polymerization
PBD	Polybutadiene
PBD-POSS	Polybutadiene-*co*-POSS
PDI	Polydispersity Index
PE	Polyethylene
PE-POSS	Polyethylene-*co*-POSS
PEO	Poly(ethylene oxide)
PEO-PPO-PEO	Poly(ethylene oxide-*b*-propylene oxide-*b*-ethylene oxide)
PET	Poly(ethylene terephthalate)

PGE	Phenyl Glycidyl Ether
pHEMA	2-(trimethylsilyloxy) ethyl methacrylate
PI	Polyisoprene
PLAM	Perforated lamellae
PMEDTA	N,N,N`,N``,N```-pentamethyldiethylenetriamine
PMMA	Poly(methyl methacrylate)
PNB	Polynorbornene
POSS	Polyhedral oligomeric silsesquioxanes
PRV	Pressure Relief Valve
PS	Polystyrene
PS-*b*-PBD	Polystyrene-*block*-Polybutadiene
PS-*b*-PMMA	Polystyrene-*block*-Poly(methyl methacrylate)
PSOH	Hydroxy-terminated polystyrene
PTFE	Polytetrafluoroethylene
Q	Silicate (SiO_4) unit
ROMP	Ring-Opening Metathesis Polymerization
SAXS	Small Angle X-ray Scattering
SBS	Styrene-Butadiene-Styrene triblock copolymer
sec-BuLi	*sec*-butyl lithium
SEM	Scanning Electron Microscopy
T	Organosilsesquioxane ($RSiO_{3/2}$) unit
T_7	Trisilanol POSS
T_8	Fully condensed POSS
T_g	Glass transition temperature
TBAF	*Tert*-butyl ammonium fluoride
T_{ODT}	Order-Disorder Transition Temperature
TEM	Transmission Electron Microscopy
TGA	Thermogravimetric Analysis
THF	Tetrahydrofuran
TMS	Tetramethylsilane
UEMA	Urethane ethyl methacrylate
WAXD	Wide-Angle X-ray Diffraction
χ	Flory-Huggins parameter

CHAPTER 1

INTRODUCTION

Study and design of self-assembling structures, primarily inspired by self-assembly occurring in nature, has attracted considerable interest in the last two decades.[1, 2] Self-assembly can be defined as "the autonomous organization of components into patterns or structures without human intervention".[3] A cornerstone article written by Whitesides *et al.* in 1991 describes the fundamental molecular interactions on which self-assembling systems can be built.[4] Molecular self-assembly is found everywhere in the design of biological structures.[5] Molecular self-assembly is of interest to chemists as it represents a potential method to build non-biological structures with dimensions of 1 to 100 nm, so-called nanostructures.[6] In fact, it is very challenging to build structures of several tens of nanometers using only organic chemistry reactions. The fundamental building block of organic chemistry, the C-C bond, measures only 0.15 nm in length. Design of nanostructures, involves many fields of expertise: interface and colloid science,[7] molecular recognition,[8] electronic fabrication,[9] polymer science,[10] electrochemistry,[11] zeolites and clay chemistry[12] and others. An increasing interest in nanotechnologies stems from potential technological applications that could be developed using self-assembly concepts.[13]

Of particular relevance to the present work is the field of hybrid organic-inorganic materials, which includes zeolites and clay chemistry.[14] Hybrid organic-inorganic materials are broadly defined as synthetic materials containing both organic and inorganic components. Hybrid organic-inorganic materials can be categorized as two types depending on the way they are synthesized. On one hand, it is possible to

synthesize organic-inorganic materials following an engineering top-down approach. In this case, mesoscopic organic and inorganic components are mixed together with the assistance of an external source of energy such as heat or mechanical work. Polymer clay hybrids such as nylon-clay hybrids are but one example of such a system.[15] On the other hand, organic-inorganic materials can be synthesized using a bottom-up approach. In this case, organic monomers are used in conjunction with inorganic monomers. After subsequent polymerization of both components, hybrid organic-inorganic materials with tunable properties at a nanoscopic level are obtained. Only a few types of nanoparticles have been used as inorganic self-assembling scaffolds, partially due to the limited number of chemically well-defined inorganic nanoparticles available. Fullerenes,[16] carbon nanotubes,[17] cadmium-selenide quantum dots,[18] polyoxometalates,[19] carboranes[20] and Polyhedral Oligomeric SilSesquioxane (POSS)[21] are a few examples of well-defined nanosized particles. The work presented in this thesis is concerned with the self-assembly of organic-inorganic materials based on POSS.

This introductory chapter is divided into three sections. The first section is a review of POSS-based organic-inorganic materials developed in the last five years. The second section deals with synthesis and morphology of organic block copolymers and the third section is a literature survey of hybrid organic-inorganic materials synthesized and self-assembled in the presence of a template directing agent.

1.1 Organic-Inorganic Nanocomposites Based on Polyhedral Oligomeric Silsesquioxane (POSS)

1.1.1 POSS Synthesis and Properties as an Inorganic Additive in an Organic Matrix

The term silsesquioxane refers to structures with the empirical formula $RSiO_{1.5}$, where R is hydrogen, alkyl, alkylene, aryl or arylene group. From a nomenclature stand point, triorganosiloxy ($R_3SiO_{1/2}$), diorganosiloxane ($R_2SiO_{2/2}$), organosilsesquioxane ($RSiO_{3/2}$) and silicate (SiO_4) units are referred as M, D, T and Q units respectively (Figure 1.1). The first oligomeric organosilsesquioxane were isolated along with other volatile compounds by Scott in 1946 through thermolysis of polymeric products obtained from cohydrolysis of methyltrichlorosilane and dimethylchlorosilane.[22] Condensation of alkyl trichlorosilane to give T_7 silsesquioxane was first reported by Brown *et al.*[23]

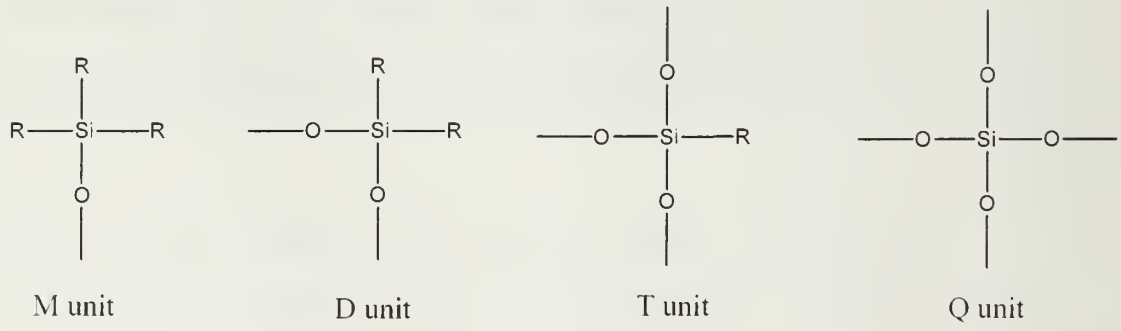

Figure 1.1 Nomenclature of Silicon-Containing Structures

Upon acid- or base-catalyzed hydrolytic condensation of an alkyl trichlorosilane, a number of products are obtained.[24-26] Among the obtained products, two are of particular interest: the non-fully condensed POSS cube (T_7) and the fully condensed POSS cube (T_8). T_7 can be further functionalized by the so-called corner capping reaction with an alkyl trichlorosilane bearing a reactive/polymerizable group (Figure 1.2). POSS particles can be approximated as spheres with a diameter of 1.5 nm. By

changing the alkyl group of the alkyl trichlorosilane, the organic periphery of the POSS particles can be modified. POSS particles crystallize in a hexagonal lattice, the lattice parameters being dependant upon the size of the R group.[27] A number of POSS derivatives (Figure 1.3) are now commercially available from Hybrid Plastics (www.hybridplastics.com).

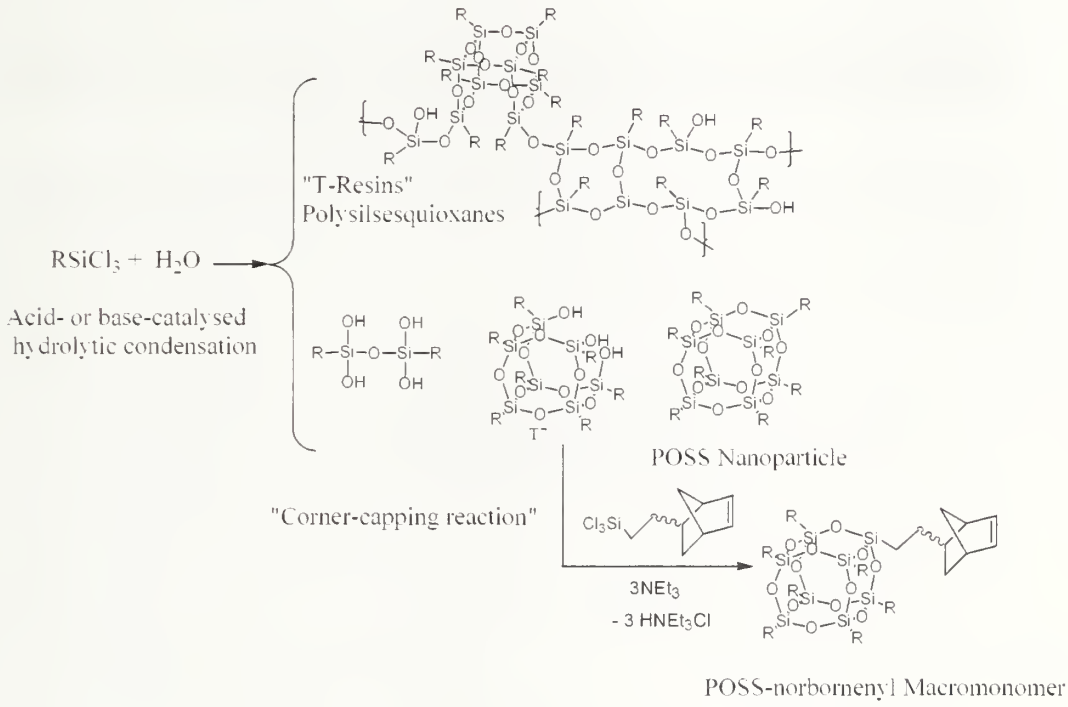

Figure 1.2 Synthesis of Silsesquioxane Derivatives by Acid- or Base-Catalyzed Hydrolytic Condensation.

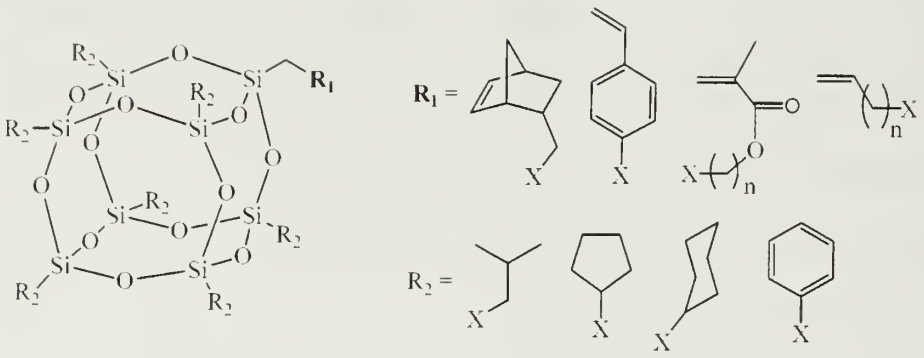

Figure 1.3 Chemical Structure of Commercially Available POSS Monomers in which R_1 is the Polymerizable Functionality, R_2 is the Organic Periphery, and x is the Point of Attachment.

Properties enhancement seen in POSS-reinforced polymer systems include the following (www.hybridplastics.com):

- An increased temperature of decomposition
- An increased glass transition temperature
- A reduced flammability
- A reduced heat evolution
- A lower density
- An increased oxygen permeability
- A lower thermal conductivity
- A higher oxidation resistance
- Improved mechanical properties

In the following section, incorporation of POSS particle in various polymer systems is reviewed. The references covered in this thesis were mainly published between 2001 and 2006 as two reviews are available on the work accomplished before 2001.[21, 28] In these two reviews, synthesis of styrene/styryl-POSS polymers and

copolymers.[29] norbornene/norbornyl-POSS polymers and copolymers.[30, 31] and ethylene/vinyl-POSS copolymers[32] are discussed. A few recent reviews have also been published.[33-35] Certain references are presented in greater detail in the following section to give an insight into the versatility of POSS chemistry.

1.1.2 POSS-Reinforced Epoxy Resins

Epoxy resins are among the most commercially successful materials known, especially as composite matrices, but also as coating materials and adhesives.[36] A number of publications dealing with the incorporation of POSS particles into epoxy resins have been published in the past couple of years.[37-40] A recent review by Joshi *et al.* covers some aspects of this chemistry.[33]

Abad *et al.* synthesized an epoxy network using the chemicals depicted in Figure 1.4.[37] PGE, DGEBA and BSA stand for Phenyl Glycidyl Ether, Diglycidyl Ether of Bisphenol A and 4,4'-[1,3 phenylenebis-(1-methylethylidene)]BiS(Aniline) respectively. The epoxy network was formed in a two step process. First, POSS with R_2 = isobutyl (IbuPOSS-Epoxide) was reacted with an equimolar amount of BSA. Second, this precursor was reacted with a stoichiometric amount of DGEBA to generate an organic-inorganic hybrid material. Thermal and morphological studies were performed. An increase in T_g was observed by DSC. This is due to the hindering of polymer chain motion by their covalent attachment to POSS clusters. A macrophase separation between POSS-rich regions and epoxy-rich regions was observed by Scanning Electron Microscopy (SEM) and Differential Scanning Calorimetry (DSC). Mechanical properties (rubbery modulus, fracture toughness, tensile modulus) of POSS-modified epoxy resins are found to be equivalent or better than non-modified epoxy

resins. Similarly, an increase of the decomposition temperature usually occurs upon POSS addition in the epoxy network.

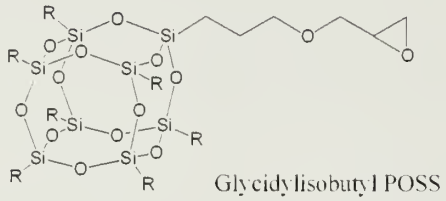

Glycidylisobutyl POSS

R = Isobutyl

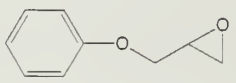

PGE

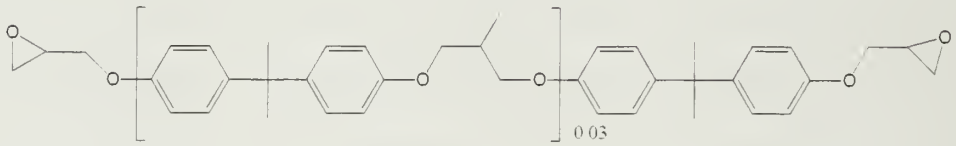

DGEBA

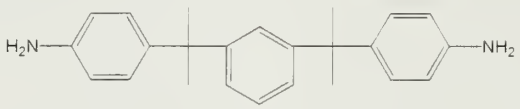

BSA

Figure 1.4 Monomers Used for the Synthesis of POSS-Reinforced Epoxy Network in Ref. 34

A few general concepts can be formulated from this work. Incorporation of a POSS particle into an organic polymeric system tends to increase the T_g of the polymer due the size of a POSS particle and/or its crystallization behavior. The large size of POSS particles hinder segmental motion resulting in an increased T_g of the overall materials. Also, the incompatibility between organic segments and POSS particles tend to result in a macrophase (or microphase) separation.

Along the same lines, the Matějka's group[39] reported on the structure and morphology of POSS-reinforced epoxy networks. An epoxy-amine network of DGEBA cross-linked with poly(oxypropylene)diamine D2000 (Jeffamine) was

modified with covalently bonded or physically blended POSS particles. Monofunctional and multifunctional epoxy-POSS particles were used. It was observed by SAXS, TEM and WAXS that the POSS particles have a strong tendency towards aggregation and crystallization. Interestingly enough, in the case of a POSS-containing epoxy network with dangling POSS (POSS loading of 50 wt%), POSS lamellae were observed.

1.1.3 Incorporation of POSS Particles in a Resist Formulation for Nanolithography.

Recently, there has been interest in incorporating POSS particles in photoresist formulations to enhance the etch resistance of the resulting polymer.[41-46] In particular, Jakubek *et al.*[44] incorporated POSS into acrylate-based resists (Figure 1.5) for 157 nm lithography. In this system, POSS was expected to increase the etch resistance as well as decrease the absorption at 157 nm. In **Polymer 2**, the methacrylate segment was replaced by α-trifluoromethylacrylate to further decrease the absorption at 157 nm.

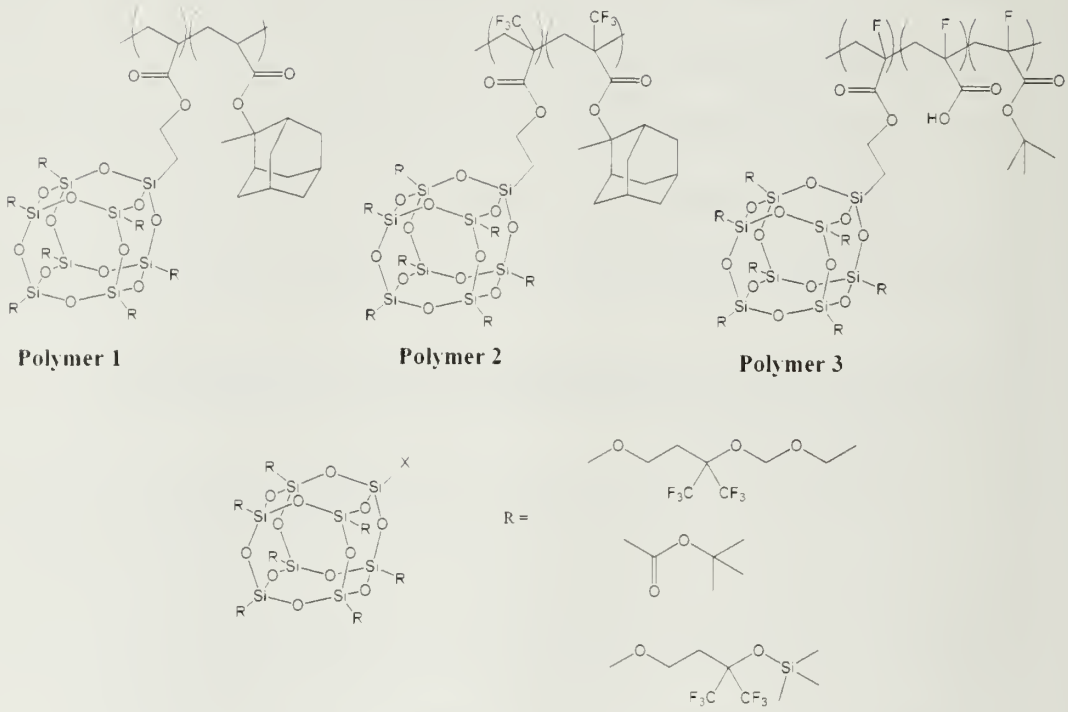

Figure 1.5 POSS-Containing Acrylate Resists (From Ref. 44)

1.1.4 POSS-Reinforced Thermoplastics

1.1.4.1 Polyimide-Based Materials

Polyimides are very attractive materials due to their good oxidation resistance and hydrolytic stability toward acidic environments. They are comparable to PET and better than nylon 6/6. The high temperature resistance of polyimides is excellent, with continuous use temperatures of 300-350 °C possible.[47] Many reports described the incorporation of POSS particles into polyimides[48-55] using different strategies.

Figure 1.6 describes the strategy used by Wright *et al.*[56] to incorporate POSS particles into a polyimide. The resulting polymer showed better atomic oxygen resistance,[57] making it suitable for Low Earth Orbit (LEO) applications.[51]

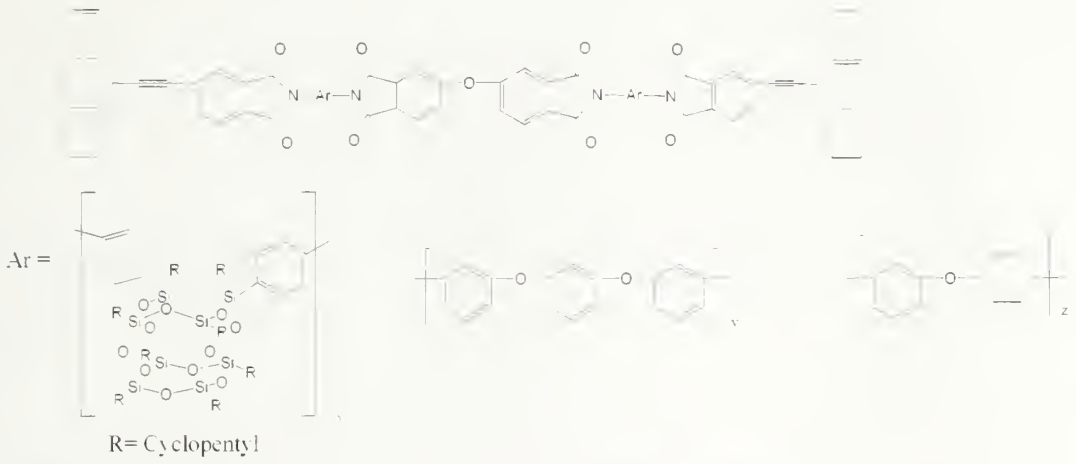

Figure 1.6 Top: Polyimide Polymer. Bottom, from Left to Right: POSS Diamine, 1,3-bis(3-aminophenoxy)benzene and 3,4'-oxydianiline (From Ref. 56).

1.1.4.2 Polyolefin Based Materials

POSS particles have been incorporated in polyolefin, either by direct blending[58, 59] or by covalent attachment to the olefin backbone.[32, 60-63] Zheng *et al.* used ring-opening metathesis polymerization (ROMP)[64] of cyclooctene and norbornyl-POSS to obtain a random copolymer. Subsequent diimide reduction of the backbone unsaturations afforded a polyethylene-POSS random copolymer (Figure 1.7). Another preparative method consisted of using a metallocene catalyst (dichloro[*rac*-ethylenebis(indenyl)]zirconium) with MAO as a cocatalyst to copolymerize ethylene and norbornyl-POSS.[65] The POSS-modified polyethylene showed an increase thermo-oxidative resistance as well as the appearance of a modulus plateau above 175°C

indicating the absence of melt flow usually observed in non-modified polyethylene. This behavior was explained by the tendency of POSS to aggregate and crystallize.

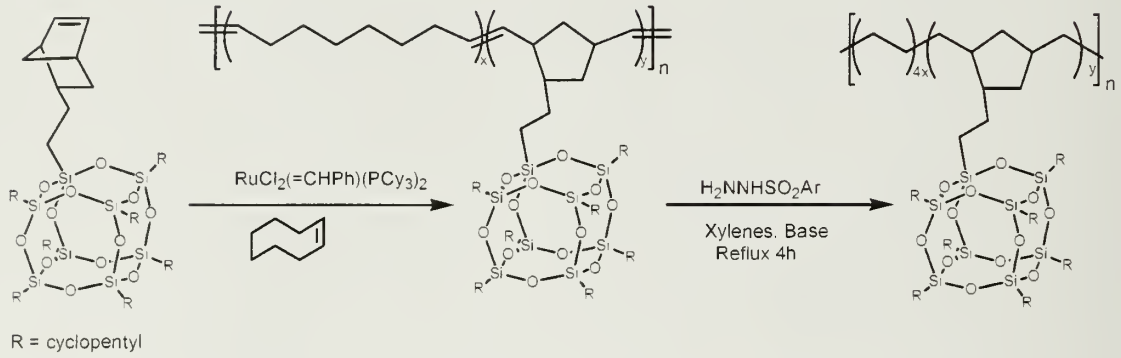

Figure 1.7 Two Step Synthesis of Polyethylene-POSS Random Copolymer (From Ref 62.).

Physical blending of POSS with ethylene-propylene copolymer[59] resulted in a solid-like rheological behavior compared with the liquid like rheological behavior of the neat resin. Aggregation and crystallization of POSS particles were the origin of the phenomena observed.

To conclude this section, most of the literature on POSS-modified systems is centered on properties improvements induced by the incorporation of POSS in commodity polymers. Morphological studies have been carried out mostly to understand the effect of changes in nanoarchitecture on macroscopic properties. Typically, an increase in mechanical properties as well as thermal properties is observed, due to the tendency of POSS particles to aggregate and crystallize. The size of POSS particles also plays a critical role in segmental motion in the polymer matrix, often resulting in an increase of T_g compared to the initial material. POSS particles can also act as fillers when well-dispersed in an organic matrix.

1.1.5 Self-Assembly of POSS-Modified Organic Polymers

As of today, only a few publications have reported on the aggregation and self-assembly of POSS particles in the range of several tens of nanometers. As previously mentioned, POSS particles have been regarded mainly as inorganic fillers, not as nanoscopic building blocks to design mesoscale structures. In the following section, examples of publications hinting at self-assembly behavior of POSS-modified materials are presented.

In 2000, Jeon *et al.*[31, 66] observed formation of POSS cylinders and spheres in a polynorbornene matrix. The cylinders are locally well-ordered, as confirmed by Wide Angle X-Ray Scattering (WAXS) and Transmission Electron Microscopy (TEM). Noteworthy is the fact that the polymers studied are random copolymers of norbornyl-POSS and norbornene. As discussed in the next section, a long-range order microphase separation is usually observed in block copolymers, not in random copolymers. The cylinders had a larger diameter with cyclopentyl-POSS than with cyclohexyl-POSS. Leu *et al.*[53, 54] reported on the synthesis of polyimide-tethered POSS nanocomposites by using a POSS diamine as comonomer. For POSS loadings greater or equal to 10 mol%, lamellae formation was observed. The persistence length of the lamellae can be up to 100 nm. A 2-dimensional POSS network is the highest possible architecture due to geometry constraints on POSS particle. POSS particles crystallize in a hexagonal 3-dimensional lattice. As one vertice of the cube is tethered to the main chain, 3-dimensional crystallization is impossible. The Matějka group [39] found that POSS-modified epoxy resins exhibited a lamellae morphology for a POSS loading of 50 wt%.

All the systems described above are based on random copolymers of POSS-particles and organic monomers. The Matyjaszewski group was the first to report on living polymerization of POSS particles by Atom Transfer Radical Polymerization (ATRP) (Figure 1.8).[67-69] Dimethyl 2,6-dibromoheptanedioate was used as a difunctional initiator to polymerize n-butylacrylate. The catalyst/ligand system has Copper (I) Bromide (Cu(I)Br) and N,N,N',N'',N''-pentamethyldiethylenetriamine (PMEDTA). The n-butylacrylate difunctional macroinitiator was then chain extended with CpPOSS-MA (POSS bearing one methyl methacrylate unit and having a cyclopentyl periphery). The resulting ABA triblock copolymer exhibited narrow molecular weight distribution (PDI=1.2). Surprisingly enough, the degree of polymerization of the POSS block did not exceed 10, probably because of the bulkiness of the POSS monomer. Cylinders of poly(n-butyl acrylate) in a POSS matrix were observed by TEM for the p(MA-POSS)$_{10}$-*b*-pBA$_{201}$-*b*-p(MA-POSS)$_{10}$ polymer, where the subscripts indicate the degree of polymerization of each block. The cylinders were locally well ordered but macroscopically disordered. In reference 69, Matyjaszewski reviewed different architectures that can be obtained using a similar strategy, starting with a multifunctional initiator. Star or comb polymers incorporating POSS particles are hypothesized.

Drazkowski et *al.*[70] attached POSS to Styrene-Butadiene-Styrene (SBS) triblock copolymers via hydrosilylation between the pendant vinyl group of the butadiene block and a POSS-hydride compound. The effect of the periphery of the POSS cube on the triblock copolymer morphology was studied. Incorporation of a POSS particle with a phenol periphery (Ph-POSS) into the SBS material resulted into a partial plastization of

the polystyrene domains by the Ph-POSS particles. This causes a significant decrease in the overall lamellae *d* spacing and the order-disorder transition temperature, T_{ODT}, with increasing amounts of Ph-POSS attachment. As the POSS periphery was changed from cyclohexenyl to cyclohexyl to cyclopentyl, the interactions between POSS-PS weakens and the *d* spacing and T_{ODT} become less dependent on the amounts of POSS attachment.

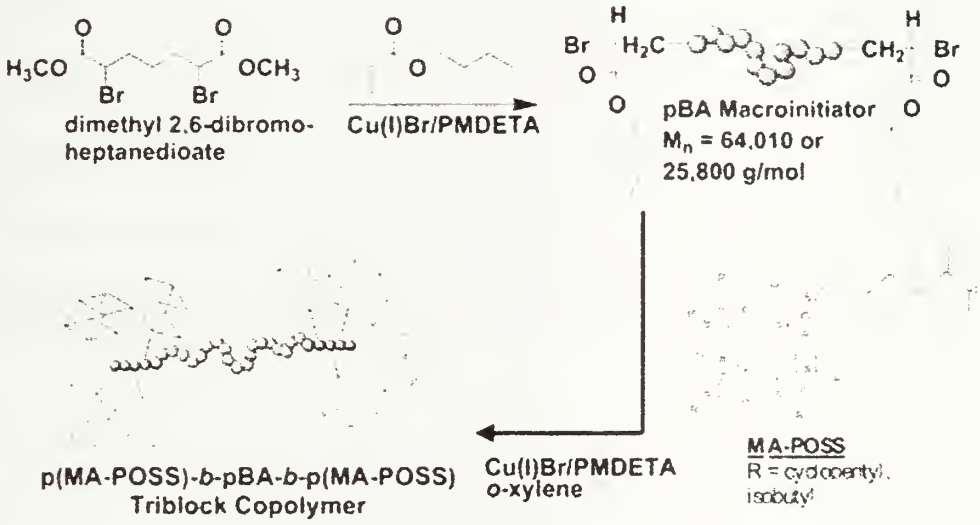

Figure 1.8 Synthetic Methodology for the Preparation of ABA Triblocks Containing a Poly(*N*-Butyl Acrylate) Middle Segments and Outer Segments of P(MA-POSS). In the First Step, Difunctional pBA Macroinitiator is Prepared by the ATRP of BA From a Dimethyl 2,6-Dibromoheptanedioate Initiator. Subsequent Chain Extension of the pBA Macroinitiator with MA-POSS Yielded the ABA Triblock Copolymer (from Ref. 68.)

A few other reports hinting at a self-assembly behavior of POSS containing systems are of interest. Intasanta *et al.*[71] used a strategy similar to the Matyjaszewski group to develop poly(methacrylate-*b*-MA-POSS) block copolymer and studied its phase separation behavior as thin films. Cylinders of POSS particles lying parallel to the surface at the air/film interface were observed.

Carroll *et al.*[72, 73] studied the crystallization behavior versus the hydrogen bonding of diaminopyridine-POSS when mixed together with thymine-functionalized polymer or gold particle. It was shown that both crystallization and hydrogen bonding occurs simultaneously.

In conclusion, POSS has been incorporated in a wide variety of organic polymers as an inorganic filler to reinforce materials' mechanical properties. The tendency of POSS to aggregate and crystallize is correlated to the observed changes in mechanical and thermal properties. Only recently have a few research groups studied POSS as an inorganic building block that can promote meso-scale self-assembly. One of the main goals of the present work is to describe the synthesis and the study of the morphology of well-defined organic/inorganic block copolymers incorporating POSS particles.

1.2 Synthesis and Morphology of Organic Block Copolymers

1.2.1 Block Copolymer Synthesis

Block copolymers consist of two or more homopolymer segments tethered through a covalent bond. Block copolymers are generally synthesized by living polymerization techniques.[74-77] Sequential monomer addition is the preferred method to obtain blocks with defined molecular weight and polydispersity. Anionic polymerization was the first polymerization technique to be used to synthesize block copolymers.[78] Anionic initiating species are very reactive towards impurities like moisture, oxygen and carbon dioxide. Therefore, very specialized techniques have been developed to circumvent these problems. High vacuum along with extremely pure reagents and solvents are needed to successfully polymerize a monomer in a living

fashion. [79-81] Cationic polymerization and group transfer polymerization (GTP) are two other examples of living polymerization.[77] Anionic polymerization will be the main polymer syntheses techniques used to conduct the research presented in this thesis.

1.2.2 Block Copolymer Morphology

Self-organization of block copolymers can be divided into three categories. In dilute solution, block copolymers can form micelles, cylindrical micelles and vesicles. At higher concentration, lyotropic phases can be observed. In bulk, several microphases are observed (Figure 1.6).[82]

The type of phase separation observed in a given block copolymer system depends on the volume fraction of each homopolymer (*f*), the interaction parameters between the different homopolymers and the interaction parameter between homopolymers and solvent (χ parameter or Flory-Huggins parameter). The χ parameter scales as 1/T where T is the temperature in degree Kelvin. The size of the phases scales with the degree of polymerization (N) of the polymer.[83] Phase dimensions in block copolymers range from a few nanometers to several hundreds of nanometers (so-called mesoscale structure). Structures obtained are therefore smaller than what is currently achievable using lithography while being much larger than organic molecules made by conventional organic reactions. The phase diagram of block copolymers can be obtained by plotting χN as a function of *f*. As shown on the phase diagram in Figure 1.10, it is possible to predict the structure of a given block copolymer after microphase separation. The phase diagram is as follows: crystalline lamellar (*cLam*), amorphous lamellar (*Lam*), hexagonal packed cylinders (*Hex*), bicontinuous cubic structure (*Gyr*, shaded area)

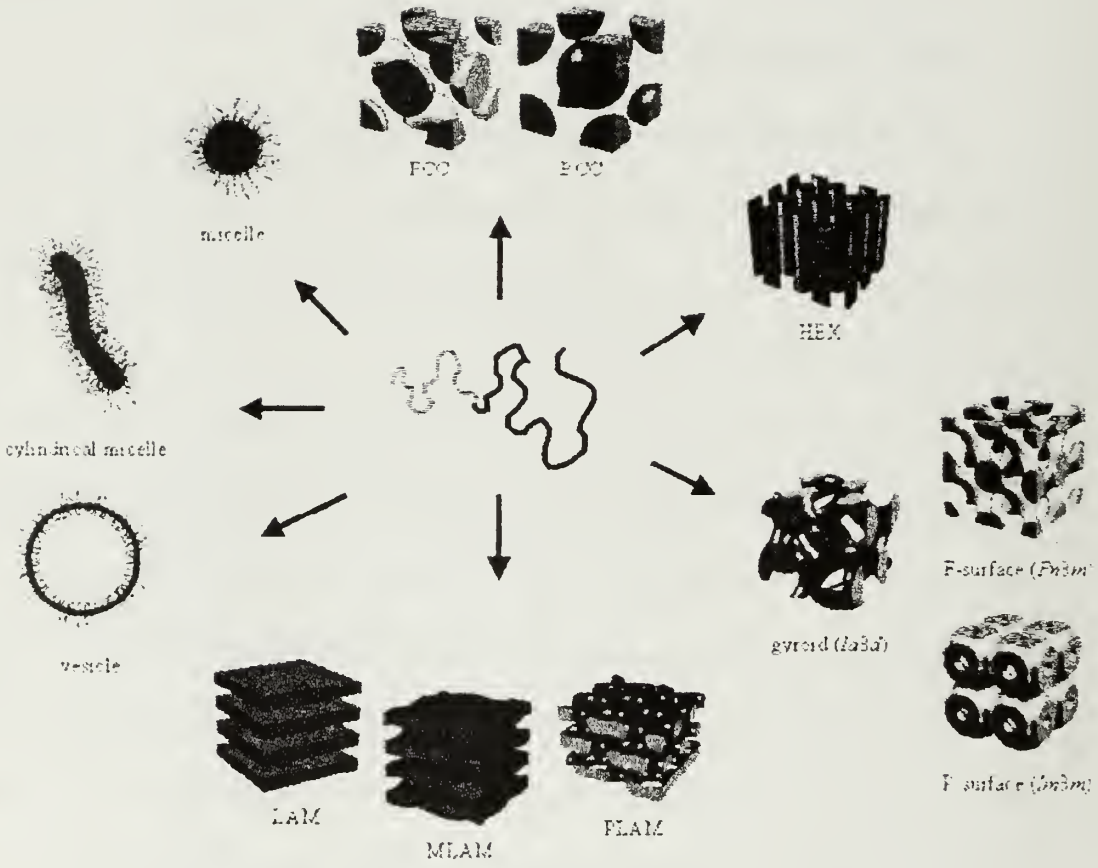

Figure 1.9 Self-organization Structures of Block Copolymers and Surfactants: Spherical Micelles, Cylindrical Micelles, Vesicles, *fcc*- and *bcc*- Packed Spheres (FCC, BCC), Hexagonally Packed Cylinders (HEX), Various Minimal Surfaces (Gyroid, F Surface, P Surface), Simple Lamellae (LAM) as well as Modulated and Perforated Lamellae (MLAM, PLAM). (from Ref. 82)

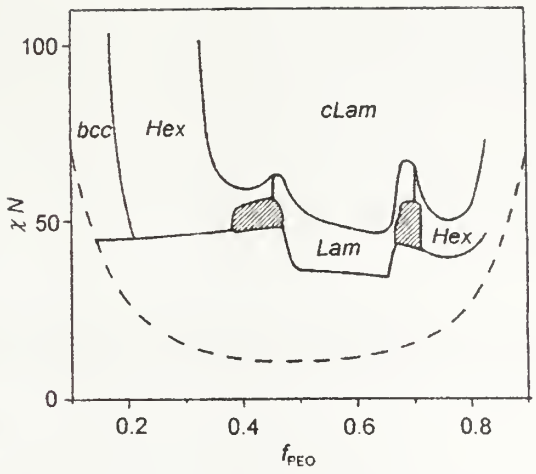

Figure 1.10 Phase Diagram for the System Poly(isoprene-*b*-ethylene oxide). (From Ref. 111)

Given their ordered microphase separation, block copolymers are studied for a variety of applications such as contact lenses, waveguides, scratch resistant coating, data storage device, masks for lithography, chemical filters, biosensors, electrolytes and dental fillings.[12, 13, 84-88]

1.3 Hybrid Organic-Inorganic Polymers and their Self-Assembly on Nanoscale

Hybrid organic-inorganic systems have attracted a great deal of attention in the scientific community. They represent a class of materials that combines properties of both organic and inorganic materials. Improved mechanical, thermal, oxidative properties are targeted when inorganic and organic components are mixed within the same matrix. To synthesize hybrid organic-inorganic materials, a top-down or a bottom-up approach can be used. Polymer-clay nanocomposites are an example of top-down approach used to generate hybrid organic-inorganic materials.[15, 89, 90]

This section discusses the bottom-up approach. There are several routes to synthesize hybrid organic-inorganic systems. Three of them will be discussed here.

First, mixing inorganic nanoparticles with block copolymers is described. Second, synthesizing block copolymers with both organic and inorganic components is a possible strategy. Finally, synthesis of sol-gel networks by using a block copolymer as a template-directing agent is reviewed.

1.3.1 Mixing of Inorganic Particles with Block Copolymers.

It is possible to generate hybrid organic-inorganic materials by mixing inorganic nanoparticles with block copolymers. Inorganic nanoparticles can exhibit interesting behavior such as electronic properties and possibly paramagnetism or ferromagnetism.[91] In principle, the inorganic nanoparticle should have enough affinity for the block copolymer template to prevent aggregation and macrophase separation. Aggregation tends to weaken mechanical or optical properties of the resulting materials. Unmodified inorganic particles tend to aggregate in the polymer matrix independent of the kind of material and their size. To avoid this aggregation, the use of functional polymers which interact with the surface of the particles,[92] or surface modification of the particles to change their character[93] can be successfully applied. A very nice example of particle modification was reported by E.L. Thomas' group at MIT.[94] Gold particles (3.5 nm diameter) stabilized with linear alkyl chain end-capped with a thiol ($C_{18}H_{37}SH$) and silica particles (21.5 nm diameter) stabilized with hexamethylenedisilazane. When mixed with a poly(styrene-*b*-ethylene/propylene) block copolymer, the silica nanoparticles were found to align in the middle of the ethylene/propylene block while the gold nanoparticles were aligned along the styrene-*b*-ethylene/propylene block interface. Theoretical studies have also predicted the aggregation behavior of nanoparticles within a block copolymer matrix.[95-98] Physical blending of POSS and an

organic matrix often results in macrophase separation. Poorer mechanical properties are observed in this case.[99]

1.3.2 Synthesis of Block Copolymers Containing an Organic and an Inorganic Block.

Only a few examples of hybrid organic-inorganic block copolymers synthesized by chain growth mechanism and have been reported, due to the limited number of inorganic monomers available. Polyferrocenylsilanes are one example of inorganic polymer that can be used to build organic-inorganic block copolymers.[100] Manners' group reported that anionic ring opening polymerization of [1]Silaferrocenophane proceeds in a living fashion (Figure 1.11).[101] Well-defined organometallic/organic/inorganic multiblock copolymers were synthesized from a combination of poly(ferrocenyldimethylsilane), polystyrene, and poly(dimethylsiloxane) blocks.

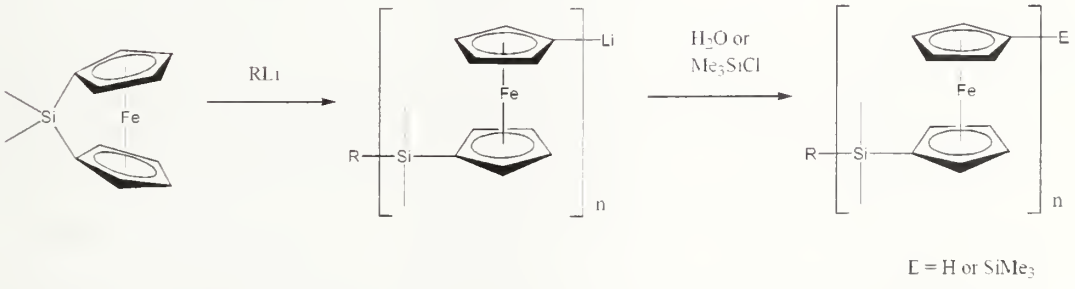

Figure 1.11 Anionic Polymerization of [1]Silaferrocenophane Initiated by an Organolithium Compound.

Cheng *et al.*[102, 103] employed a diblock copolymer of poly(styrene-*b*-ferrocenyldimethylsilane) (PS/PFS), in which the organometallic PFS provides an excellent (10:1) etching contrast in oxygen plasma.

Another approach to incorporate inorganic molecules and particularly metals into organic polymers consists of incorporating metal ligands into the organic polymer. Subsequent complexation of the polymer with a metal gives rise to the desired material.[104] Properties such as paramagnetism, supramagnetism, magnetic properties for data storage, enhanced conductivities and non-linear optical properties have been observed in organic molecules incorporating inorganic metals.[105, 106]

1.3.3 Organic-Inorganic Network by the Sol-gel Approach Employing Diblock Copolymers as a Template-Directing Agent

Organizing inorganic matter with organic molecules at a mesoscale was first discovered by scientists at the Mobil Corporation 1992.[107] Since then, numerous applications using these materials as catalysts, for gas sensing, and others applications have emerged. Choice of the organic template to spatially control the mineralization process will dictate the size of the features obtained in the final material. Given their size, polymers are very convenient to generate features of several tens of nanometers in dimension.

Of particular interest for this work is the sol-gel polymerization of metal alkoxides in presence of a preformed organic polymer. A variety of metal alkoxides (Si, Ti, Zr, Sn, Al) have been used to generate the inorganic network. Mainly alkoxysilane will be discussed in the following section. A typical application area for hybrid materials are optical systems that require homogeneous and transparent materials which cannot be obtained from mixtures that are already macroscopically phase separated. Therefore, it is necessary to use polymers that have interactions with the inorganic network, e.g. hydrogen bonding to residual silanol groups. Poly(vinyl

pyridine), poly(methylmethacrylate), polyamides, poly(ethylene oxide), polyethersulfones, have been successfully as template-directing agent in the formation of organic-inorganic networks. [108-110]

Noteworthy is the work accomplished by Stucky *et al.* in which an amphiphilic block copolymer (poly(ethylene oxide-*b*-propylene oxide-*b*-ethylene oxide)) (PEO-PPO-PEO) is used as organic structure-directing agent in conjunction with an alkoxysilane (tetraethoxysilane or tetramethoxysilane). [111-113] The alkoxysilane was found to segregate in the hydrophilic block of the PEO-PPO-PEO upon mixing. After polymerization of the alkoxy silane hexagonal interpenetrating networks of organic and inorganic materials were obtained. It is possible to further calcine the sample while maintaining the morphology. Mesoporous silica was obtained this way.
Following the same type of idea, Wiesner *et al.* [114, 115] have been developing sol-gel chemistry in which the alkoxysilane (3-(glycidyloxypropyl)trimethoxysilane, GLYMO) bears a polymerizable organic group. GLYMO was copolymerized with aluminum *sec*-butoxide in the presence of poly(isoprene-*b*-ethylene oxide) (PI-PEO) as template-directing agent. Polyisoprene is more hydrophobic than polypropylene oxide resulting in a more pronounced segregation of the alkoxysilane in the hydrophilic block. By varying the volume fraction of PI with respect to PEO and by changing the weight percent of inorganic precursor for a given amount of block copolymer, a variety of organic-inorganic morphologies were obtained in the bulk (Figure 1.12). Nano-objects such as spheres or lamellae could be obtained by dissolving the PI block in a good solvent. Mesoporous solid were obtained after calcination at 600°C. The morphology of the precursor was maintained after calcination.

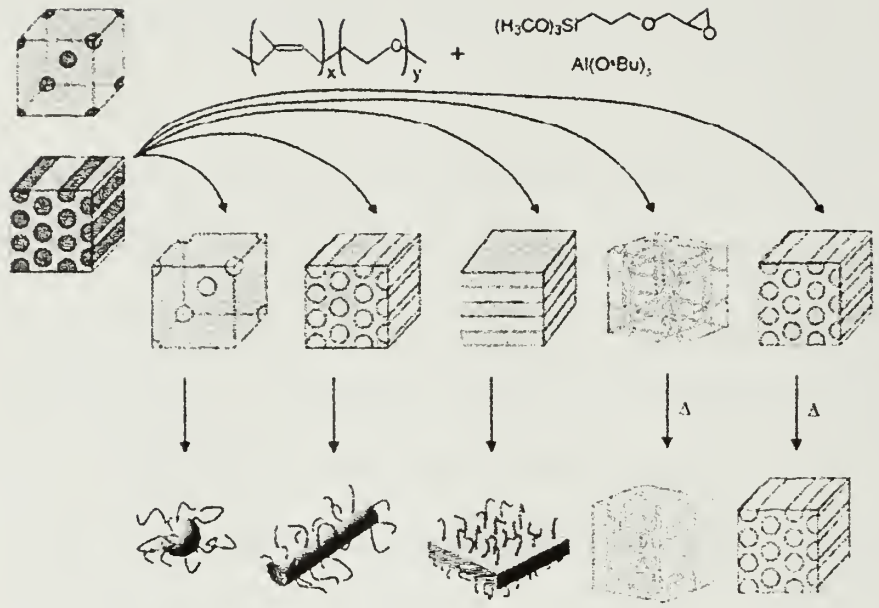

Figure 1.12 Schematic Drawing for the Preparation of Nano-Objects as Well as Mesoporous Materials Obtained by Mixing Different Amount of Inorganic Precursor With Block Copolymer. Single "Hairy" Nano-Objects of Different Shapes are Isolated by Dissolution. Calcinations at About 600 °C Lead to Mesoporous Materials With Preserved Morphologies. (from Ref. 115)

1.4 Thesis Summary

Apart from the sol-gel approach, there are only a few ways to build block copolymers of organic-inorganic materials. POSS is going to be used as an inorganic macromer to build mesoscale structures. First POSS was incorporated into a random copolymer of POSS and butadiene via ROMP (Ring Opening Metathesis Polymerization) of cyclooctadiene (Chapter 2). Model hemitelechic POSS-polystyrene has been synthesized by anionic polymerization (Chapter 3.) In order to increase the POSS content in the polymer, a series of poly(styrene-*b*-POSS) was synthesized and characterized (Chapter 4). The morphology study revealed highly ordered microphase separated structures. Chapter 5 summarizes the design and construction of a manifold to safely handle and polymerize ethylene oxide and 1,3-butadiene.

1.5 References

(1) Lindsey, J. S. *New J. Chem.* **1991,** 15, (2-3), 153-180.

(2) Sarikaya, M.; Tamerler, C.; Jen, A. K. Y.; Schulten, K.; Baneyx, F. *Nature Materials* **2003,** 2, (9), 577-585.

(3) Whitesides, G. M.; Grzybowski, B. *Science* **2002,** 295, (5564), 2418-2421.

(4) Whitesides, G. M.; Mathias, J. P.; Seto, C. T. *Science* **1991,** 254, (5036), 1312-1319.

(5) Yurchenco, P. D.; Birk, D. E.; Mecham, R. P., *Extracellular matrix assembly and structure*. Academic Press: San Diego, 1994; p 468.

(6) Glotzer, S. C. *Science* **2004,** 306, (5695), 419-420.

(7) Jonas, U.; del Campo, A.; Kruger, C.; Glasser, G.; Boos, D. *Proc. Natl. Acad. Sci. U. S. A.* **2002,** 99, (8), 5034-5039.

(8) Lehn, J. M. *Science* **2002,** 295, (5564), 2400-2403.

(9) Rueckes, T.; Kim, K.; Joselevich, E.; Tseng, G. Y.; Cheung, C. L.; Lieber, C. M. *Science* **2000,** 289, (5476), 94-97.

(10) McLeish, T. *Science* **1997,** 278, (5343), 1577-1578.

(11) Penner, R. M.; Heben, M. J.; Longin, T. L.; Lewis, N. S. *Science* **1990,** 250, (4984), 1118-1121.

(12) Corriu, R. J. P. *Angew. Chem., Int. Ed. Engl.* **2000,** 39, (8), 1376-1398.

(13) Lai, W. Y.-C.; Pau, S.; López, O. D. In *Nanofabrication: technologies, devices, and applications*, 2004; SPIE--the International Society for Optical Engineering: 2004; p 450.

(14) Loy, D. A. *MRS Bulletin* **2001,** 26, (5), 364-408.

(15) Kawasumi, M. *J. Polym. Sci., Part A: Polym. Chem.* **2004,** 42, (4), 819-824.

(16) Braun, T.; Schubert, A. P.; Kostoff, R. N. *Chem. Rev.* **2000,** 100, (6), 2475-2475.

(17) Ajayan, P. M. *Chem. Rev.* **1999,** 99, (7), 1787-1799.

(18) Alivisatos, A. P. *Science* **1996,** 271, (5251), 933-937.

(19) Katsoulis, D. E. *Chem. Rev.* **1998,** 98, (1), 359-387.

(20) Leites, L. A. *Chem. Rev.* **1992,** 92, (2), 279-323.

(21) Li, G. Z.; Wang, L. C.; Ni, H. L.; Pittman, C. U. *Journal of Inorganic and Organometallic Polymers* **2001,** 11, (3), 123-154.

(22) Scott, D. W. *J. Am. Chem. Soc.* **1946,** 68, (3), 356-358.

(23) Brown, J. F.; Vogt, L. H. *J. Am. Chem. Soc.* **1965,** 87, (19), 4313-4317.

(24) Feher, F. J.; Terroba, R.; Jin, R. J.; Wyndham, K. D.; Lucke, S.; Brutchey, R.; Nguyen, F. *Polym. Mater. Sci. Eng.* **2000,** 82, 301.

(25) Loy, D. A.; Shea, K. J. *Chem. Rev.* **1995,** 95, (5), 1431-1442.

(26) Baney, R. H.; Itoh, M.; Sakakibara, A.; Suzuki, T. *Chem. Rev.* **1995,** 95, (5), 1409-1430.

(27) Waddon, A. J.; Coughlin, E. B. *Chem. Mater.* **2003,** 15, (24), 4555-4561.

(28) Schwab, J. J.; Lichtenhan, J. D. *Applied Organometallic Chemistry* **1998,** 12, (10-11), 707-713.

(29) Haddad, T. S.; Lichtenhan, J. D. *Macromolecules* **1996,** 29, (22), 7302-7304.

(30) Bharadwaj, R. K.; Berry, R. J.; Farmer, B. L. *Polymer* **2000,** 41, (19), 7209-7221.

(31) Mather, P. T.; Jeon, H. G.; Romo-Uribe, A.; Haddad, T. S.; Lichtenhan, J. D. *Macromolecules* **1999,** 32, (4), 1194-1203.

(32) Tsuchida, A.; Bolln, C.; Sernetz, F. G.; Frey, H.; Mulhaupt, R. *Macromolecules* **1997,** 30, (10), 2818-2824.

(33) Joshi, M.; Butola, B. S. *Journal of Macromolecular Science-Polymer Reviews* **2004,** C44, (4), 389-410.

(34) Pan, Q. W.; Fan, X. H.; Chen, X. F.; Zhou, Q. F. *Progress in Chemistry* **2006,** 18, (5), 616-621.

(35) Pu, K. Y.; Fan, Q.; Wang, L. H.; Huang, W. *Progress in Chemistry* **2006,** 18, (5), 609-615.

(36) *Epoxy Resins, Chemistry and Technology*. Marcel Dekker: New York, 1988.

(37) Abad, M. J.; Barral, L.; Fasce, D. P.; Williams, R. J. J. *Macromolecules* **2003,** 36, (9), 3128-3135.

(38) Choi, J.; Harcup, J.; Yee, A. F.; Zhu, Q.; Laine, R. M. *J. Am. Chem. Soc.* **2001,** 123, (46), 11420-11430.

(39) Matejka, L.; Strachota, A.; Plestil, J.; Whelan, P.; Steinhart, M.; Slouf, M. *Macromolecules* **2004,** 37, (25), 9449-9456.

(40) Ni, Y.; Zheng, S. X.; Nie, K. M. *Polymer* **2004,** 45, (16), 5557-5568.

(41) Tegou, E.; Bellas, V.; Gogolides, E.; Argitis, P. *Microelectron. Eng.* **2004,** 73-74, 238-243.

(42) Tegou, E.; Bellas, V.; Gogolides, E.; Argitis, P.; Eon, D.; Cartry, G.; Cardinaud, C. *Chem. Mater.* **2004,** 16, (13), 2567-2577.

(43) Eon, D.; Cartry, G.; Fernandez, V.; Cardinaud, C.; Tegou, E.; Bellas, V.; Argitis, P.; Gogolides, E. *Journal of Vacuum Science & Technology B* **2004,** 22, (5), 2526-2532.

(44) Jakubek, V.; Liu, X. Q.; Vohra, V. R.; Douki, K.; Kwark, Y. J.; Ober, C. K.; Markley, T. J.; Robertson, E. A.; Carr, R. V. C.; Marsella, J. A.; Conley, W.; Miller, D.; Zimmerman, P. *Journal of Photopolymer Science and Technology* **2003,** 16, (4), 573-580.

(45) Ali, M. A.; Gonsalves, K. E.; Agrawal, A.; Jeyakumar, A.; Henderson, C. L. *Microelectron. Eng.* **2003,** 70, (1), 19-29.

(46) Wu, H. P.; Hu, Y. Q.; Gonsalves, K. E.; Yacaman, M. J. *Journal of Vacuum Science & Technology B* **2001,** 19, (3), 851-855.

(47) Odian, G.. Principles of Polymerization, Third Edition. In *Principles of Polymerization, Third Edition*, John Wiley & Sons, I.. Ed. 1991; pp 158-162.

(48) Lee, Y. J.; Huang, J. M.; Kuo, S. W.; Lu, J. S.; Chang, F. C. *Polymer* **2005,** 46, (1), 173-181.

(49) Chen, Y. W.; Kang, E. T. *Mater. Lett.* **2004,** 58, (29), 3716-3719.

(50) Huang, J. C.; Xiao, Y.; Mya, K. Y.; Liu, X. M.; He, C. B.; Dai, J.; Siow, Y. P. *J. Mater. Chem.* **2004,** 14, (19), 2858-2863.

(51) Phillips, S. H.; Haddad, T. S.; Tomczak, S. J. *Current Opinion in Solid State & Materials Science* **2004,** 8, (1), 21-29.

(52) Tamaki, R.; Choi, J. W.; Laine, R. M. *Chem. Mater.* **2003,** 15, (3), 793-797.

(53) Leu, C. M.; Chang, Y. T.; Wei, K. H. *Chem. Mater.* **2003,** 15, (19), 3721-3727.

(54) Leu, C. M.; Reddy, G. M.; Wei, K. H.; Shu, C. F. *Chem. Mater.* **2003,** 15, (11), 2261-2265.

(55) Huang, J. C.; He, C. B.; Xiao, Y.; Mya, K. Y.; Dai, J.; Siow, Y. P. *Polymer* **2003,** 44, (16), 4491-4499.

(56) Wright, M. E.; Schorzman, D. A.; Feher, F. J.; Jin, R. Z. *Chem. Mater.* **2003,** 15, (1), 264-268.

(57) Gonzalez, R. I.; Phillips, S. H.; Hoflund, G. B. *Journal of Spacecraft and Rockets* **2000,** 37, (4), 463-467.

(58) Joshi, A.; Butola, B. S. *Polymer* **2004,** 45, (14), 4953-4968.

(59) Fu, B. X.; Gelfer, M. Y.; Hsiao, B. S.; Phillips, S.; Viers, B.; Blanski, R.; Ruth, P. *Polymer* **2003,** 44, (5), 1499-1506.

(60) Zheng, L.; Farris, R. J.; Coughlin, E. B. *Abstracts of Papers of the American Chemical Society* **2000,** 220, U318-U318.

(61) Zheng, L.; Kasi, R. M.; Farris, R. J.; Coughlin, E. B. *Abstracts of Papers of the American Chemical Society* **2001,** 221, U367-U367.

(62) Zheng, L.; Farris, R. J.; Coughlin, E. B. *J. Polym. Sci., Part A: Polym. Chem.* **2001,** 39, (17), 2920-2928.

(63) Zheng, L.; Waddon, A. J.; Farris, R. J.; Coughlin, E. B. *Macromolecules* **2002,** 35, (6), 2375-2379.

(64) Grubbs, R. H., *Handbook of metathesis*. Weinheim [Germany] : Wiley-VCH: 2003.

(65) Zheng, L.; Farris, R. J.; Coughlin, E. B. *Macromolecules* **2001,** 34, (23), 8034-8039.

(66) Jeon, H. G.; Mather, P. T.; Haddad, T. S. *Polym. Int.* **2000,** 49, (5), 453-457.

(67) Pyun, J.; Miller, P. J.; Matyjaszewski, K. *Abstracts of Papers of the American Chemical Society* **2000,** 219, U390-U390.

(68) Pyun, J.; Matyjaszewski, K.; Wu, J.; Kim, G. M.; Chun, S. B.; Mather, P. T. *Polymer* **2003,** 44, (9), 2739-2750.

(69) Pyun, J.; Xia, J. H.; Matyjaszewski, K. *Synthesis and Properties of Silicones and Silicone-Modified Materials* **2003,** 838, 273-284.

(70) Drazkowski, D. B.; Lee, A.; Haddad, T. S.; Cookson, D. J. *Macromolecules* **2006,** 39, (5), 1854-1863.

(71) Intasanta, N.; ; Russell, T. P.; ; Coughlin, E. B. In *Ultrathin films of self-assembled organic-inorganic hybrid nanoparticle block copolymers*, Abstracts of Papers of the American Chemical Society, Anaheim, 2004; Anaheim, 2004.

(72) Carroll, J. B.; Frankamp, B. L.; Rotello, V. M. *Chemical Communications* **2002,** (17), 1892-1893.

(73) Carroll, J. B.; Waddon, A. J.; Nakade, H.; Rotello, V. M. *Macromolecules* **2003,** 36, (17), 6289-6291.

(74) Kennedy, J. P. *J. Polym. Sci., Part A: Polym. Chem.* **1999,** 37, (14), 2285-2293.

(75) Patten, T. E.; Matyjaszewski, K. *Acc. Chem. Res.* **1999,** 32, (10), 895-903.

(76) Hawker, C. J. *Acc. Chem. Res.* **1997,** 30, (9), 373-382.

(77) Odian, G., *Principles of Polymerization, Third Edition*, John Wiley & Sons, Inc: 1991.

(78) Szwarc, M. *Nature* **1956,** 178, (4543), 1168-1169.

(79) Morton, M.; Fetters, L. J. *Rubber Chem. Technol.* **1974,** 48, 359.

(80) Hadjichristidis, N.; Iatrou, H.; Pispas, S.; Pitsikalis, M. *J. Polym. Sci., Part A: Polym. Chem.* **2000,** 38, (18), 3211-3234.

(81) Uhrig, D.; Mays, J. W. *J. Polym. Sci., Part A: Polym. Chem.* **2005,** 43, (24), 6179-6222.

(82) Hamley, I. W., *The Physics of Block Copolymers*, Oxford University Press: New York, 1998.

(83) Bates, F. S. *Science* **1991,** 251, (4996), 898-905.

(84) Forster, S. *Colloid Chemistry I* **2003,** 226, 1-28.

(85) Ulrich, R.; Du Chesne, A.; Templin, M.; Wiesner, U. *Advanced Materials* **1999,** 11, (2), 141-146.

(86) Thurn-Albrecht, T.; Schotter, J.; Kastle, C. A.; Emley, N.; Shibauchi, T.; Krusin-Elbaum, L.; Guarini, K.; Black, C. T.; Tuominen, M. T.; Russell, T. P. *Science* **2000,** 290, (5499), 2126-2129.

(87) Tseng, G. Y.; Ellenbogen, J. C. *Science* **2001,** 294, (5545), 1293-1294.

(88) Forster, S.; Plantenberg, T. *Angewandte Chemie-International Edition* **2002,** 41, (5), 689-714.

(89) Ray, S. S.; Okamoto, M. *Progress in Polymer Science* **2003,** 28, (11), 1539-1641.

(90) Giannelis, E. P. *Advanced Materials* **1996,** 8, (1), 29-&.

(91) Godovski, D. Y. *Thermal and Electrical Conductivity of Polymer Materials* **1995,** 119, 79-122.

(92) Nagata, K.; Kodama, S.; Kawasaki, H.; Deki, S.; Mizuhata, M. *J. Appl. Polym. Sci.* **1995,** 56, (10), 1313-1321.

(93) Zhang, C. L.; Xu, T.; Butterfield, D.; Misner, M. J.; Ryu, D. Y.; Emrick, T.; Russell, T. P. *Nano Letters* **2005,** 5, (2), 357-361.

(94) Bockstaller, M. R.; Lapetnikov, Y.; Margel, S.; Thomas, E. L. *J. Am. Chem. Soc.* **2003,** 125, (18), 5276-5277.

(95) Thompson, R. B.; Ginzburg, V. V.; Matsen, M. W.; Balazs, A. C. *Science* **2001,** 292, (5526), 2469-2472.

(96) Lamm, M. H.; Chen, T.; Glotzer, S. C. *Nano Lett.* **2003,** 3, (8), 989-994.

(97) Lee, J. Y.; Balazs, A. C.; Thompson, R. B.; Hill, R. M. *Macromolecules* **2004,** 37, (10), 3536-3539.

(98) Zhang, X.; Chan, E. R.; Glotzer, S. C. *J. Chem. Phys.* **2005,** 123, (18).

(99) Kopesky, E. T.; Haddad, T. S.; Cohen, R. E.; McKinley, G. H. *Macromolecules* **2004,** 37, (24), 8992-9004.

(100) Kulbaba, K.; Manners, I. *Macromolecular Rapid Communications* **2001,** 22, (10), 711-724.

(101) Ni, Y. Z.; Rulkens, R.; Manners, I. *J. Am. Chem. Soc.* **1996,** 118, (17), 4102-4114.

(102) Cheng, J. Y.; Ross, C. A.; Thomas, E. L.; Smith, H. I.; Vancso, G. J. *Advanced Materials* **2003,** 15, (19), 1599-+.

(103) Cheng, J. Y.; Ross, C. A.; Thomas, E. L.; Smith, H. I.; Vancso, G. J. *Appl. Phys. Lett.* **2002,** 81, (19), 3657-3659.

(104) Manners, I. *Science* **2001,** 294, (5547), 1664-1666.

(105) Archer, R. D., *Inorganic and organometallic polymers*. Wiley-VCH: New York, 2001.

(106) Manners, I. *Angew. Chem., Int. Ed. Engl.* **1996,** 35, (15), 1603-1621.

(107) Kresge, C. T.; Leonowicz, M. E.; Roth, W. J.; Vartuli, J. C.; Beck, J. S. *Nature* **1992,** 359, (6397), 710-712.

(108) Kickelbick, G. *Progress in Polymer Science* **2003,** 28, (1), 83-114.

(109) Soler-Illia, G.; Crepaldi, E. L.; Grosso, D.; Sanchez, C. *Current Opinion in Colloid & Interface Science* **2003,** 8, (1), 109-126.

(110) Sanchez, C.; Julian, B.; Belleville, P.; Popall, M. *J. Mater. Chem.* **2005,** 15, (35-36), 3559-3592.

(111) Yang, P. D.; Deng, T.; Zhao, D. Y.; Feng, P. Y.; Pine, D.; Chmelka, B. F.; Whitesides, G. M.; Stucky, G. D. *Science* **1998,** 282, (5397), 2244-2246.

(112) Yang, P. D.; Zhao, D. Y.; Margolese, D. I.; Chmelka, B. F.; Stucky, G. D. *Nature* **1998,** 396, (6707), 152-155.

(113) Zhao, D. Y.; Feng, J. L.; Huo, Q. S.; Melosh, N.; Fredrickson, G. H.; Chmelka, B. F.; Stucky, G. D. *Science* **1998,** 279, (5350), 548-552.

(114) Templin, M.; Franck, A.; DuChesne, A.; Leist, H.; Zhang, Y. M.; Ulrich, R.; Schadler, V.; Wiesner, U. *Science* **1997,** 278, (5344), 1795-1798.

(115) Simon, P. F. W.; Ulrich, R.; Spiess, H. W.; Wiesner, U. *Chem. Mater.* **2001,** 13, (10), 3464-3486.

CHAPTER 2

POLYMER NANOCOMPOSITES THROUGH CONTROLLED SELF-ASSEMBLY OF CUBIC SILSESQUIOXANE SCAFFOLDS

2.1 Introduction

2.1.1 Background

The formation of ordered structures at the nanometer length scale requires strategies that are able to harness the fundamental forces of self-assembly to direct the generation of higher ordered motifs from the basic building block constitutents.[1-3] The utilization of non-covalent interactions, both intra- and intermolecular remains one of the principle methods upon which nanoscale aggregates are constructed. For polymers, success has been achieved using organic block copolymers to generate a range of differing nanometer length scale morphologies in the solid state. The generation of these structures is driven by reducing surface free energy between chemically linked, yet incompatible, blocks.[4, 5] A limitation remains however in that long annealing times are needed to approach thermodynamically favorable structures in block copolymer morphologies. Comparable nanoscale morphological structures have been obtained for inorganic-polymeric structures using sol-gel preparative methods utilizing amphiphilic surfactants as templates.[6-8] There is however the associated problem of maintaining the desired structure upon removal of the surfactants. Considerable challenges remain regarding the construction of robust nanostructured materials using suitable building blocks via a bottom-up approach. Controlling associative interactions of scaffolds is certainly an attractive route. However, implicit in this approach is the understanding of the interplay of non-covalent interactions. This understanding would enable one to

manipulate a polymeric structure. Choosing a suitable primary chemical sequence would afford desired organization of the material into a secondary structure at length scales considerably longer than those of the individual polymer chain.

Polyhedral oligomeric silsesquioxanes (POSS®) are a family of molecularly precise nearly isotropic molecules with diameters ranging between 1-3 nm depending on the number of silicon atoms in the central cage and the peripheral substitution groups surrounding this core.[9] A cubic T_8 silsesquioxane unit has an inorganic cubic core comprised of a Si_8O_{12} core surrounded by eight tunable alkyl substitution groups (Figure 2.1). It has an approximate spherical diameter of 1.5 nm when R is a cyclopentyl group. POSS has been recognized as well-defined building blocks for nanostructured materials.[10-13] Efficient synthetic methods have also been developed whereby one corner can be selectively substituted by a functional group X capable of undergoing polymerization. This has provided the possibility to incorporate inorganic POSS cages into organic polymer chains.[9-11, 13-33] The cubic silsesquioxane unit can be viewed as a nanoparticle for both its size and filler function, or a well-defined macromonomer for its ability to undergo polymerization. In this chapter, we also demonstrate its use as a scaffold to generate lateral ordering as a consequence of polymer-POSS interactions.

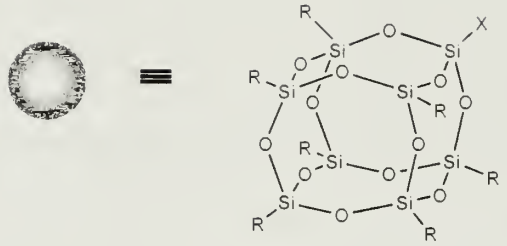

Figure 2.1 Structure o Cubic Silsesquioxanes (POSS®). Cubic Silsesquioxane is a Well-defined Molecule Having an Inorganic Core Comprised of Si_8O_{12} Surrounded by Eight Tunable Substitution Groups. Each Unit Can Be Treated as a Sphere Represented by a Green Sphere in all the Following Figures.

2.1.2 Design Rationale

A body of work has shown that octa-alkyl substituted cubic silsesquioxane nanoparticles $R_8Si_8O_{12}$ form hexagonal (or equivalently rhombohedral) crystal structures. [34-39] Based on X-ray studies from Larsson[35] and recent work from this laboratory.[40] each cubic silsesquioxane unit can be regarded as being nearly spherical. The three-dimensional crystal structure of POSS can be viewed by arranging each POSS sphere in a plane on a hexagonal array and stacking these planes in ABCA sequence. When the POSS spheres are attached along the polymer chains, the crystal packing of the cubic silsesquioxane units is constrained by their covalent attachment to the polymer chain. As a result, a bilayer or lamellar-like structure is formed where POSS spheres are packed hexagonally within planes and two planes are stacked together. In other words, the covalently connected chains serve as the source of crystallization confinement, preventing the development of spherical packing in three

dimensions, and therefore results in a 2-dimensional raft-like structure. A schematic drawing is shown in Figure 2.2. The specific interactions between particles originate from intermolecular van der Waals forces resulting in the stable construction of a nano-layered structure. In previous studies of polyethylene-POSS copolymers, X-ray diffraction data supported this proposed structure.[40, 41] However, the competing co-crystallization of polyethylene frustrates the POSS assembly, and no large scale POSS nanostructures were observed in real space imaging techniques. In the present study, a low glass transition temperature amorphous polymer, 1,4-polybutadiene, was selected as the backbone polymers, thus providing a rubbery liquid-like matrix to allow the pendant POSS units to self-assemble in the absence of competing polymer crystallization.

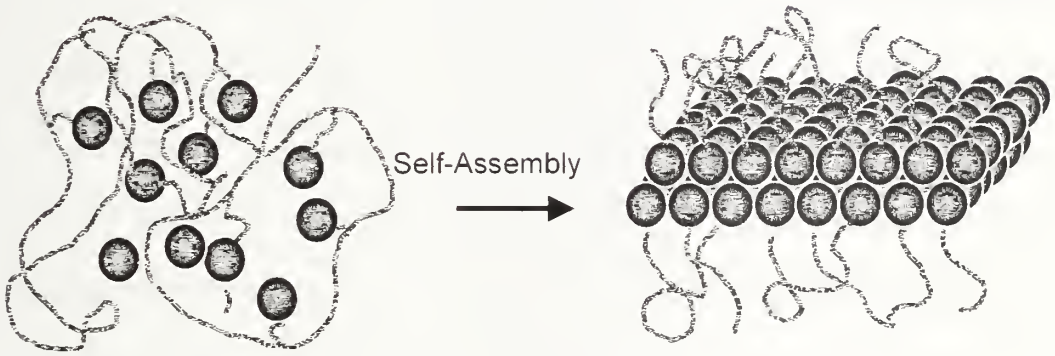

Figure 2.2 Synthesis of Polymer Nanocomposites Through Controlled Self-Assembly of Cubic Silsesquioxane (POSS) Nanoparticles. POSS Preferentially Aggregates and Crystallizes into an Ordered Lattice within the Polymer Matrix. The Covalently Bonded Polymer Chains Serve as the Source of Confinement to Limit POSS Growth in a Two-Dimensional Lattice.

2.2 Experimental Section

2.2.1 Materials

Cyclopentyl-POSS-norbornene macromonomer 1-[2-(5-norbornen-2-yl)ethyl]-3,5,7,9,11,13,15-heptacyclopentylpentacyclo[9.5.1.1^{3,9}.1^{5,15}.1^{7,13}]octasiloxane (POSS-norbornene, **1**) was provided by Hybrid Plastics. The catalyst $RuCl_2(=CHPh)(PCy_3)_2$ was purchased from Strem Chemical. Other reagents were obtained from Aldrich. Cyclooctadiene and methylene chloride were vacuum transferred from CaH_2 prior to use.

2.2.2 Polymerization Procedures for Polybutadiene-POSS Copolymers

9.74 mg (12 μmol) of $RuCl_2(=CHPh)(PCy_3)_2$ was dissolved in 1 mL of CH_2Cl_2 and added to a solution of 0.65 g cyclooctadiene (6 mmol, 500 equiv.) and 0.072 g POSS-norbornene **1** (0.070 mmol, 10 wt %) in 4 mL of CH_2Cl_2 in the glovebox. The reaction mixture was stirred for 24 hours under nitrogen at room temperature. The solutions remained homogenous throughout the entire reaction. The reaction was stopped by injection of 1 mL CH_2Cl_2 with a trace amount of ethyl vinyl ether and 2,6-di-tert-butyl-4-methylphenol. The copolymers were precipitated in 100 mL methanol, recovered by decanting the solvent and dried overnight under vacuum at room temperature. A purple solid was obtained in 85% yield. The polymerizations were repeated using varying amounts of **1**, 0, 10, 20, 30, 40, 50 wt %, to prepare a range of copolymers (Table 2.1).

2.2.3 Polymer Characterization

2.2.3.1 NMR

^{1}H spectra were obtained in chloroform-*d* at 300 MHz using a Bruker DPX-300 FT-NMR spectrometer. ^{13}C NMR spectra were recorded in chloroform-*d* with a Bruker DPX-300 FT-NMR spectrometer operating at 75 MHz. High temperature NMR were recorded in tetrachloroethane-d_2 with a Bruker AMX-500 FT NMR spectrometer operating at 125 MHz. Gel permeation chromatography was performed using a Polymer Lab LC1120 HPLC pump equipped with a Waters differential refractometer detector. The mobile phase was THF with a flow rate of 1 mL/min. Separations were performed using 10^5 Å, 10^4 Å and 10^3 Å Polymer Lab columns. Molecular weights were calibrated versus narrow molecular weight polystyrene standards.

2.2.3.2 DSC

Differential scanning calorimetry was performed under a continuous nitrogen purge on a Mettler-Toledo DSC 822^{e}. Octane (Aldrich, 99%+), pentane (Aldrich, 99%+), deionized water, indium and zinc were used to perform the calibration. Samples having a mass between 2.5 and 11 mg were used. Data were gathered using a scan rate of 10 °C/min on the first scan.

2.2.3.3 TGA

Thermogravimetric analysis was carried out using a TA Instruments TGA 2950 thermogravimetric analyzer with a heating rate of 10°C/min from room temperature to 700 $^{\circ}$ C under a continuous nitrogen or air purge (40 mL/min for both air and nitrogen).

2.2.3.4 TEM

Specimens for TEM, WAXD and SAXS were cast from 5 wt % toluene or methylene chloride solutions overnight in the hood. Bulk film samples for electron microscopy were microtomed in a Leica Ultracut cryoultramicrotome. Sections approximately 50-100 nm thick were cut with a Diatome diamond knife at a sample temperature of -110°C, a knife temperature of -100°C and a cryogenic sample chamber of -120°C. The only exception was the sample **PBD-POSS-1** because of the difficulty to handle a viscous liquid at room temperature. It was deposited onto the TEM grids directly from a dilute methylene chloride solution (~0.1 wt %) and the solvent was evaporated within minutes. TEM studies were performed using a JEOL 100 CX transmission electron microscope operated at 100 kV.

2.2.3.5 WAXD

Wide angle X-ray diffraction was carried out on a Siemens D500 instrument in normal/transmission mode (0.3 incident slit beam divergence) with Ni-filtered Cu K_α radiation (1.54 Å wavelength). Data were obtained with the incident beam normal to the plane of the film.

2.2.3.6 SAXS

Small angle X-ray scattering was performed using Ni-filtered Cu Kα radiation (1.54 Å wavelength) from a Rigaku rotating anode (operated at 40 kV, 200 mA). The X-ray was collimated by a set of three pinholes. A CCD detector (Siemens Hi-Star), located at a camera length of 875.2 mm, was used to record scattering patterns.

2.3 Results and Discussion

2.3.1 Polymerization

To demonstrate the concept of controlled self-assembly of cubic silsesquoixane scaffolds, a series of random copolymers comprising polybutadiene (PBD) and POSS spheres was designed. The copolymers were synthesized utilizing ring-opening metathesis copolymerization (ROMP) of 1,5-cyclooctadiene and a cubic silsesquioxane bearing a polymerizable norbornene group **1** using the catalyst $RuCl_2(=CHPh)(PCy_3)_2$ (Figure 2.3).[42] ROMP of cyclooctadiene provides exclusively 1,4-polybutadiene as the polymer backbones. The mole ratio of cyclooctadiene to catalyst was fixed at 500:1 to yield moderately high molecular weight polybutadiene. Increasing concentrations of POSS were used in the reaction feeds to afford a series of random copolymers. The molecular weight characterization data of the PBD-POSS copolymers is listed in Table 2.1. All of these copolymers have M_w values of between 67-88 kg/mol, and the corresponding polydispersities are in the range of 1.7-2.0.

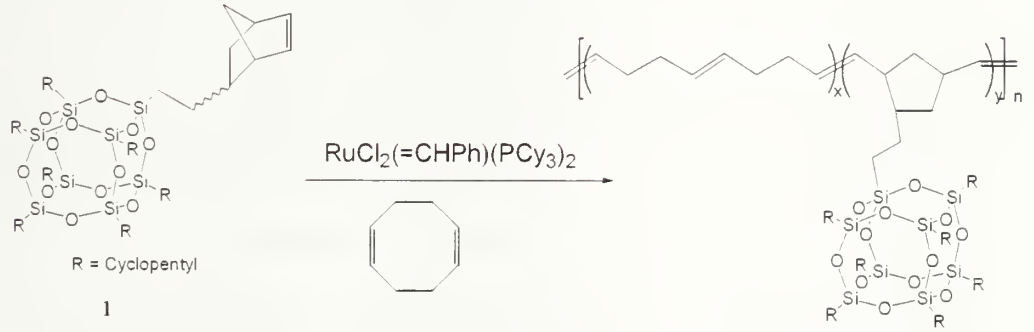

Figure 2.3 Synthesis of PBD-POSS Copolymers. The Copolymers were Synthesized by Ring-Opening Metathesis Copolymerization of 1,5-Cyclooctadiene and POSS Bearing a Polymerizable Norbornene Group

Using ^{1}H-NMR to determine the level of incorporation of POSS macromonomer in the copolymers revealed a steady increase as the amount of POSS in the feed was increased. Samples with different incorporation of POSS (12 - 53 wt %) were obtained

simply by changing the feed ratio between cyclooctadiene and POSS. The physical appearance of the isolated products changes drastically from a viscous liquid at 0 wt % POSS to elastomeric materials with 23 wt % or greater POSS loadings. The ^{1}H NMR also reveals no residual POSS-norbornene macromonomer in the copolymers. However the conversion of cyclooctadiene to 1,4-polybutadiene was not complete under the relatively dilute solution polymerization condition (0.65 g cyclooctadiene in 5 mL CH_2Cl_2), the thermodynamic equilibrium among copolymer, cyclic oligomer and residue monomer resulted in the maximum conversion being roughly 80%. Dilute solution polymerization was chosen instead of neat bulk polymerization, or concentrated conditions, simply due to the limited solubility of POSS macromonomer (~100 mg/mL). The wt% and mol% of POSS in the copolymers obtained from ^{1}H-NMR agrees with the feed ratio if the overall conversion of cyclooctadiene is considered. We believe that the backbone sequences of these copolymers are random, not blocky, based on the efficient cross-metathesis mechanism between polymer chains as described previously.[29] Although the POSS-norbornene has much higher ROMP activity than cyclooctadiene, sufficiently long reaction times (24 hours) were chosen to allow significant inter-chain cross metathesis to occur to ultimately afford random copolymers. The evidence for the random microstructures comes from ^{1}H-NMR studies of the final copolymers, the copolymer with 53 wt % POSS in $C_2D_2Cl_4$ at 100 °C does not show any characteristic olefinic peaks from homopolymer of POSS-norbornene (Figure 2.4). Therefore no significant amount of POSS-norbornene block segments is present in the copolymers.

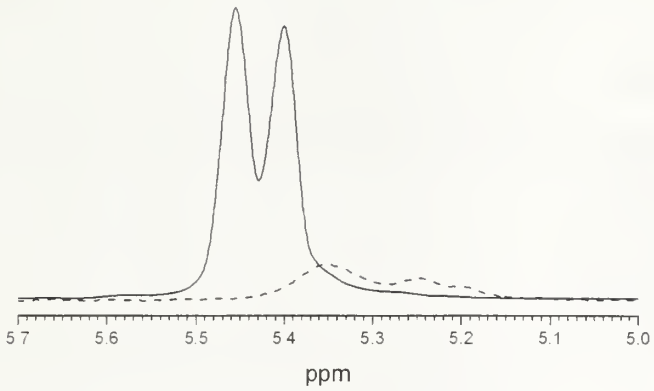

Figure 2.4 Olefinic Region ^{1}H-NMR Spectra of Poly(butadiene-POSS-53 wt %) Copolymer (Entry 6 Table 1, Solid Line) and Poly(POSS-Norbornene) (Dashed Line) at 100 °C in $C_2D_2Cl_4$.

Table 2.1 Summary of Molecular Weight Data of PBD- POSS Copolymers

Entry	Sample	POSS (wt %) in Feed	POSS in Copolymer[a]		Yield	M_w[b] (kg mol)	PDI[b]	trans cis[c]
			wt %	Mol %	%			
1	**PBD**	0	0	0	76	68	1.7	61 39
2	**PBD-POSS-1**	10	12	1.4	85	67	1.7	56 44
3	**PBD-POSS-2**	20	23	3	84	71	1.8	53 47
4	**PBD-POSS-3**	30	33	5	86	74	1.8	57 43
5	**PBD-POSS-4**	40	43	7.5	88	79	1.9	55 45
6	**PBD-POSS-5**	50	53	10.8	87	88	2	51 49

[a] As determined by ^{1}H-NMR in $CDCl_3$.
[b] Weight average molecular weight as determined by GPC in THF, versus narrow molecular weight polystyrene standards.
[c] Trans/cis ratio of backbone unsaturations as determined by ^{13}C-NMR of olefin region in $CDCl_3$.

2.3.2 DSC

The DSC data of PBD-POSS were collected and are shown in Figure 2.5. The lowest trace is a polybutadiene control. Each successive trace moving upwards in the graph are increasing POSS wt%. Two clear transitions can be observed on all the curves in this graph. A glass transition temperature is shown around -95 °C corresponding to T_g of 1,4-polybutadiene. A slight increase of T_g is observed in all of the PBD-POSS samples. The second peak around -10 °C comes from the melting transition of trans 1,4-polybutadiene. Due to the lack of 1,2-units and relatively high trans content in PBD, a regular packing and crystallization of the chains becomes possible. With increasing POSS content in copolymers, the melting temperatures decreases from 5 °C to –20 °C from **PBD-POSS-1** to **PBD-POSS-5**. This observation can be explained by the existence of POSS units in the copolymers, which disrupt the crystallization of PBD. A similar behavior was observed in PE- and PP-POSS

copolymers, though at a much higher temperature range.[30] No significant transition is noticed from room temperature up to 400 °C where the copolymers begin to degrade.

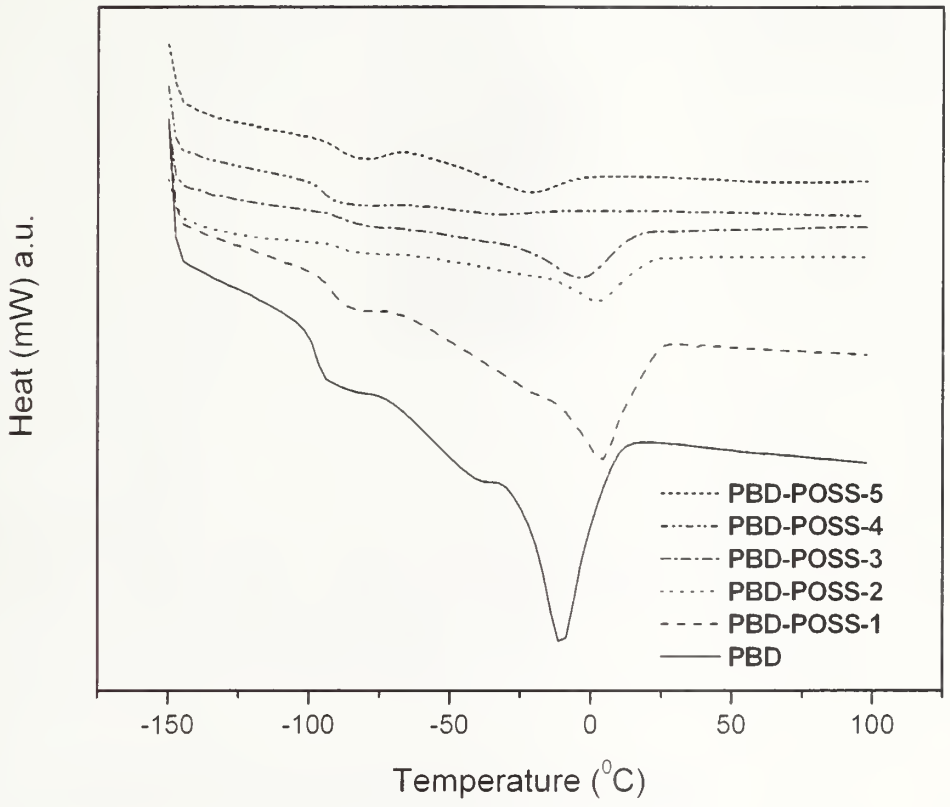

Figure 2.5 DSC Traces of PBD and PBD-POSS Copolymers.

2.3.3 TGA

Under nitrogen, POSS-norbornene gives a char yield of 20.8 wt% (Figure 2.6). The temperature at 5 %wt loss is equal to 311°C. The decomposition temperature at 5 wt% for polybutadiene is equal to 413°C and is only slightly affected upon POSS incorporation. The char yield obtained for each polymer is proportional to the amount of POSS present in the polymer.

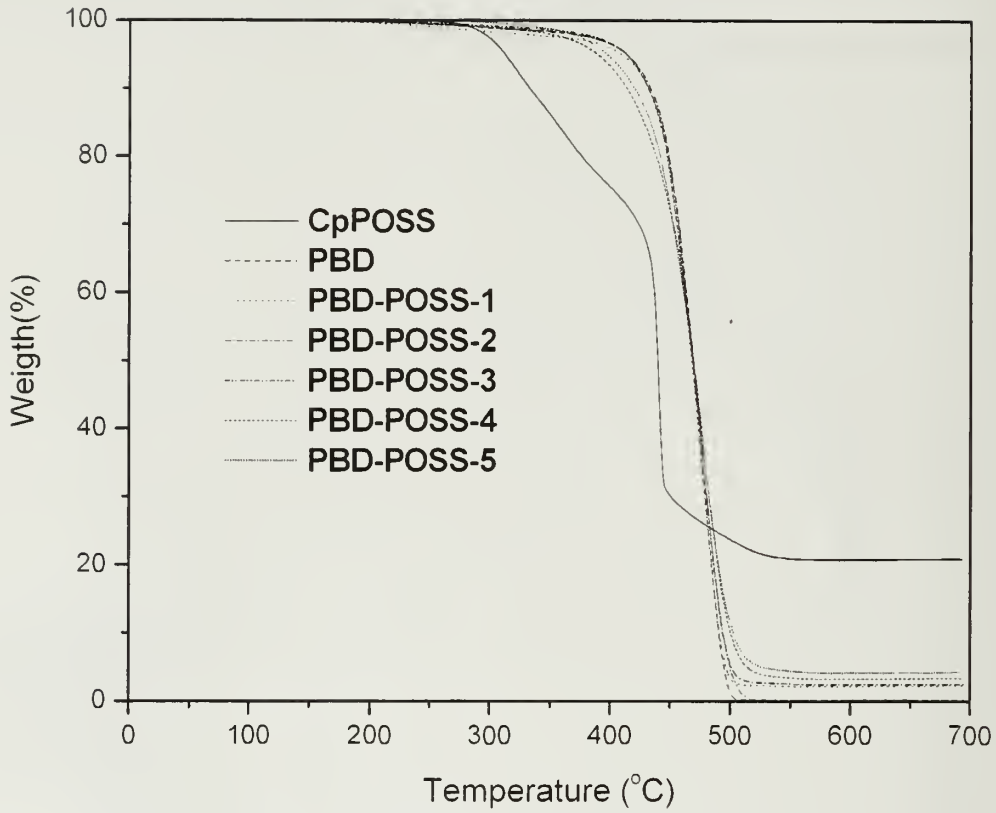

Figure 2.6 TGA of PBD-POSS Series Under N_2.

The TGA traces of the PBD-POSS series under air exhibit an interesting behavior (Figure 2.7). First, the char yield of POSS-norbornene at 700°C is equal to approximately 50%. This can be explained by a conversion of the POSS cage to silica. In fact, it has been shown that the POSS cage has the ability to be converted into silica upon treatment with oxygen plasma.[43] The same phenomenon is assumed to be taking place in the case of the PBD-POSS series. This phenomenon is the origin of the higher char yield obtained for the copolymers in air compared to nitrogen. Moreover, polymer oxidation leading to higher mass is occurring, explaining the mass increase of the sample between 100°C and 300°C.

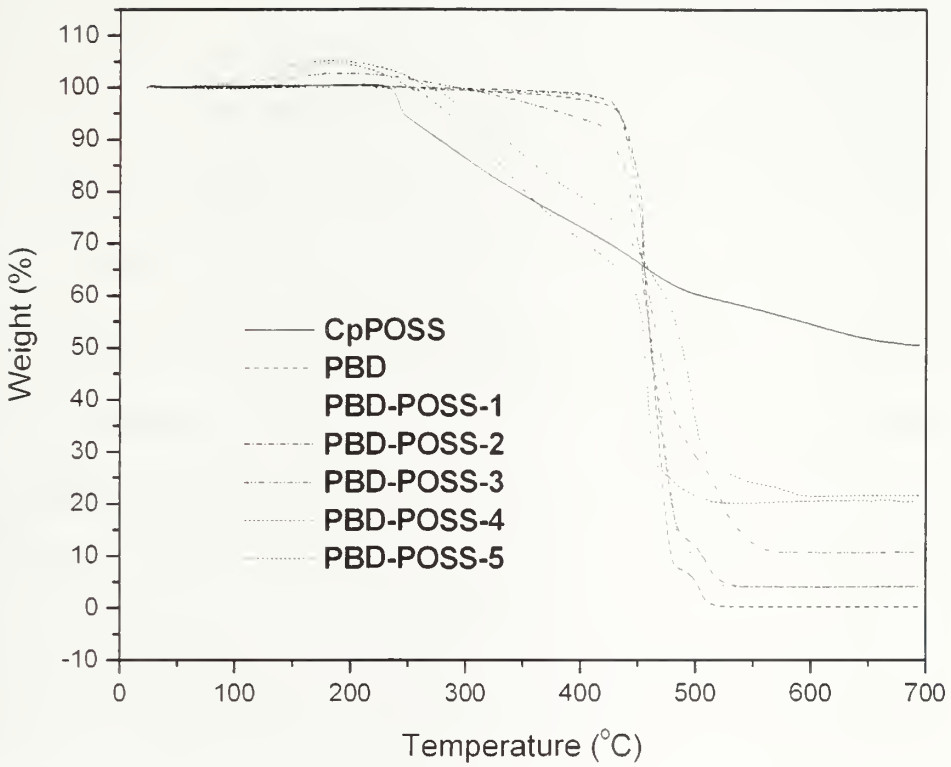

Figure 2.7 TGA of PBD-POSS Series Under Air

2.3.4 WAXD

Wide angle X-ray diffraction, which provides information about crystalline structure, was used to examine these PBD-POSS samples for POSS aggregation and precise information of the POSS crystalline lattice. Shown in Figure 2.8 are the diffraction profiles of **PBD-POSS-1** to **PBD-POSS-5**. For comparison, traces of PBD and POSS are also drawn. The pure PBD shows a broad peak at 2θs of 19.5° (4.55 Å), corresponding to an amorphous halo. The pure POSS shows strong reflections at 2θs of 8.2° (10.8 Å), 11.0° (8.03 Å), 12.1° (7.31 Å) and 19.0° (4.66 Å). These reflections are

associated with the hexagonal crystalline structure of POSS from 101, 110, 012 and 300/113/330 diffraction planes with a hexagonal unit cell of a = 16.06 Å and c = 17.14 Å.[40] It is clear that the copolymers show features which are characteristic of the structures of the two separate components. For **PBD-POSS-1**, the sample with the lowest POSS content in this series, the WAXD is dominated by the PBD amorphous halo. However, an additional peak at $2\theta = 8.3°$ (10.6 Å) corresponds to the POSS reflections. As the POSS content increases, the reflections from the POSS component increase in intensity compared with the halo from PBD. At the highest POSS content, 53% wt % (10.8 mol %), the sample shows only a weak PBD amorphous halo and strong 101, 110 diffractions from POSS, leading to the conclusion that more and more POSS particles aggregate together to form a crystalline raft-like structure with increasing of POSS concentrations. The strong diffraction from the 300/113/330 POSS diffraction planes at observed at $2\theta = 19°$ is a broad peak overlapping with the amorphous halo diffracted from PBD due to close peak positions. In contrast to the sharp diffraction in the POSS, the broadening at 19° is attributed to the anisotropic shape of the crystals.[41] In a constrained crystal lattice, the diffraction planes associated with the two long dimensions (length and width in a lamellar structure) show sharp diffraction, while diffractions associated with the one short dimension (thickness) show the broadest peaks.

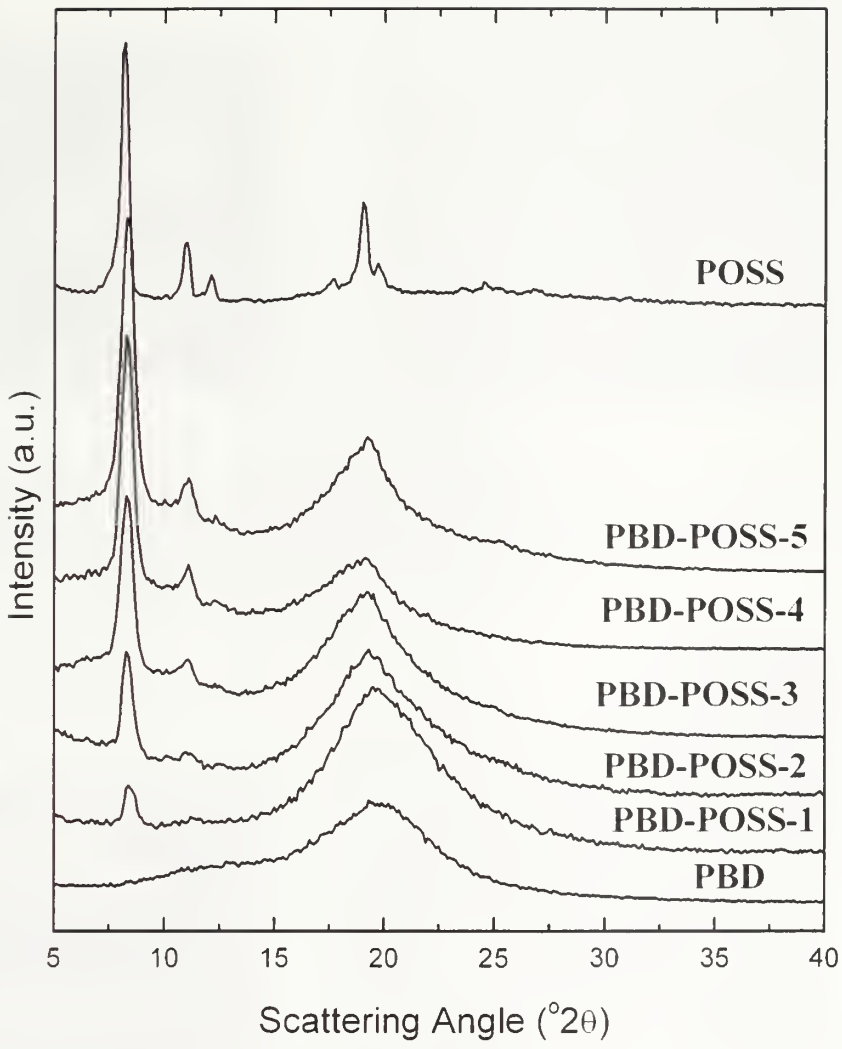

Figure 2.8 WAXD of PBD-POSS. The Sharp Diffraction Peaks at 8.3° (10.6 Å) and 11.1° (7.96 Å) Indicate Crystalline Aggregation of POSS Nanoparticles in PBD-POSS Random Copolymers.

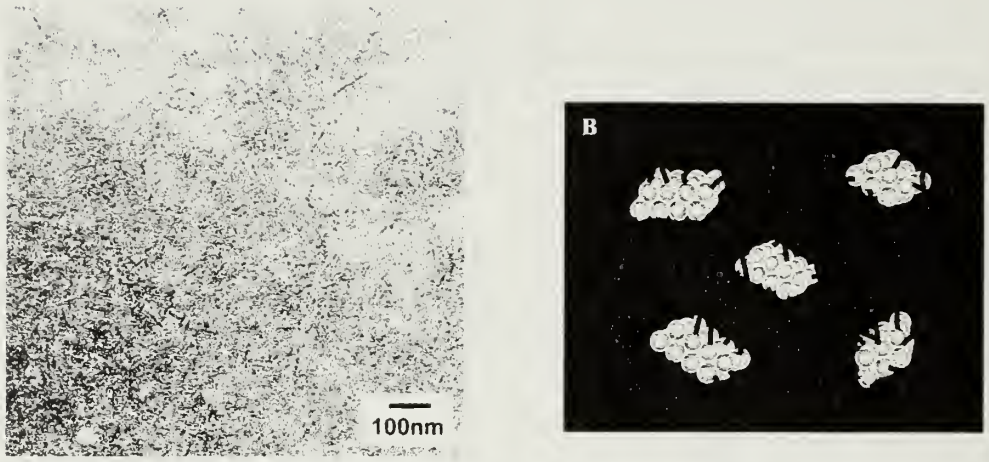

Figure 2.9 TEM of PBD-POSS-1 (left). The Copolymers of Low POSS Concentration Aggregate into Short Randomly Oriented Lamellae with Lateral Dimensions of Approximately 50 nm. Schematic Drawing of PBD-POSS Assembly at Low POSS Concentration (Right)

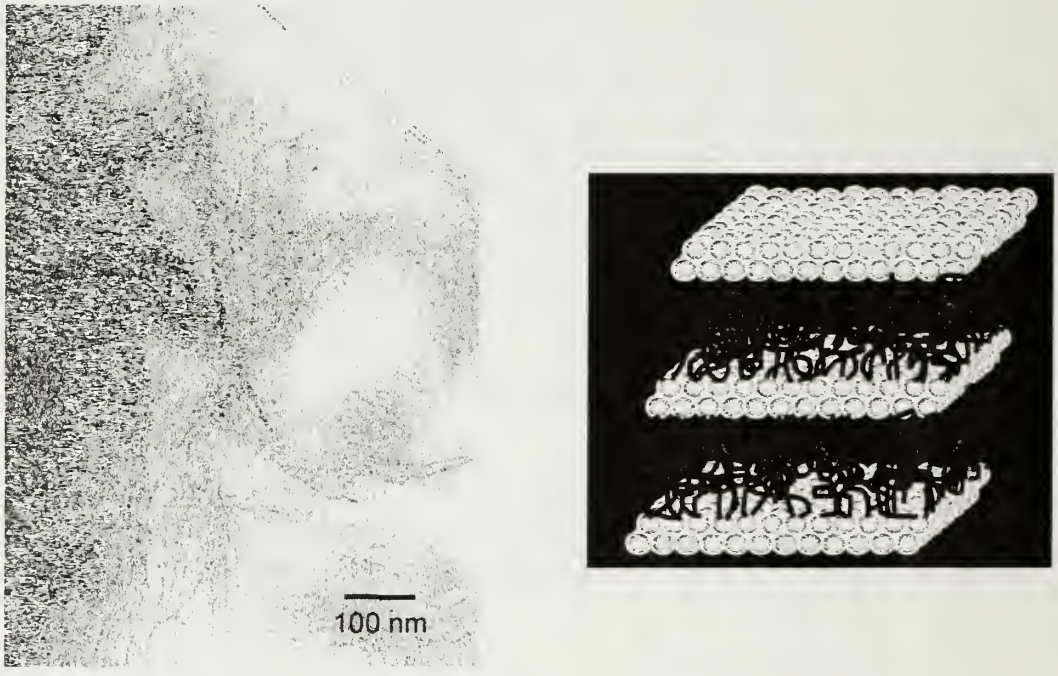

Figure 2.10 TEM of PBD-POSS-4 (left). The Copolymers of High POSS Concentration Form Continuous Lamellar Morphology with Lateral Length on the Order of Microns. Schematic Drawing of PBD-POSS Assembly at High POSS Concentration (Right).

2.3.5 TEM

Although the WAXD data indicate anisotropic crystalline aggregation of POSS nanoparticles in PBD-POSS random copolymers, this does not unambiguously prove the nanoscale morphology formed by POSS particles. As a result, transmission electron microscopy studies were performed. The contrast in a TEM micrograph originates from diffraction and mass-thickness contrast between dissimilar domains. POSS, due to its silicon content, has higher mass contrast than PBD chains which are comprised solely of carbon and hydrogen. In addition, the crystalline POSS domains as observed by WAXD diffract electrons more effectively than amorphous PBD. Both of these effects render POSS darker in TEM imaging without the need to resort to a staining agent. Shown in Figures 2.9 and 2.10 are two natural contrast TEM micrographs of PBD-POSS random copolymers with 12 and 43 wt % POSS incorporation. In Figure 2.9, POSS aggregates are directly observed as short randomly oriented lamellae with the lateral dimensions of approximately 50 nm. The thickness of the lamellae is found to be approximately 3 ~ 5 nm and corresponds to roughly twice the diameter of a POSS nanoparticles. The morphology observed here is comparable to that of fully exfoliated nylon-6/clay nanocomposites.[44] A notably feature of this sample is that this particular morphology was formed within one minute, the time required for solvent evaporation. Increasing the incorporation ratio of POSS to 43 wt %, results in continuous lamellae with lateral lengths on the order of microns (Figure 2.10). The irregular lamellar spacing observed in the image is possibly a combination of both POSS lamella twisting and the random nature of the copolymers. The morphology bears similarity to the lamellar morphology formed by precise diblock copolymers. Interestingly, our

experimental morphological results agree well with the computational result from Glotzer *et al.* on oligomeric tethered nanoparticles.[45] They predicted a similar nanostructure formation (Figure 3a and b in reference 44) using a system of oligomers tethered to specific locations on nanoparticles. The difference is that the simulation was carried out in a solvent and the nanostructure was based on thermodynamically driven immiscibility of tethers and nanoparticles. The favorable particle-particle interaction to form the crystalline packing of POSS was not considered.

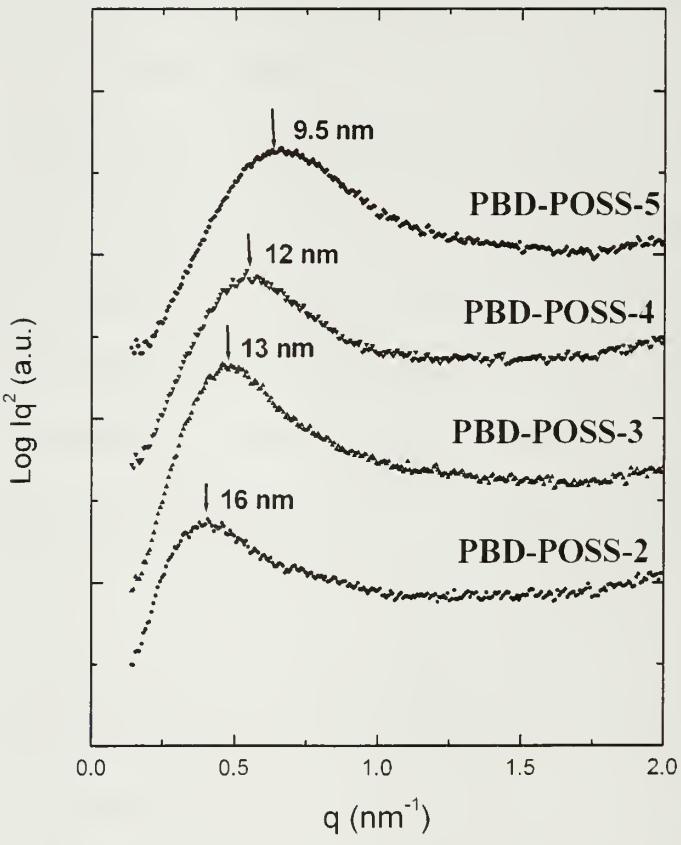

Figure 2.11 SAXS of PBD-POSS. The Lamellar Morphology Formed *via* Self-Assembly of POSS Particles is Further Supported by the Data of Small Angle X-Ray Scattering. The Peak Positions Correspond to the Spacing Between Lamellae.

2.3.6 SAXS

The lamellar morphology formed *via* controlled self-assembly of POSS particles is further supported by the data of small-angle X-ray scattering (Figure 2.11), where broad maxima are observed. The peak positions correspond to the spacing d between lamellae. The value can be simply calculated using the equation $d = 2\pi q$, where $q = 4\pi \lambda \sin(\theta/2)$ is the scattering vector. For example, the average distance between POSS layers is ~12 nm in the **PBD-POSS-4** sample. The lack of higher order reflections is a result of the random nature of the copolymers. The shift of broad maxima indicates that the spacing changes on the basis of the POSS concentrations. In a higher POSS concentration sample, such as **PBD-POSS-5**, the inter-lamellar distance is much smaller due to the relatively lower PBD content between two layers.

It is important to point out the difference between PBD-POSS nanocomposites and polymer clay nanocomposites in terms of their overall preparation, despite the similar morphologies observed under certain conditions. Polymer clay nanocomposites are one of the first successful demonstrations to emerge from the rapidly expanding field of nanoscale science.[44, 46, 47] They have shown substantial improvements in tensile strength, and heat distortion temperature achieved at relatively low loadings of inorganic layered clays within a host polymer matrix. The attempt to disperse clay layers in a polymer matrix always encounters the problem of unfavorable interactions between the hydrophilic surface of clays and hydrophobic polymers. This results in an incomplete dispersal or limited exfoliation. As a result, true polymer clay nanocomposites are successful only in a limited set of selected systems despite the fact that numerous attempts have been done to incorporate clay filler in a broad range of

polymeric materials. Generally speaking, the approach to obtain polymer clay nanocomposites involves a top-down strategy with a goal of separating macroscopic mineral clays into nanometer sized individual layers. In contrast, the approach pursued in this work is to build the inorganic layered nanostructure using suitable self-assembly building blocks in a bottom-up approach. By switching the synthetic approach from top-down to bottom-up, the unfavorable interactions between the organic and inorganic components has been changed into a favorable factor. This approach can easily lead to a "homogenous" organic-inorganic composite with a few nanometer thick inorganic layered filler uniformly distributed throughout the polymer matrix. Several of the novel properties documented in polymer/clay systems associated with the anisotropic shape of inorganic fillers are expected to be observed in assembled POSS systems.

The controlled aggregation of POSS spheres from single spherical particle to the ordered lamellar structures will offer a new opportunity for further understanding and better design of composite materials. Last, but not least, this controlled self-assembly process is also noteworthy considering the random nature of the copolymers and broad molecular weight distribution (polydispersity index ~ 2). Other assembly methods, specifically surfactant and block copolymer approaches, require the use of well-defined molecules or polymers with low polydispersities. This work demonstrates that it is possible to obtain ordered nanostructure from a random copolymer system.

2.4 Conclusion

A series of random copolymers of PBD and POSS bearing a polymerizable norbornene group was designed and successfully synthesized using ROMP copolymerization. The POSS loading in copolymers varies from 0 to 53 wt % and

molecular weights are in the range of M_w 67 to 88 kg/mol. The morphology of the copolymers has been characterized by WAXD, TEM, and SAXS. The results from WAXD show that the PBD-POSS copolymers have diffraction features of both POSS and PBD. In all the polymers, POSS maintain the same crystalline structures or hexagonal packing with 2θs of 8.3° (10.6 Å) and 11.1° (7.96 Å) associated with (101) and (110) diffraction planes. TEM results indicate that the copolymers assemble into small, randomly oriented lamellae with lateral dimensions of approximately 50 nm and thickness of 3-5 nm at low POSS concentration. These nanostructures extend to longer, continuous lamellar morphology with increasing POSS concentration. The spacing between lamellae can be changed by the relative ratio between POSS and PBD as shown with SAXS. The periodical spacing varies from 16 nm with 23 wt % POSS to 9.5 nm with 53 wt % POSS. All of these results clearly show the formation of self-assembled layered nanostructure of POSS aggregates. This design, based on associative interaction between POSS and limited crystal growth imposed by covalent attachment to a polymer backbone may open the door to the design of ordered polymer materials at nanometer length scales that are well beyond the length scales of the primary sequences.

2.5 References

(1) Whitesides, G. M.; Mathias, J. P.; Seto, C. T. *Science* **1991,** 254, (5036), 1312-1319.

(2) Ikkala, O.; ten Brinke, G. *Science* **2002,** 295, (5564), 2407-2409.

(3) Hartgerink, J. D.; Beniash, E.; Stupp, S. I. *Science* **2001,** 294, (5547), 1684-1688.

(4) Matsen, M. W.; Bates, F. S. *Macromolecules* **1996,** 29, (4), 1091-1098.

(5) Muthukumar, M.; Ober, C. K.; Thomas, E. L. *Science* **1997,** 277, (5330), 1225-1232.

(6) Aksay, I. A.; Trau, M.; Manne, S.; Honma, I.; Yao, N.; Zhou, L.; Fenter, P.; Eisenberger, P. M.; Gruner, S. M. *Science* **1996,** 273, (5277), 892-898.

(7) Yang, H.; Kuperman, A.; Coombs, N.; MamicheAfara, S.; Ozin, G. A. *Nature* **1996,** 379, (6567), 703-705.

(8) Lu, Y. F.; Ganguli, R.; Drewien, C. A.; Anderson, M. T.; Brinker, C. J.; Gong, W. L.; Guo, Y. X.; Soyez, H.; Dunn, B.; Huang, M. H.; Zink, J. I. *Nature* **1997,** 389, (6649), 364-368.

(9) Lichtenhan, J. D., Silsesquioxane-Based Polymers. In *Polymeric Materials Encyclopedia*, Salamone, J. C., Ed. CRC Press: Boca Raton: 1996; pp 7768-7777.

(10) Choi, J.; Harcup, J.; Yee, A. F.; Zhu, Q.; Laine, R. M. *J. Am. Chem. Soc.* **2001,** 123, (46), 11420-11430.

(11) Tamaki, R.; Tanaka, Y.; Asuncion, M. Z.; Choi, J.; Laine, R. M. *J. Am. Chem. Soc.* **2001,** 123, (49), 12416-12417.

(12) Cassagneau, T.; Caruso, F. *J. Am. Chem. Soc.* **2002,** 124, (27), 8172-8180.

(13) Tamaki, R.; Choi, J.; Laine, R. M. *Chem. Mater.* **2003,** 15, (3), 793-797.

(14) Lichtenhan, J. D.; Vu, N. Q.; Carter, J. A.; Gilman, J. W.; Feher, F. J. *Macromolecules* **1993,** 26, (8), 2141-2142.

(15) Lichtenhan, J. D.; Otonari, Y. A.; Carr, M. J. *Macromolecules* **1995,** 28, (24), 8435-8437.

(16) Haddad, T. S.; Lichtenhan, J. D. *Macromolecules* **1996,** 29, (22), 7302-7304.

(17) Tsuchida, A.; Bolln, C.; Sernetz, F. G.; Frey, H.; Mulhaupt, R. *Macromolecules* **1997,** 30, (10), 2818-2824.

(18) Lee, A.; Lichtenhan, J. D. *Macromolecules* **1998,** 31, (15), 4970-4974.

(19) Romo-Uribe, A.; Mather, P. T.; Haddad, T. S.; Lichtenhan, J. D. *J. Polym. Sci., Part B: Polym. Phys.* **1998,** 36, (11), 1857-1872.

(20) Schwab, J. J.; Lichtenhan, J. D. *Appl. Organometal. Chem.* **1998,** 12, (10-11), 707-713.

(21) Lee, A.; Lichtenhan, J. D. *J. Appl. Polym. Sci.* **1999,** 73, (10), 1993-2001.

(22) Mather, P. T.; Jeon, H. G.; Romo-Uribe, A.; Haddad, T. S.; Lichtenhan, J. D. *Macromolecus* **1999,** 32, (4), 1194-1203.

(23) Shockey, E. G.; Bolf, A. G.; Jones, P. F.; Schwab, J. J.; Chaffee, K. P.; Haddad, T. S.; Lichtenhan, J. D. *Appl. Organometal. Chem.* **1999,** 13, (4), 311-327.

(24) Fu, B. X.; Zhang, W. H.; Hsiao, B. S.; Rafailovich, M.; Sokolov, J.; Johansson, G.; Sauer, B. B.; Phillips, S.; Balnski, R. *High Perform. Polym.* **2000,** 12, (4), 565-571.

(25) Pyun, J.; Matyjaszewski, K. *Macromolecules* **2000,** 33, (1), 217-220.

(26) Costa, R. O. R.; Vasconcelos, W. L.; Tamaki, R.; Laine, R. M. *Macromolecules* **2001,** 34, (16), 5398-5407.

(27) Fu, B. X.; Hsiao, B. S.; Pagola, S.; Stephens, P.; White, H.; Rafailovich, M.; Sokolov, J.; Mather, P. T.; Jeon, H. G.; Phillips, S.; Lichtenhan, J.; Schwab, J. *Polymer* **2001,** 42, (2), 599-611.

(28) Li, G. Z.; Wang, L. C.; Toghiani, H.; Daulton, T. L.; Koyama, K.; Pittman, C. U. *Macromolecules* **2001,** 34, (25), 8686-8693.

(29) Zheng, L.; Farris, R. J.; Coughlin, E. B. *J. Polym. Sci., Part A: Polym. Chem.* **2001,** 39, 2920-2928.

(30) Zheng, L.; Farris, R. J.; Coughlin, E. B. *Macromolecules* **2001,** 34, (23), 8034-8039.

(31) Li, G. Z.; Wang, L.; Toghiani, H.; Daulton, T. L.; Pittman, C. U. *Polymer* **2002,** 43, (15), 4167-4176.

(32) Leu, C. M.; Chang, Y. T.; Wei, K. H. *Macromolecules* **2003,** 36, (24), 9122 - 9127.

(33) Pittman, C. U.; Li, G. Z.; Ni, H. L. *Macromol. Symp.* **2003,** 196, 301-325.

(34) Barry, A. J.; Daudt, W. H.; Domicone, J. J.; Gilkey, J. W. *J. Am. Chem. Soc.* **1955,** 77, 4248-4252.

(35) Larsson, K. *Ark. Kemi* **1960,** 16, 203-28.

(36) Larsson, K. *Ark. Kemi* **1960,** 16, 209-214.

(37) Larsson, K. *Ark. Kemi* **1960,** 16, 215-219.

(38) Auf der Heyde, T. P. E.; Burgi, H.-B.; Burgy, H.; Tornroos, K. W. *Chimia* **1991,** 45, 38-40.

(39) Zheng, L.; Waddon, A. J.; Farris, R. J.; : Coughlin, E. B. *Macromolecules* **2002,** 35, 2375-2379.

(40) Waddon, A. J.; Coughlin, E. B. *Chem. Mat.* **2003,** 15, (24), 4555-4561.

(41) Waddon, A. J.; Zheng, L.; Farris, R. J.; Coughlin, E. B. *Nano Letters* **2002,** 2, (10), 1149-1155.

(42) Schwab, P.; Grubbs, R. H.; Ziller, J. W. *J. Am. Chem. Soc.* **1996,** 118, (1), 100-110.

(43) Gonzalez, R. I.; Phillips, S. H.; Hoflund, G. B. *J. Spacecraft and Rockets.* **2000,** 37, 463-467.

(44) Kojima, Y.; Usuki, A.; Kawasumi, M.; Okada, A.; Kurauchi, T.; Kamigaito, O. *J. Polym. Sci., Part A: Polym. Chem.* **1993,** 31, (4), 983-986.

(45) Zhang, Z. L.; Horsch, M. A.; Lamm, M. H.; Glotzer, S. C. *Nano Letters* **2003,** 3, (10), 1341-1346.

(46) Giannelis, E. P. *Adv. Mater.* **1996,** 8, (1), 29-35.

(47) Pinnavaia, T. J.; Beal, G. W., *Polymer Clay Nanocomposites*. John Wiley & Sons: New York: 2001.

CHAPTER 3

TELECHELIC POLYSTYRENE-POSS COPOLYMERS AS MODEL SYSTEMS FOR THE STUDY OF WELL-DEFINED ORGANIC-INORGANIC HYBRID MATERIALS

3.1 Introduction

The combination of different inorganic additives and organic polymers, in conjunction with the appropriate processing methods, can produce hybrid materials with new properties for electrical, optical, structural or related applications.[1-3] Typically, properties such as the glass transition temperature, T_g, melting point, and stress-strain behavior or microphase separation can be altered by introducing an inorganic component into an organic polymer matrix.[4, 5] Layered organic/inorganic nanocomposites[6] and silica gel-derived hybrids[7, 8] are but two examples of organic/inorganic composites. In what is commonly called the "top-down" approach the various components are combined together with mechanical work and/or thermal energy. Blended systems suffer from a lack of further processability and control due to difficulties with dispersion of the inorganic component. On the other hand, systems such as silica gel-derived hybrids are a result of post-polymerization formation of a network that is a function of pH of the solution or the structure of the precursor. This methodology gives rise to hybrid organic/inorganic polymers which can conveniently be used for membrane or coating applications.[8] Nonetheless, the final inorganic structure is poorly defined due to the randomness of the network crosslink formation. These two approaches, component blending or post reaction crosslinking, are the most

commonly taken to prepare hybrid organic-inorganic systems. Both approaches suffer from a lack of control over the microstructure giving rise to an "ill-defined" material.

An alternative approach to generating organic/inorganic hybrid structures would be to start at the molecular level using well-defined building blocks. Relatively few studies detailing the synthesis and characterization of controlled architectures using this concept have been completed.[9-15] Expanding the scope of novel hybrid materials is of interest not only for the standpoint of the overall synthetic challenge but also critical in order to validate the self-assembly properties predicted from computational investigations.[16-18] The use of anionic polymerization to produce well-defined organic-inorganic hybrid structures has not yet been fully investigated. The synthetic utility of anionic polymerization is well documented for the synthesis of organic block copolymers.[19] Replacement of one of the organic domains in a block copolymer architecture with a well defined inorganic moiety presents the opportunity to compare, or contrast, the new hybrid copolymers obtained with their conventional organic counterparts. New chemical and physical properties are likely to be found from the resultant hybrid copolymers.

Polyhedral oligomeric silsesquioxanes (POSS) are inorganic nanosized particles, and are potential candidates to control microstructure. These building blocks are of particular interest due to its molecularly precise structure as well as its solubility in common organic solvents.[20, 21] Experimental protocols have been developed over the last 40 years so as to have good yield and control over the structure of the POSS macromer. The so-called T_8 POSS series has a cubic core with eight silicon atoms at each corner and an oxygen bridge between each silicon atom. Seven silicon atoms bear

an organic group that provides solubility, and a reactive group is generally attached to the 8th silicon atom. It is possible to incorporate this ~1.5 nm diameter macromonomer into organic polymers. Random copolymers incorporating POSS have been prepared that are either thermosets or thermoplatics.[22-32] These represent a category of new hybrid polymers with a tremendous technological potential.[2, 33] Control over the placement of the POSS within an organic polymer is possible using living/controlled polymerization methodologies. Matyjaszweski[9, 10, 34] has incorporated the POSS inorganic particle into both linear and star systems using ATRP. Amphiphilic telechelic polymers having a poly(ethylene oxide) backbone and POSS endgroups have been independently prepared by Mather and Frey.[12, 35]

3.2 Experimental Section

3.2.1 Materials

Styrene (99+%), ethylene oxide (99.5%), dibutyltin dilaurate (95%, DBTDL), *sec*-butyl lithium (1.6M in hexanes) were purchased from Aldrich Chemical Co. Toluene and benzene were purchased from Fisher. 1-[isocyanotopropyldimethylsilyl]-3,5,7,9,11,13,15-hepacyclopentylpentacyclo [9.5.1.1^{3,9}.1^{5,15}.1^{7,13}] octasiloxane (POSS) (**1**) was supplied by Hybrid Plastics, Inc. Styrene was distilled from calcium hydride, and benzene and toluene were purified using a mixture of sodium and benzophenone. Ethylene oxide was passed through a magnesium sulfate column prior to use.

3.2.2 Synthesis of Hydroxy-Terminated Polystyrene

The amount of initiator with respect to the amount of monomer is controlled so that the resulting molecular weight of the polymer is predictable. To obtain **PSOH-1**, 5

ml (43.6mmol) of styrene purified over CaH_2 were added to 50 ml of benzene. The solution was titrated with *sec*-BuLi until a faint yellow color appeared, then 3.4 ml (5.45 mmol) of *sec*-BuLi were added. A bright red color appeared and stayed throughout the reaction. The reaction was run under nitrogen at room temperature for 3 hours. Ethylene oxide was bubbled into the solution until the disappearance of the red color was observed. The polymer was precipitated in acidic methanol, dissolved in chloroform, and precipitated in methanol. The chloroform removed any trace of benzene left in the polymer. The polymer was then vacuum-dried overnight at room temperature. Unusually low polydispersities for polymers made by anionic polymerization under inert atmosphere are obtained due to measurement after purification. Lower molecular weight molecules are removed during the precipitation.

3.2.3 Synthesis of Hybrid Hemitelechelic Polystyrene-POSS

In 25 ml of toluene, 0.25g (0.28mmol) of hydroxy-terminated polystyrene (**PSOH-1**) was mixed with 0.306g (0.28mmol) of **CpPOSS-NCO**. DBTDL was added to the solution (1%wt with respect to the reactants). The solution was heated to 90°C and held at this temperature overnight under a nitrogen purge. The product was precipitated in cold methanol and vacuum-dried overnight. The same procedure was followed for each sample. A stoichiometric amount of **CpPOSS-NCO** and hydroxy-terminated polystyrene was used. Within the resolution limit of the GPC, no starting material was found after the reaction reached completion.

3.2.4 Polymer Characterization

3.2.4.1 GPC

Gel permeation chromatography (GPC) measurements were performed in tetrahydrofuran (THF) at 1.0 mL/min using a Knauer K-501 Pump with a K-2301 refractive index detector and K-2600 UV detector, and a column bank consisting of two Polymer Labs PLGel Mixed D columns and one PLGel 50 A column (1.5 x 30 cm) at 35°C. Molecular weights are reported relative to polystyrene standards.

3.2.4.2 NMR

^{1}H spectra were obtained at room temperature in chloroform-*d* at 300 MHz using a Bruker DPX-300 FT-NMR spectrometer. ^{13}C NMR spectra were recorded at room temperature in chloroform-*d* with a Bruker DPX-300 FT-NMR spectrometer operating at 75 MHz.

3.2.4.3 Thermal Analysis

Differential scanning calorimetry (DSC) was performed under a continuous nitrogen purge using a Mettler-Toledo DSC 822^{e}. Octane (Aldrich, 99%+), pentane (Aldrich, 99%+), deionized water, indium and zinc were used to perform the calibration. Samples having a mass between 2.5-11mg were used. Data was gathered using a scan rate of 10 °C/min on the second scan. Thermogravimetric analysis (TGA) was carried out using a TA Instruments TGA 2950 thermogravimetric analyzer with a heating rate of 20 °C/min from room temperature to 700 °C under a continuous nitrogen or air purge (40 mL/min for both air and nitrogen).

3.2.4.4 WAXS

Diffractometry was carried out on a Siemens D500 instrument in normal/transmission mode (0.3 incident slit beam divergence) with Ni-filtered Cu K_α radiation (1.54 Å wavelength).

3.2.4.5 SAXS

The small-angle x-ray scattering measurements were performed at beamline 15ID-D (ChemMatCARS) in the Advanced Photon Source (APS) at Argonne National Laboratory. The energy of radiation used for the experiments was 8.27 keV ($\Delta E/E \sim 10\text{-}4$), which corresponds to an X-ray wavelength of 1.50 Å. SAXS images were collected using a two-dimensional Bruker 6000 CCD X-ray detector with a 1024 x 1024 pixel array covering a 94 x 94 mm area. The sample to detector distance was 1.90 m and was calibrated using silver behenate. Each 2-D image was taken using a 10 second exposure time, and the images were integrated azimuthally to obtain a 1-D SAXS profile.

The PS-POSS and PS-OH samples were molded into 8 mm discs of 1 mm thickness. **PS-POSS-1** was annealed at 60°C for 20 min. **PS-POSS-4** and **PS-POSS-7** were annealed at 110°C for 20 min. The samples were mounted in a metal holder and placed in an electric heating cell. The samples were secured by a Kapton film and the heating cell had two Kapton windows in order to enclose the environment with minimal beam attenuation. A blank image with all of the Kapton layers was taken and subtracted form the final PS-POSS samples.

3.2.4.6 FT-IR

Fourier transform infrared (FT-IR) spectra were recorded using a Perkin-Elmer Spectrum 2000 system at room temperature. A total of 16 scans were performed and the spectral resolution was 4 cm^{-1}. Data analysis was performed using Spectrum 2000 software. Pellets were prepared from pressing a mixture of ground polymer and KBr.

3.3 Results and Discussion

3.3.1 Synthesis

The tethering of POSS to an anionically-synthesized polymer will extend the range of materials as well as the morphologies that can be achieved. The living anionic synthesis of hydroxyl-terminated polystyrene has been described in the literature.[36-38] The molecular weight range of the hydroxyl-terminated polystyrene samples was chosen so that the radius of gyration of the polymer was comparable to that of the POSS particle.[39, 40] Polystyrene chains with a number average molecular weight, M_n, of 900 g/mol and 16,000g/mol have radii of gyration of 8.5Å and 34Å, respectively, versus a radius of approximately 7.5Å for the POSS particle. Tethering of the isocyanate modified POSS particle (**CpPOSS-NCO**) to the polystyrene chains was achieved through the formation of a urethane linkage, Figure 3.1. The syntheses of amphiphilic telechelic polymers having a poly(ethylene oxide) backbone and POSS endgroups is straightforward as the purification of the final product can be achieved based on solubility differences of the reagents. In our case an efficient, highly yielding coupling reaction must be used due to the comparable solubility of POSS and polystyrene in common organic solvents.

To avoid extensive purification, an equimolar amount of **CpPOSS-NCO** with respect to the hydroxyl-terminated polystyrene was used in the urethane formation chemistry. Urethane formation was promoted by the use of dibutyltin dilaurate at 90 °C in toluene solution.

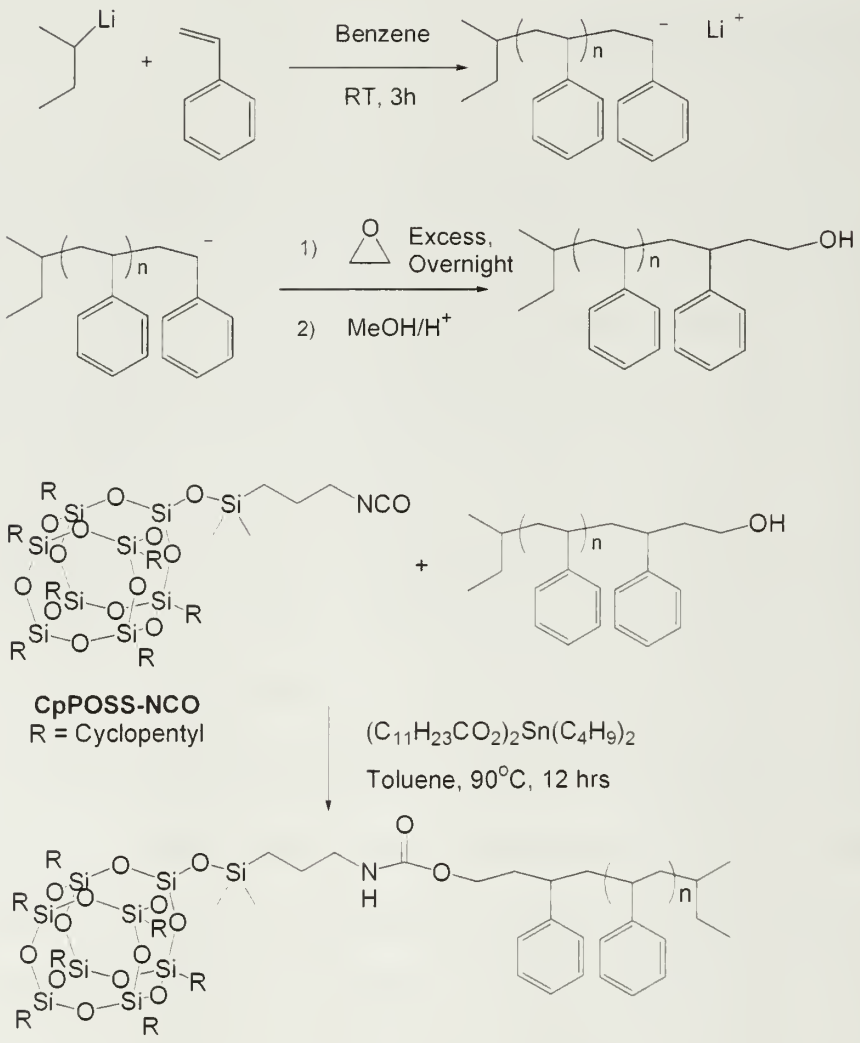

Figure 3.1 Synthesis of Hemi-Telechelic Polystyrene-POSS Hybrids

A representative synthesis of the hemi-telelchelic hybrids is the conversion of hydroxyl terminated polystyrene **PSOH-4**, M_n and PDI of 4890 g/mol and 1.11, to **PS-**

POSS-4 with a M_n and PDI of 6040 g/mol and 1.06, respectively (Entry 4 Table 3.1). The increase in molecular weight is as expected for all samples given the molar mass of **CpPOSS-NCO** (1058.56 g/mol). The retention of the narrow molecular weight distribution indicates the absence of side-reactions. Figure 3.2. An equimolar amount of polystyrene and **CpPOSS-NCO** was used and no residual starting material is seen within the resolution limit of the GPC confirming that the coupling reaction goes to completion.

Table 3.1 Molecular Weights and Polydispersities of Hydroxyl-Terminated Polystyrene Precursors and the PS-POSS Hybrids.

Entry	Sample	M_n (GPC)	PDI	T_g (°C)	Sample	M_n (GPC)	PDI	T_g (°C)
1	**PSOH-1**	873	1.11	47	**PS-POSS-1**	1.91E+03	1.07	64
2	**PSOH-2**	2.03E+03	1.11	79	**PS-POSS-2**	3.17E+03	1.11	78
3	**PSOH-3**	2.53E+03	1.11	77	**PS-POSS-3**	2.79E+03	1.12	75
4	**PSOH-4**	4.89E+03	1.11	91	**PS-POSS-4**	6.04E+03	1.06	92
5	**PSOH-5**	8.47E+03	1.05	98	**PS-POSS-5**	9.60E+03	1.06	99
6	**PSOH-6**	1.10E+04	1.06	104	**PS-POSS-6**	1.12E+04	1.07	103
7	**PSOH-7**	1.65E+04	1.06	106	**PS-POSS-7**	1.69E+04	1.06	104

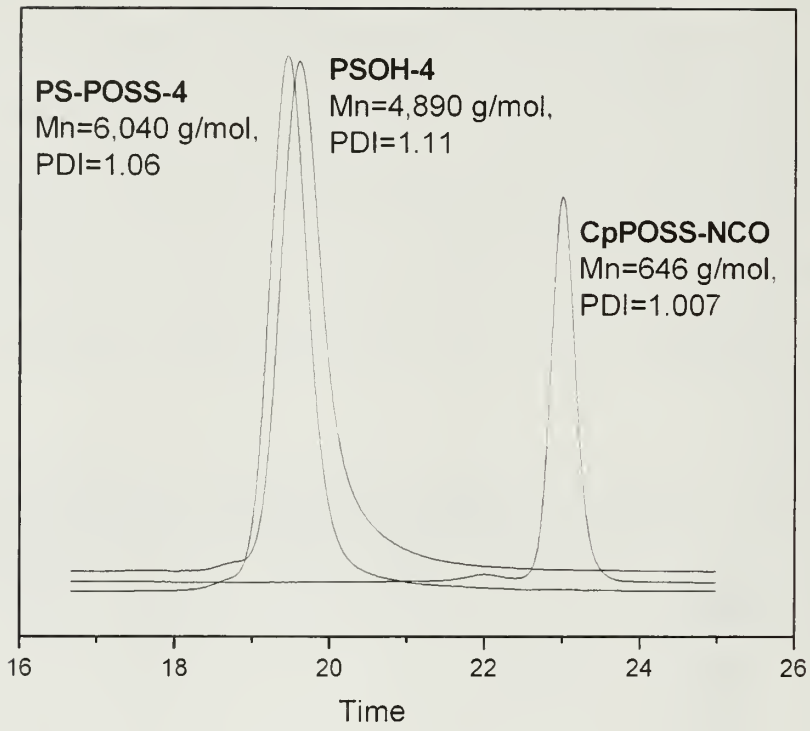

Figure 3.2 Overlays of the Gel Permeation Chromatograms for the Experiments in Entry 4 of Table 3.1.

3.3.2 NMR

The exclusive formation of the expected product can be observed by comparison of the ^{1}H NMR spectra of the two starting materials and the final product (Figure 3.3). The methylene protons α to the hydroxyl group of the PSOH shift downfield from δ 3.25 ppm to δ 3.67 ppm upon reaction. The corresponding methylene protons α to the isocyanate group in POSS shift upfield from δ 3.26 ppm to δ 3.02 ppm. The newly formed urethane N-H signal appears at δ 4.38 ppm. Integration confirms that there is one molecule of POSS per polystyrene chain. Similar conclusions are drawn from the ^{13}C NMR (Figure 3.4).

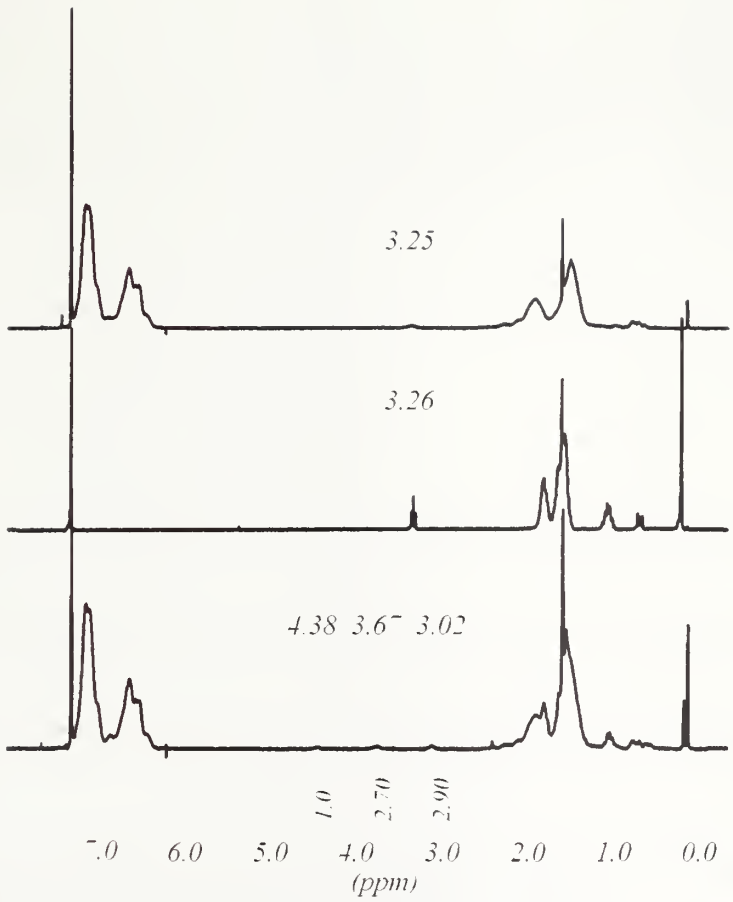

Figure 3.3 ^{1}H NMR Spectra of Hydroxyl Polystyrene PSOH-4 (Top), CpPOSS-NCO (Middle) and Hemitelechelic PS-POSS-4 (Bottom).

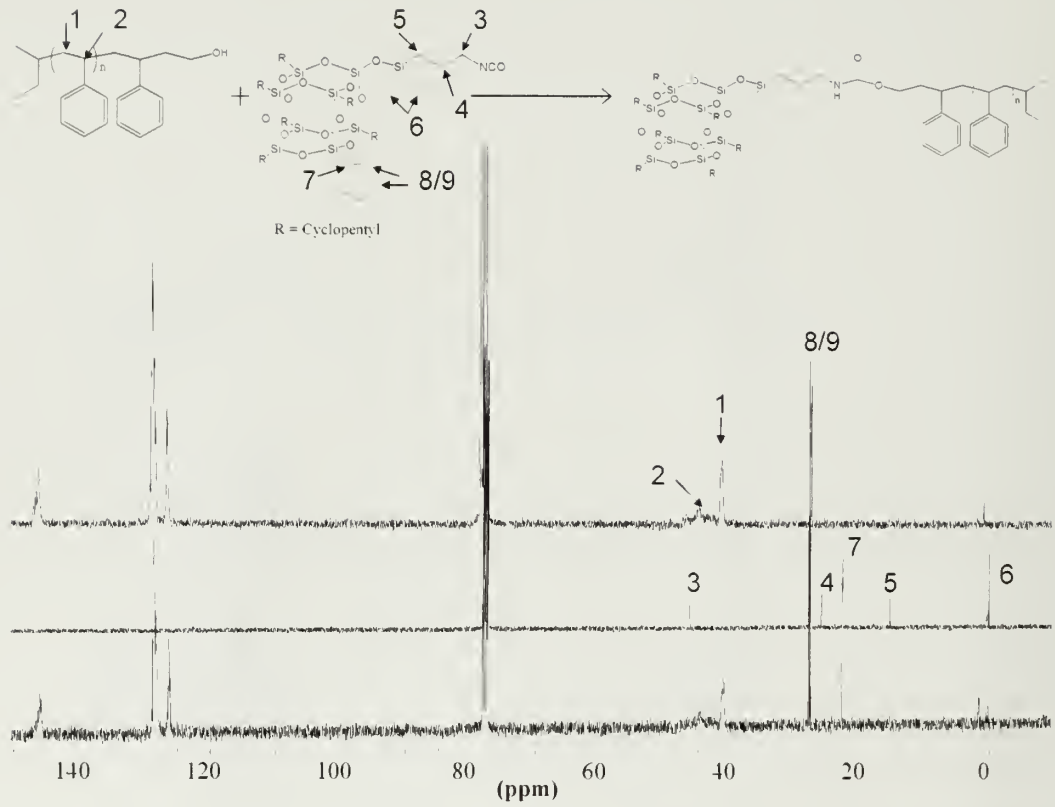

Figure 3.4 ^{13}C NMR: Hydroxyl Polystyrene PSOH-4 (Top), CpPOSS-NCO (Middle) and Hemitelechelic PS-POSS-4 (Bottom).

3.3.3 FT-IR

The FT-IR spectrum (Figure 3.5) confirmed the formation of the urethane linkage as shown by the N-H stretching absorption band at 3300 cm^{-1} and a carbonyl stretching absorption band at 1728 cm^{-1}. The isocyanate and terminal hydroxyl group absorption bands at 2272 cm^{-1} and 3400 cm^{-1} of the two starting materials respectively have disappeared. Upon heating, the N-H adsorption band intensity does not change, implying that no interchain hydrogen bonding is taking place between the urethane linkages. Thus any resultant morphology will not be dictated by hydrogen bonding in these hybrid hemi-telechelic PS-POSS polymers.

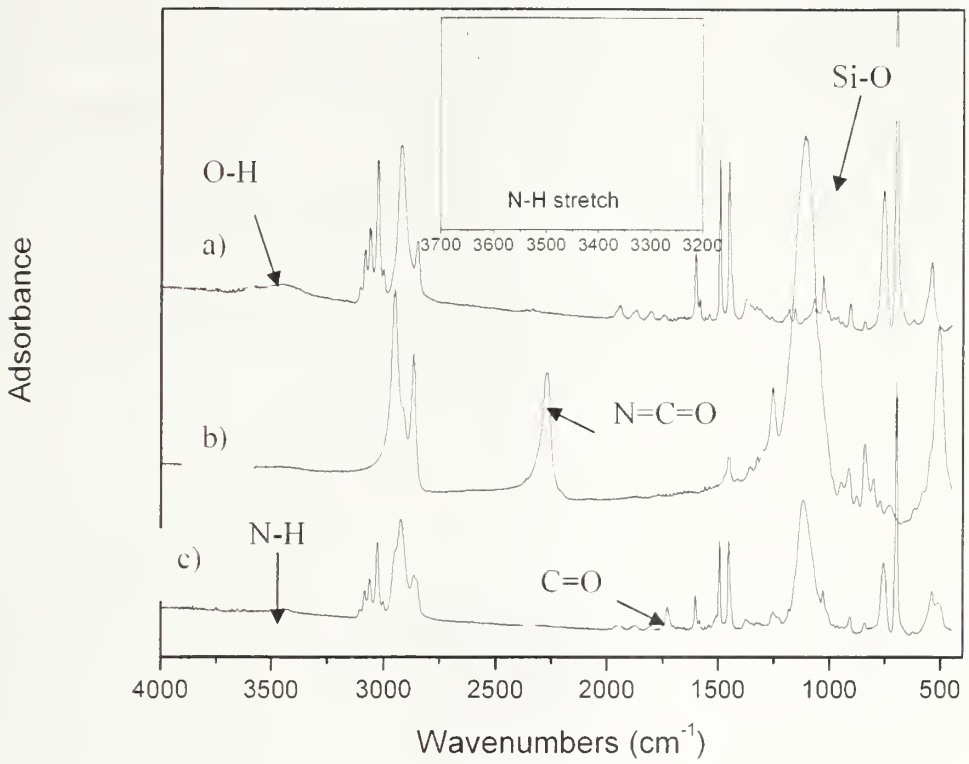

Figure 3.5 FTIR of (a) PSOH-4, (b) CpPOSS-NCO and (c) PS-POSS-4.

3.3.4 Thermal Characterization

An increase in the char yield under both air and nitrogen atmospheres is observed by TGA for **PS-POSS-4** hybrids compared to the **PSOH-4** analogs (Figure 3.6). The decomposition temperature is slightly higher for the hybrid hemitelechelic polymer than for **CpPOSS-NCO** itself. A difference is exhibited between the trace of PS-POSS under air and nitrogen atmosphere. Under nitrogen purge PSOH is observed to be more stable than PS-POSS due to the chemical linkage between the polystyrene and the POSS moiety. The linkage contains -$NHCO_2$-, which is an easily cleavable functional group. Under air purge (Figure 3.7), **PS-POSS-4** is more stable than **PSOH-4**. It is assumed that POSS decomposes in air by forming a silica-like layer, which

protects the bulk material from further oxidation.[30] On Figure 3.6 and 3.7, the line at Y = 9.5% corresponds to the mass of a POSS cage converted into silica. It can be seen that the char yield in Figure 3.6 is lower than 9.5%. Under air atmosphere, the POSS cube is totally converted into silica giving a char yield equal to 9.5%.

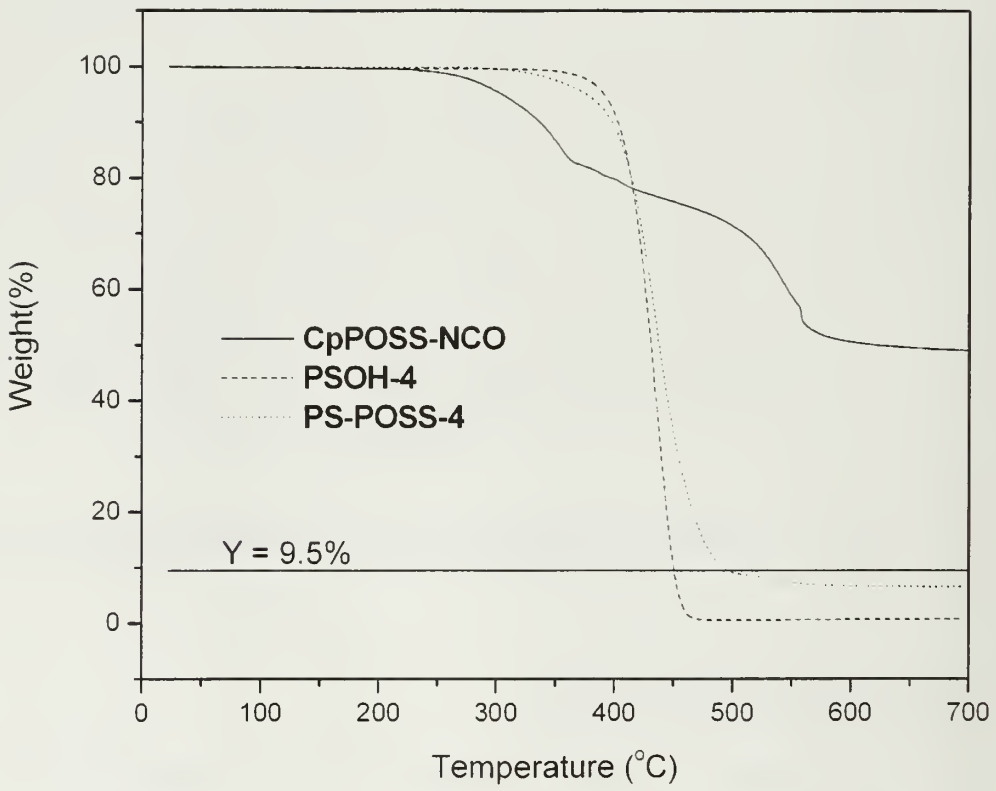

Figure 3.6 TGA of PSOH-4 and POSS-PS-4 Under N_2 Atmosphere

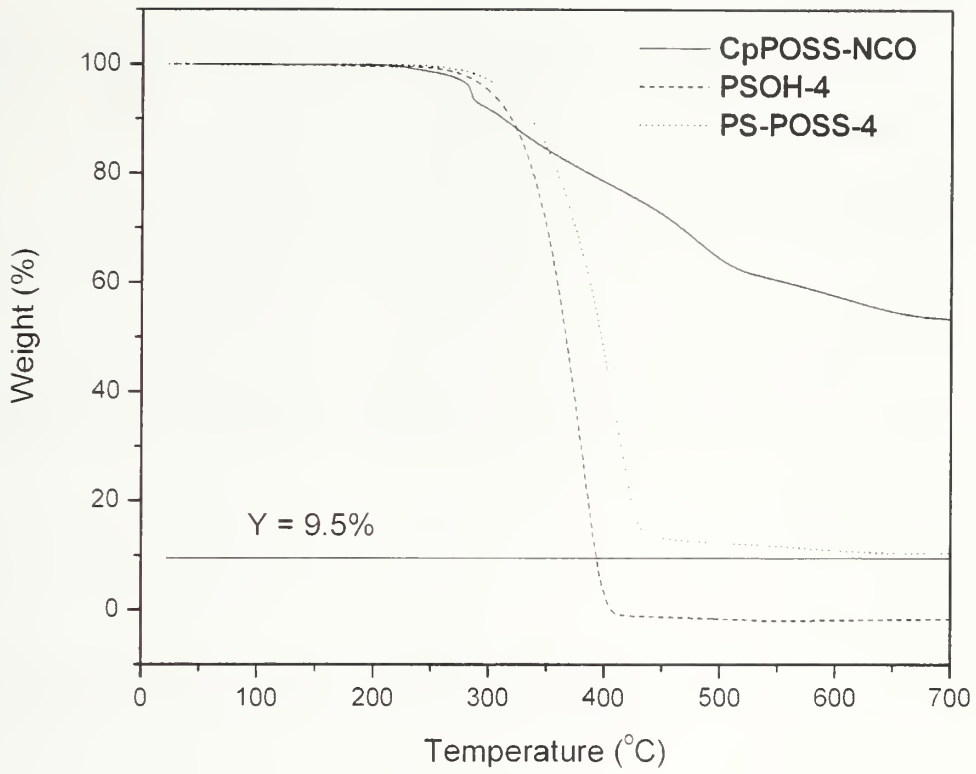

Figure 3.7 TGA of PSOH-4 and PS-POSS-4 Under Air Atmosphere

The glass transition temperature (Table 3.1) for the hydroxyl-terminated polystyrene oligomers was found to be dependent on molecular weight. The T_g varies from 47.2°C for the lowest molecular weight oligomer (**PSOH-1**) to 105.7°C for the 16.500 g/mol sample (**PSOH-7**). No difference in T_g can be observed for the corresponding PS-POSS hybrid hemi-telechelics when compared to their PS analogs, with the exception of **PSOH-1** and **PS-POSS-1**. The presence of POSS tethered at the end of the polystyrene chain does not alter the T_g, suggesting that the POSS moieties and polystyrene chains are secluded from each for the higher molecular weight samples. In the case of the shortest polystyrene chain the large molar mass of POSS is apparently sufficient to raise the T_g by 17 °C.

3.3.5 WAXS

An increase in the aggregate size of POSS domains is observed by WAXS with an increase of the weight percent of POSS (Figure 3.8). The main diffraction peak for the POSS monomer, observed at $2\theta = 8.6°$ corresponding to d spacing of ~10.8Å, increases with the weigh percent of POSS. The width of this peak indicates that the size of the aggregates is fairly small, only a few POSS cubes per aggregates. The aggregation diminishes, and perhaps is completely suppressed, as the polystyrene chain length increases.

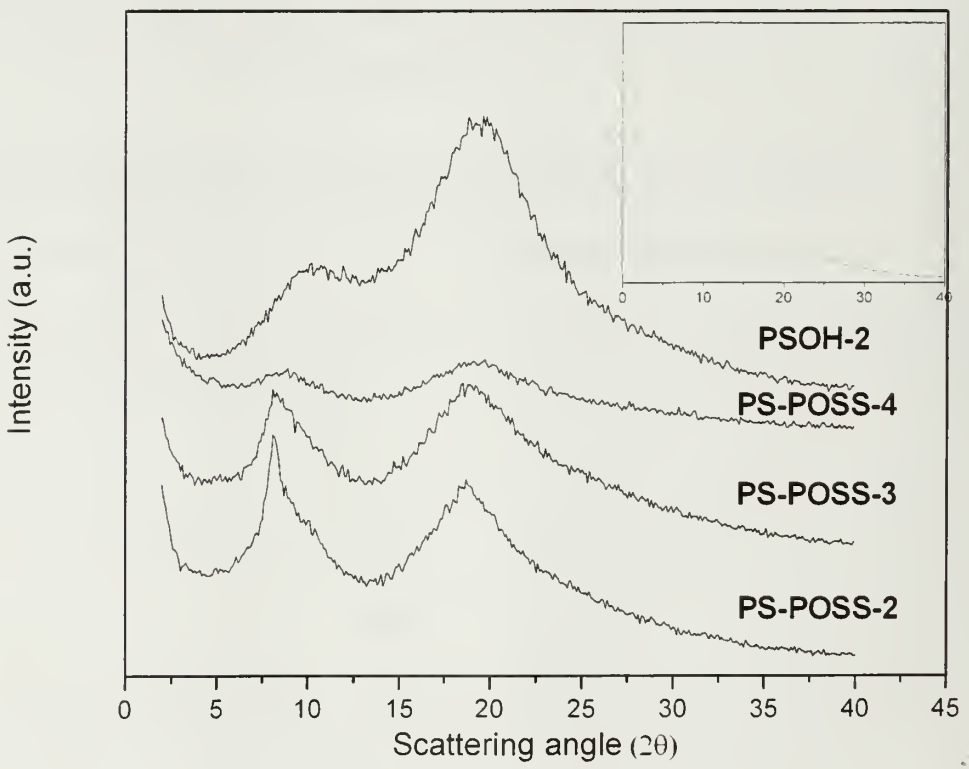

Figure 3.8 WAXS Profile of the Hybrid Polymer PS-POSS. Inset: WAXS Profile of CpPOSS-NCO.

3.3.6 SAXS

Studying a series of PS-POSS samples in SAXS enables to gain insight into the nanoscopic organization of the materials. **PS-POSS-4** and **PS-POSS-7** do not show any signal in SAXS. SAXS of **PS-POSS-1**, on the other hand, shows a diffraction pattern with a first and a second order peak. The first order peak is found at q = 0.0769 $Å^{-1}$ which correspond to a long period L = 8.17 nm. The long period found here is equal to approximately two times the radius of gyration of a polystyrene polymer with M_n = 900 g/mol.[39, 40] From these dimensional considerations, a plausible model for the organization of the hemi-telechelic PS-POSS polymer would be a head-to-head and tail-to-tail aggregation. The second order peak is a proof of the mesoscopic organization of the system. SAXS measurements of **PS-POSS-1** were carried at 60°C, above the T_g of the polymer. An equilibrium state in the liquid phase was obtained that way.

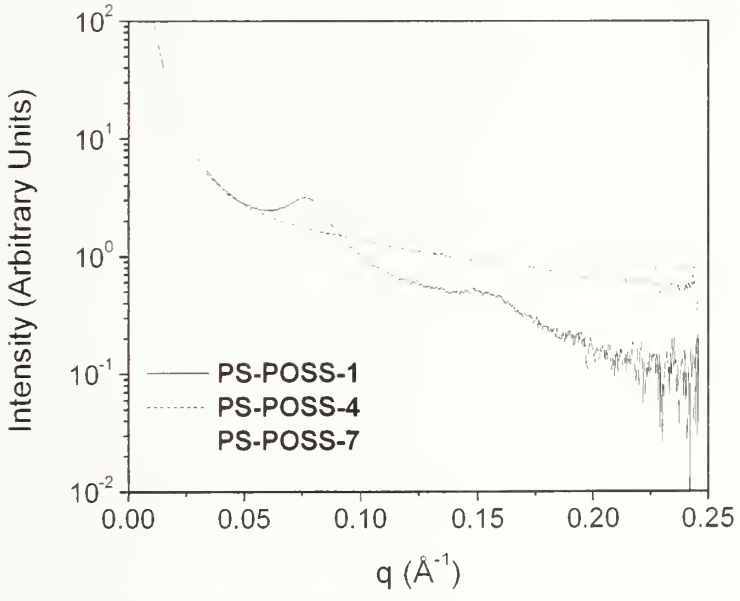

Figure 3.9 SAXS of PS-POSS Series

3.4 Conclusion

In summary, a synthetic protocol for preparing well-defined POSS-polystyrene hemi-telechelic hybrids has been developed. These model systems provided an experimental opportunity to probe the ordering, or aggregation behavior, of inorganic nanoparticles within polymeric matrices. Furthermore, the versatility of the chemistry used provides an extension of traditional block copolymers currently available for study to include organic-inorganic block copolymers.

3.5 References

(1) Kickelbick, G. *Prog. Polym. Sci.* **2003,** 28, (1), 83-114.

(2) Gonsalves, K. E.; Merhari, L.; Wu, H. P.; Hu, Y. Q. *Adv. Mater.* **2001,** 13, (10), 703-714.

(3) Barton, T. J.; Bull, L. M.; Klemperer, W. G.; Loy, D. A.; McEnaney, B.; Misono, M.; Monson, P. A.; Pez, G.; Scherer, G. W.; Vartuli, J. C.; Yaghi, O. M. *Chem. Mater.* **1999,** 11, (10), 2633-2656.

(4) Pinnavaia, T. J.; Beal, G. W.. *Polymer Clay Nanocomposites*. John Wiley & Son: New York, 2001.

(5) Kojima, Y.; Usuki, A.; Kawasumi, M.; Okada, A.; Kurauchi, T.; Kamigaito, O. *J. Polym. Sci., Part A: Polym. Chem.* **1993,** 31, (4), 983-986.

(6) Giannelis, E. P. *Adv. Mater.* **1996,** 8, (1), 29-35.

(7) Corriu, R. J. P. *Angew. Chem., Int. Ed. Engl.* **2000,** 39, (8), 1376-1398.

(8) Wen, J. Y.; Wilkes, G. L. *Chem. Mater.* **1996,** 8, (8), 1667-1681.

(9) Pyun, J.; Matyjaszewski, K.; Wu, J.; Kim, G. M.; Chun, S. B.; Mather, P. T. *Polymer* **2003,** 44, (9), 2739-2750.

(10) Pyun, J.; Matyjaseweski, K. *Macromolecules* **1999,** 33, 217-220.

(11) Pyun, J.; Miller, P. J.; Matyjaszewski, K. *Abstracts of Papers of the American Chemical Society* **2000,** 219, U390-U390.

(12) Kim, B. S.; Mather, P. T. *Macromolecules* **2002,** 35, (22), 8378-8384.

(13) Riggs, J. E.; Guo, Z. X.; Carroll, D. L.; Sun, Y. P. *J. Am. Chem. Soc* **2000,** 122, (24), 5879-5880.

(14) Song, T.; Dai, S.; Tam, K. C.; Lee, S. Y.; Goh, S. H. *Langmuir* **2003,** 19, (11), 4798-4803.

(15) Song, T.; Dai, S.; Tam, K. C.; Lee, S. Y.; Goh, S. H. *Polymer* **2003,** 44, (8), 2529-2536.

(16) Zhang, Z. L.; Horsch, M. A.; Lamm, M. H.; Glotzer, S. C. *Nano Lett.* **2003,** 3, (10), 1341-1346.

(17) Thompson, R. B.; Ginzburg, V. V.; Matsen, M. W.; Balazs, A. C. *Science* **2001,** 292, (5526), 2469-2472.

(18) Lamm, M. H.; Chen, T.; Glotzer, S. C. *Nano Lett.* **2003,** 3, (8), 989-994.

(19) Hadjichristidis, N.; Pitsikalis, M.; Pispas, S.; Iatrou, H. *Chem. Rev.* **2001,** 101, (12), 3747-3792.

(20) Brown, J. F.; Vogt, L. H. *J. Am. Chem. Soc.* **1965,** 87, 4313-4317.

(21) Voronkov, M. G.; Lavrent'yev, V. I., Polyhedral Oligosilsesqioxanes and Their Homo Derivatives. In *Top. Curr. Chem.*, Boschke, F. L., Ed. Springer-Verlag: Berlin, 1982; Vol. 102, pp 199-236.

(22) Lee, A.; Lichtenhan, J. D. *J. Appl. Polym. Sci.* **1999,** 73, (10), 1993-2001.

(23) Shockey, E. G.; Bolf, A. G.; Jones, P. F.; Schwab, J. J.; Chaffee, K. P.; Haddad, T. S.; Lichtenhan, J. D. *Appl. Organometal. Chem.* **1999,** 13, (4), 311-327.

(24) Lichtenhan, J. D.; Otonari, Y. A.; Carr, M. J. *Macromolecules* **1995,** 28, (24), 8435-8437.

(25) Haddad, T. S.; Viers, B. D.; Phillips, S. H. *Journal of Inorganic and Organometallic Polymers* **2001,** 11, (3), 155-164.

(26) Romo-Uribe, A.; Mather, P. T.; Haddad, T. S.; Lichtenhan, J. D. *J. Polym. Sci., Part B: Polym. Phys.* **1998,** 36, (11), 1857-1872.

(27) Lee, A.; Lichtenhan, J. D. *Macromolecules* **1998,** 31, (15), 4970-4974.

(28) Mather, P. T.; Jeon, H. G.; Romo-Uribe, A.; Haddad, T. S.; Lichtenhan, J. D. *Macromolecus* **1999,** 32, (4), 1194-1203.

(29) Costa, R. O. R.; Vasconcelos, W. L.; Tamaki, R.; Laine, R. M. *Macromolecules* **2001,** 34, (16), 5398-5407.

(30) Zheng, L.; Farris, R. J.; Coughlin, E. B. *J. Polym. Sci., Part A: Polym. Chem.* **2001,** 39, 2920-2928.

(31) Zheng, L.; Kasi, R. M.; Farris, R. J.; Coughlin, E. B. *J. Polym. Sci., Part A: Polym. Chem.* **2002,** 40, (7), 885-891.

(32) Liu, H. Z.; Zhang, W.; Zheng, S. X. *Polymer* **2005,** 46, (1), 157-165.

(33) Xiao, S.; Nguyen, M.; Gong, X.; Cao, Y.; Wu, H. B.; Moses, D.; Heeger, A. J. *Advanced Functional Materials* **2003,** 13, (1), 25-29.

(34) Miller, P. J.; Kickelbick, G.; Nakagawa, Y.; Diamanti, S.; Pacis, C.; Matyjaszewski, K. *Abstracts of Papers of the American Chemical Society* **1998,** 215, U394-U395.

(35) Knischka, R.; Dietsche, F.; Hanselmann, R.; Frey, H.; Mulhaupt, R.; Lutz, P. J. *Langmuir* **1999,** 15, (14), 4752-4756.

(36) Morton, M.; Fetters, L. J. *Rubber Chem. Technol.* **1974,** 48, 359.

(37) Quirk, R. P.; Ma, J. J. *J. Polym. Sci., Part A: Polym. Chem.* **1988,** 26, (8), 2031-2037.

(38) Hadjichristidis, N.; Iatrou, H.; Pispas, S.; Pitsikalis, M. *J. Polym. Sci., Part A: Polym. Chem.* **2000,** 38, (18), 3211-3234.

(39) Ballard, D. G. H.; Wignall, G. D.; Schelten, J. *Eur. Polym. J.* **1973,** 9, (9), 965-969.

(40) Wignall, G. D.; Ballard, D. G. H.; Schelten, J. *Eur. Polym. J.* **1974,** 10, (9), 861-865.

CHAPTER 4

MODEL ORGANIC-INORGANIC HYBRID DIBLOCK COPOLYMERS BASED ON POSS FOR THE ORDERING OF SILICA PRECURSOR VIA SELF-ASSEMBLY

4.1 Introduction

Hybrid organic-inorganic materials have attracted considerable interest over the past few years.[1-3] The ability to combine physical properties of organic and inorganic matter in the same material opens up avenues toward the development of new hybrid functional organic-inorganic nanocomposites. One of the driving forces for the synthesis of new hybrid organic inorganic materials is their use in an increasing number of state-of-the art applications. Hybrid organic-inorganic materials have been successfully used for protective and decorative coatings,[4] microelectronics,[5] photovoltaic cell applications [6] and optics.[7]

Due to the inherent incompatibility between organic and inorganic materials, various synthetic strategies were developed to enable the fabrication of such hybrid materials.[8] Numerous theoretical studies on hybrid organic inorganic materials have been conducted and showed a very promising potential for the self-assembly of such materials.[9-11] From an experimental standpoint, either a "bottom-up" or a "top-down" approach can be used to synthesize hybrid organic-inorganic materials. Clay nanocomposites are a typical example of a "top-down" strategy in which the incompatibility between the organic and the inorganic counterpart is overcome by using an external source of energy such as heat or mechanical work.[12] The "bottom-up" strategy utilizes molecular precursor that can generate a hybrid organic-inorganic

material upon chemical reaction. Successful examples of this strategy include sol-gel chemistry in which a metal alkoxides are hydrolyzed forming so-called "oxo-polymers".[13] Although very successful at combining organic and inorganic matter in the same material, conventional sol-gel chemistry does not enable control over the material at a mesoscopic level that is at a length scale of tens to hundreds of nanometers. Long-range order of hybrid organic-inorganic materials is critical to enable applications such as catalysis, membrane and separation technology and molecular engineering.[14] A typical approach to address this challenge is the use of organic structures formed through self-assembly as structure-directing agents.[15] Low molecular weight surfactants and amphiphilic block copolymers have been used to achieve this goal. Specifically, Wiesner et al. have developed a strategy in which an amphiphilic poly(isoprene-*b*-ethylene oxide) block copolymer is used as a template-directing agent for two metal alkoxides, (3-glycidyloxypropyl-) trimethoxysilane and aluminum *sec*-butoxide.[16] The metal alkoxides segregate preferentially within the polyethylene oxide block, mimicking its microstructure and upon hydrolytic condensation spheres, cylinders and lamellae of inorganic materials in an organic matrix were obtained. A drawback of this method is the fact that there is little control over the structure of the hybrid material at a molecular level. An alternative approach consists in utilizing a well-defined inorganic building block and incorporating it into an organic matrix. In this chapter, we describe the use of POSS as a nanoscopic inorganic building block incorporated in a diblock copolymer to generate unique hybrid organic-inorganic material with long range order.[17] A POSS particle with a cyclopentyl periphery and an isocyanate functional group has a diameter of approximately 1.5nm. POSS particles

crystallize in a hexagonal packing.[18] POSS has been successfully incorporated as filler for material reinforcement in several different polymeric systems[19] such as styrene/styryl-POSS polymers and copolymers,[20] norbornene/norbornyl-POSS polymers and copolymers,[21] ethylene/vinyl-POSS copolymers.[22] POSS-reinforced epoxy resins[23] and polyimides incorporating POSS.[24] As of today, only a few reports are concerned with utilizing POSS as a building block to generate mesoscopically-ordered structures.[25] Zheng et al.[26] used Ring Opening Metathesis Polymerization (ROMP) of cyclooctadiene in conjunction with POSS-norbornyl to generate random copolymers of POSS and polybutadiene. Incompatibility between the two components and crystallization of POSS induced microphase separation in the material. Alternating lamellae of POSS and polybutadiene could be observed by TEM for POSS loading of 30 wt% and above. Pyun et al.[27] have used Atom Transfer Radical Polymerization (ATRP) to synthesize ABA triblock copolymers with the A block being POSS block. Microphase separation could be observed on specific samples. Following a similar synthetic strategy, Intasanta et al.[28] have showed that a block copolymer of POSS and poly(methyl metacrylate) forming POSS cylinders in bulk could be cast on a silica wafer, oriented perpendicular to the surface and thermally transformed into silica giving rise to well ordered silica poles on a surface. Because of steric hindrance POSS can be polymerized to a maximum degree of polymerization of 10 by ATRP.

This chapter describes the synthesis of a series of poly(styrene-*b*-POSS) block copolymers. A homopolymer of hydroxyethyl methacrylate POSS was synthesized by free radical polymerization to measure the density of the POSS block. Subsequently, poly(styrene-*b*-hydroxyethyl methacrylate) precursors were synthesized via anionic

polymerization, providing starting materials with controlled molecular weight and low polydispersity (below 1.1). An isocyanate-functionalized POSS could be added to the second block via a urethane linkage formation. This strategy enabled a degree of polymerization of POSS of up to 41 in the present study. The volume fraction of each block was varied so that lamellae and cylinders could be obtained. Microphase separation of block copolymers as well as POSS crystallization induced phase separation. Finally, bulk morphology was studied with small angle X-rays scattering (SAXS) and transmission electron microscopy (TEM).

4.2 Description of the High-Vacuum Technique

Anionic polymerization under high-vacuum has been described in great details in excellent manuscripts.[29-31]. In the following section, a brief description of the vacuum line and the type of reactor used will be given.

4.2.1 Vacuum Line

As shown on Figure 1, a similar design as the one described by Hadjichristidis and coworkers was used in our laboratory.[30] For safety reasons, a triple stage oil diffusion pump (Wheeler oil diffusion pump, Arizona State University) was used instead of a mercury diffusion pump. Two cold traps were placed between the main manifold and the oil diffusion pump to avoid contamination of the diffusion pump oil with organic substances. The performance of this oil diffusion pump (pumping speed and ultimate vacuum) are similar to what is obtained with a mercury diffusion pump.

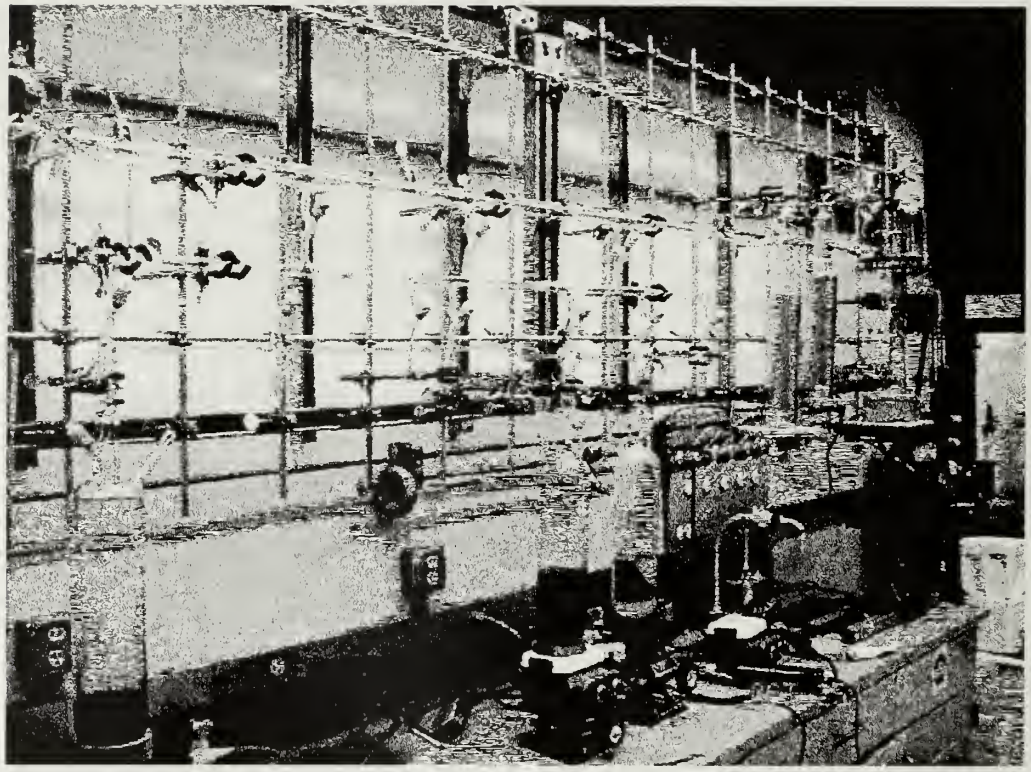

Figure 4.1 Picture of the High-Vacuum Manifold

4.2.2 Custom-Made Reactors and Experimental Protocol

The reactors used to perform anionic polymerization under high vacuum were custom-made. The principles used to design a reactor always follow the same rules. The quantity of reagents necessary for a reaction are first purified and stored under vacuum. A break-seal (a thin membrane of glass) enables to keep high-vacuum in the ampoule and will be broken by a glass-covered magnet in the next step. The monomers are then attached to the reactor. The resulting reactor is docked to the vacuum line, evacuated, flame-dried and the necessary quantity of solvent is distilled into the reactor. The reactor is then flame-sealed under vacuum and the break-seals of the reagents are broken in an order following the reaction scheme. In Figure 4.2, a typical reactor used for the polymerization of 2-(trimethylsilyloxy) ethyl methacrylate (p-HEMA) is shown.

The red ampoule contains a known amount of living polystyrene of known molecular weight, endcapped with diphenylethylene. On the other arm, the two ampoules pointing up are methanol and lithium chloride in THF. The flask attached to the side arm is a purge section. Finally, on the glass tube pointing down will be attached the p-HEMA ampoule. Once the reactor is cleaned and the purge section removed, THF is cooled down to -78°C. The break-seals of the polystyrene and the lithium chloride ampoules are then ruptured. In the final step, p-HEMA is slowly distilled in the reactor by warming up the ampoule to approximately 50°C. After an hour of reaction, methanol is introduced into the reactor to terminate the reaction.

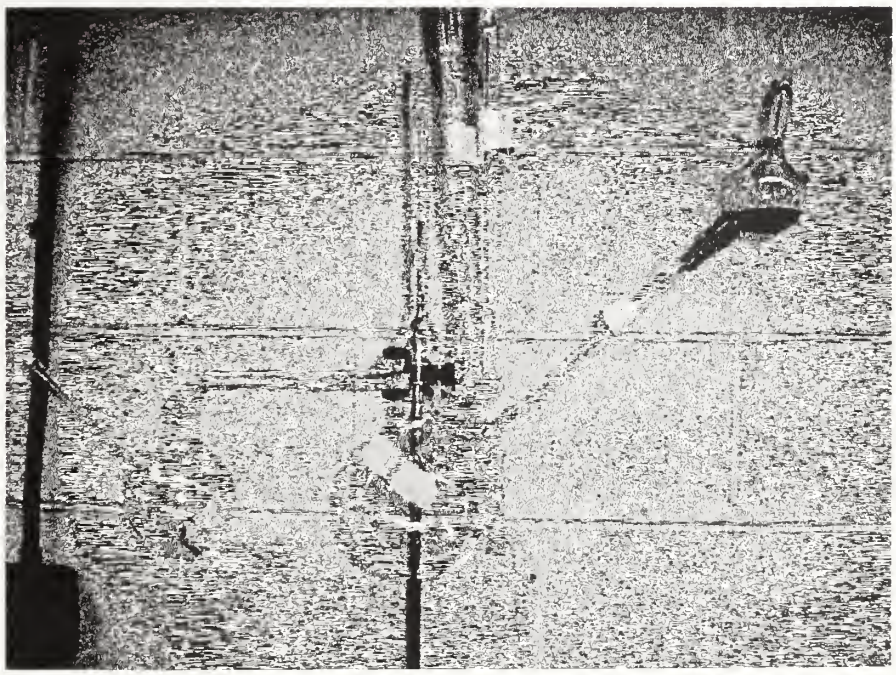

Figure 4.2 Typical Reactor Used for the Polymerization of Methacrylate

4.3 Experimental Section

4.3.1 Materials

The purification of styrene (Aldrich), diphenylethylene (Aldrich), 2-(trimethylsilyloxy) ethyl methacrylate (Aldrich, pHEMA), *sec*-butyl chloride (Aldrich) and lithium chloride (Aldrich, 99.998%) to the standards required for anionic polymerization has been described elsewhere.[32] Dibutyltin dilaurate (DBTDL, 95%), tetrabutyl ammonium fluoride (TBAF, 1M in THF), 2-hydroxyethyl methacrylate (98%) and lithium granules were purchased from Aldrich Chemical Co and used as received. 2,2'-Azobis(2-methylpropionitrile) (AIBN, 98%, Aldrich) was recrystallized from methanol. Toluene, tetrahydrofuran and benzene were purchased from Fisher and purified following known protocols.[32] Reagent grade hexane and methanol were purchased from Fisher and used as received. 1-due to a more-3,5,7,9,11,13,15-hepacyclopentylpentacyclo [9.5.1.13,9.15,15.17,13] octasiloxane (**CpPOSS-NCO**) and 1-[isocyanotopropyldimethylsilyl]-3,5,7,9,11,13,15-hepacyclopentylpentacyclo [9.5.1.13,9.15,15.17,13] octasiloxane (**IbuPOSS-NCO**) were supplied by Hybrid Plastics, Inc. *Sec*-butyl lithium was synthesized from *sec*-butyl chloride and lithium granules in hexanes. *Sec*-butyl lithium was titrated by polymerizing a known amount of styrene and analyzing the resulting polymer by GPC with respect to a polystyrene calibration.

4.3.2 Synthesis

4.3.2.1 Polymerization Procedure for Polystyrene-HEMA Copolymer P(S_{537}-*b*-$pHEMA_{41}$)

Poly(styrene-*b*-2-(trimethylsilyloxy) ethyl methacrylate) (P(S-*b*-pHEMA)) precursors were polymerized by anionic polymerization under high vacuum. In a typical experiment, 3.25ml of *sec*-BuLi ([*s*-BuLi] = 0.07 M in hexanes, 0.228 mmol) were introduced under vacuum in 100ml of benzene. Subsequently, 12.5ml of styrene (0.109 mol) were added and reacted overnight. 0.63 ml Diphenyl ethylene ([DPE] = 0.72M, 0.454 mmol) was added to the reaction mixture and the reaction was left for two days at room temperature (M_n (GPC) = 55,800 g/mol, PDI = 1.03). The solution was then split in 4 ampoules and each ampoule was reacted with a different amount of 2-(trimethylsilyloxy) ethyl methacrylate). An ampoule containing 28.4 ml of living polystyrene solution in benzene was added at room temperature to a reactor containing 100 ml of THF and 2 ml of LiCl ([LiCl] = 0.59 M, 1.18 mmol). The reactor was then cooled down to -78 °C using a dry ice/Isopropanol mixture and 0.47 ml of pHEMA were distilled in the reactor. As soon as the first drop of pHEMA reached the reaction solution, the red color typical of diphenylethylene lithium disappeared. The reaction was left at -78 °C for 1 hour and was terminated by a few drop of methanol. Subsequently, the solution was concentrated in a rotovapor and precipitated in methanol. M_n (^{1}H NMR), and polydispersity (GPC) were equal to 64,100 g/mol, and 1.03 respectively. The number average molecular weight is calculated by comparing the ration of the aromatic protons at δ 7.3-6.3 ppm (5 protons) to the HEMA methylene α to the urethane linkage (2 protons).

^{1}H NMR (400 MHz, $CDCl_3$): δ 7.11 (m, 3H), δ 6.60 (m, 2H), δ 4.00 (m, 2H), δ 3.75 (m, 2H), δ 1.88 (m, 1H), δ 1.45 (m, 2H), δ 0.92 (m, 9H), δ 0.139 (s, 9H)

^{13}C NMR (100 MHz, $CDCl_3$): δ 177.3, 145.4, 128.03, 125.7, 65.9, 60.0, 54.5, 43.9, 40.7, 34.8, 34.6, 31.7, 25.7, 22.8, 20.8, 14.2, 1.4, -0.34

4.3.2.2 Removal of the Trimethylsilyl Protecting Group from P(S_{537}-*b*-pHEMA$_{41}$) to Obtain P(S_{537}-*b*-HEMA$_{41}$).

In a typical experiment, 0.4322 g (0.276 mmol of trimethylsilyl protecting group) of **P(S_{537}-*b*-pHEMA$_{41}$)** were dissolved in 100 ml of THF and subsequently cooled down to 0°C. TBAF (2ml, 2 mmol) was added to the reaction flask. After an hour of reaction, the solution was passed through a silica gel column using THF as the eluant, to remove the side products from the reaction. The solution was concentrated and precipitated in cold hexane for **P(S_{537}-*b*-pHEMA$_{41}$)**. The other polymers were precipitated in MeOH. A final polymer mass of 0.3528g (85% yield) was obtained after all the purification steps. A M_n (^{1}H NMR) of 61,140 g/mol was obtained along with a PDI of 1.04. From the GPC, the amount of coupling was approximately equal to 2%.

^{1}H NMR (400 MHz, $CDCl_3$): δ 7.11 (m, 3H), δ 6.60 (m, 2H), δ 4.13 (m, 2H), δ 3.86 (m, 2H), δ 1.88 (m, 1H), δ 1.45 (m, 2H),δ 0.92 (m, 9H)

^{13}C NMR (100 MHz, $CDCl_3$): δ 145.4, 128.03, 125.7, 43.9, 40.7, 34.8, 34.6, 31.7, 29.2, 25.4, 22.8, 20.8 18.9, 14.2, 11.5

4.3.2.3 Addition of POSS to P(S_{537}-*b*-pHEMA$_{41}$) to Afford P(S_{537}-*b*-UEMA-IbuPOSS$_{41}$)

The reaction was carried out using standard Schlenk technique. **P(S_{537}-*b*-HEMA$_{41}$)** (0.3528g, 0.236 mmol of alcohol) was dissolved in 6ml of dry toluene along

with 0.912g of **IbuPOSS-NCO** (0.94 mmol). DBTDL (0.1 ml, 0.17 mmol) was then added to the solution and the reaction mixture was heated up at 90°C over night. The final polymer was precipitated twice in a 2:1 MeOH:hexane mixture, filtered and dried overnight in a vacuum oven at room temperature. M_n = 68,680 g/mol (THF GPC), PDI = 1.03.

^{1}H NMR (400 MHz, $CDCl_3$): δ 7.11 (m, 3H), δ 6.60 (m, 2H), δ 5.65 (s, 1H), δ 4.25 (t, 2H), δ 4.09 (t, 2H), δ 3.14 (t, 2H), δ 1.88 (m, 10H), δ 1.45 (m, 2H), δ 0.98 (d, 42H), δ 0.64 (m, 16H), δ 0.14 (s, 6H)

^{13}C NMR (100 MHz, $CDCl_3$): δ 156.2, 145.4, 128.03, 125.7, 59.6, 44.0, 40.5, 35.0, 29.8, 25.8, 23.9, 23.8, 22.60, 22.55, 22.50, 14.9, -0.26

4.3.2.4 Synthesis of IbuPOSS-UEMA Monomer

In a 50 ml flask containing 20ml of dry THF was added **IbuPOSS-NCO** (1.19g, 1.2 mmol), 2-hydroxyethyl methacrylate (0.75 ml, 6.18 mmol), DBTDL (0.2 ml, 0.34 mmol) and CuCl (5 mg, 0.05 mmol). The solution was refluxed for 1 hr at 65°C and the final product was purified by silica gel flash chromatography using a 1:1 hexane:ethyl acetate mixture as eluant. The solvent was removed with a rotovapor and the white powder was dried overnight under vacuum at room temperature. (79.2 % yield).

^{1}H NMR (400 MHz, $CDCl_3$): δ 6.13 (s, 1H), δ 5.58 (s, 1H), δ 4.75 (s,1H), δ 4.31 (s, 4H), δ 3.17 (q, 2H, J = 6.9 Hz), δ 1.95 (s, 3H), δ 1.86 (m, 7H), δ 1.68 (m, 2H), δ 0.95 (d, 42H, J = 6.8 Hz), δ 0.61 (t, 16H, J = 4.8 Hz), δ 0.13 (s, 6H).

^{13}C NMR (100 MHz, $CDCl_3$): δ 165, 158, 157.5, 125.9, 63.0, 62.4, 43.9, 25.7, 23.8, 23.6, 22.42, 22.40, 18.3, 14.8, -0.39. MS-FAB: m/z = 1104.2 (theo: 1104.84)

4.3.2.5 Synthesis IbuPOSS-Propane for DSC Measurements

Propanol (0.96ml, 12.8 mmol), DBTDL (0.05 ml, 0.08 mmol) and **IbuPOSS-NCO** (0.7182g, 0.74mmol) were added to a 20 ml flask containing 10 ml of THF. The solution was refluxed for 2 hours. The product of the reaction was precipitated into cold methanol affording a white solid and was dried overnight in a vacuum oven. (Yield = 15.8%)

^{1}H NMR (400 MHz, $CDCl_3$): δ 4.62 (s, 1H), δ 4.00 (q, 2H, J = 6.8 Hz), δ 3.14 (t, 2H, J = 6.4 Hz), δ 1.86 (m, 7H), δ 1.68 (m, 4H), δ 0.95 (d, 45H, J = 6.8 Hz), δ 0.61 (t, 16H, J = 4.8 Hz), δ 0.13 (s, 6H).

^{13}C NMR (100 MHz, $CDCl_3$): δ 156.77, 43.79, 23.87, 23.84, 23.69, 22.50, 22.45, 22.42, 14.79, 10.37, -0.361. MS-FAB: m/z = 1034.3 (theo: 1034.8)

4.3.2.6 Radical Polymerization of IbuPOSS-UEMA Using AIBN as an Initiator to Afford P(IbuPOSS-UEMA).

In a 20 ml vial containing 1.8 ml of benzene, AIBN (2.5 mg, 0.015 mmol) and **IbuPOSS-UEMA** (1g, 0.84 mmol) were added. After dissolving the powder, the solution was degassed by bubbling nitrogen for 20 min. The reaction flask was heated up at 60°C for 2 hr, after which gelation of the solution occurred. THF (20ml) was added to dissolve the gel and the resulting solution was precipitated in methanol. The unreacted **IbuPOSS-UEMA** was removed via a soxhlet extraction with methanol for 3 days. (Yield = 47%). M_n (THF GPC) = 670,000 g/mol with respect to polystyrene standards. PDI = 1.23

^{1}H NMR (400 MHz, $CDCl_3$): δ 4.23 (m, 4H), δ 3.12 (t, 2H), δ 1.85 (m,9H), δ 1.52 (m, 4H), δ 0.96 (m, 52H), δ 0.61 (t, 16H), δ 0.13 (s, 6H).

^{13}C NMR (100 MHz, $CDCl_3$): δ 156.1, 141.2, 31.6, 25.71, 23.84, 23.81, 22.66, 22.44, 22.39.

4.3.3 Polymer Characterization

4.3.3.1 GPC

Gel permeation chromatography (GPC) measurements were performed in tetrahydrofuran (THF) at 1.0 mL/min using a Knauer K-501 Pump with a K-2301 refractive index detector and K-2600 UV detector, and a column bank consisting of two Polymer Labs PLGel Mixed D columns at 25°C. Molecular weights are reported relative to polystyrene standards (Polymer Labs, Inc.).

Preparative GPC was carried out in THF at 5 ml/min using a pump (HP Series 1050) with a refractive index detector (HP 1047A) and one Polymer Labs ResiPore 3μm (300 x 7.5mm) columns. THF solutions containing 25mg/ml of polymers were used.

4.3.3.2 NMR

^{1}H NMR and ^{13}C NMR spectra were recorded at 400 MHz and 100 MHz on a Bruker NMR spectrometer at room temperature in deuterated chloroform.

4.3.4 Thermal analysis

Differential scanning calorimetry was performed under a continuous nitrogen purge on a Mettler-Toledo DSC 822^{e}. Octane (Aldrich, 99%+), pentane (Aldrich, 99%+), deionized water, indium and zinc were used to perform the calibration. Samples having a mass between 2.5 and 11 mg were used. Data were gathered using a scan rate of 10 °C/min on the first scan. Thermogravimetric analysis (TGA) was carried out using a TA Instruments TGA 2950 thermogravimetric analyzer with a

heating rate of 10 ° C/min from room temperature to 600°C under a continuous nitrogen flow (40 mL/min).

4.3.5 TEM

Specimens for TEM and SAXS were cast from 5 wt % toluene for a week. Morphology was studied on the as-cast films and they were further annealed at 120°C *in vacuo* for four days. Bulk film samples for electron microscopy were microtomed in a Leica Ultracut cryoultramicrotome. Sections approximately 50-100 nm thick were cut with a Diatome diamond knife at a sample temperature of -110°C, a knife temperature of -100°C and a cryogenic sample chamber of -120°C. TEM studies were performed using a JEOL 100 CX transmission electron microscope operated at 100 kV. No staining was needed to observe contrast in TEM.

4.3.6 SAXS

Small angle X-ray scattering was performed using Ni-filtered Cu Kα radiation (1.54 Å wavelength) from a Rigaku rotating anode (operated at 40 kV, 200 mA). The X-ray was collimated by a set of three pinholes. A CCD detector (Siemens Hi-Star), located at a camera length of 875.2 mm, was used to record scattering patterns.

4.3.7 Film Density Measurement

Density of **Poly(IbuPOSS-UEMA)** homopolymer was measured according to the ASTM D 792-00 standard. 0.1g of **Poly(IbuPOSS-UEMA)** were melt pressed between two capton films at 200°C for 30 min. The resulting film was subjected to the ASTM D 792-00 standard. A density of 1.06 was found.

4.4 Results and Discussion

4.4.1 Synthesis of Poly(Styrene-*b*-pHEMA) by Sequential Anionic Polymerization (Figure 4.4.).

In this chapter, the nomenclature used for the block copolymers is such that each block is called by the name of the monomer. S stands for styrene, pHEMA for protected hydroxyethyl methacrylate, HEMA for deprotected pHEMA and UEMA-xPOSS for POSS-NCO reacted with the pendant alcohol group of the HEMA block, where x is either isobutyl (Ibu) or cyclopentyl (Cp). The number in subscript after the monomer corresponds to the degree of polymerization of the monomer.

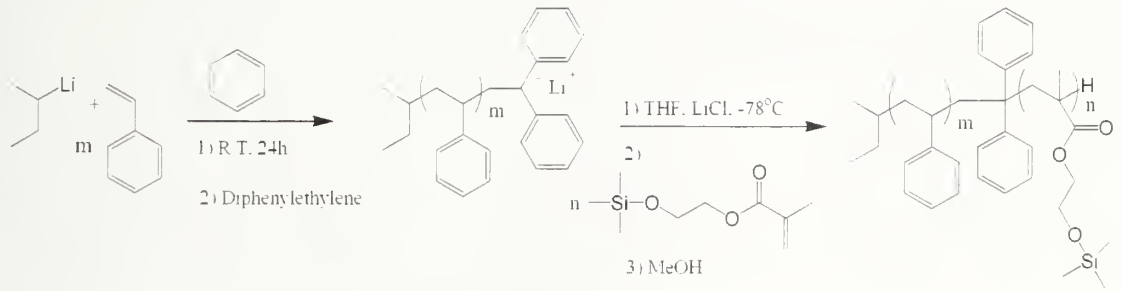

Figure 4.3 Synthesis of Poly(Styrene-*b*-(Trimethylsilyloxy) ethyl methacrylate) by Anionic Polymerization

Sequential anionic polymerization was chosen to synthesize the Poly(styrene-*b*-pHEMA) block copolymer precursors because of the ability to precisely control the molecular weight and the polydispersity. The synthetic scheme is shown on Figure 4.3. Styrene polymerization was initiated by *sec*-butyl lithium in benzene and a 2 to 3 times excess DPE was added to the solution. Polystyrene end-capped with diphenylethylene was split into several ampoules enabling the synthesis of a series of diblock copolymers with an identical first block. An increase of molecular weight while maintaining a low polydispersity (below 1.1) upon addition of the methacrylate monomer can be seen on Figure 4.4.

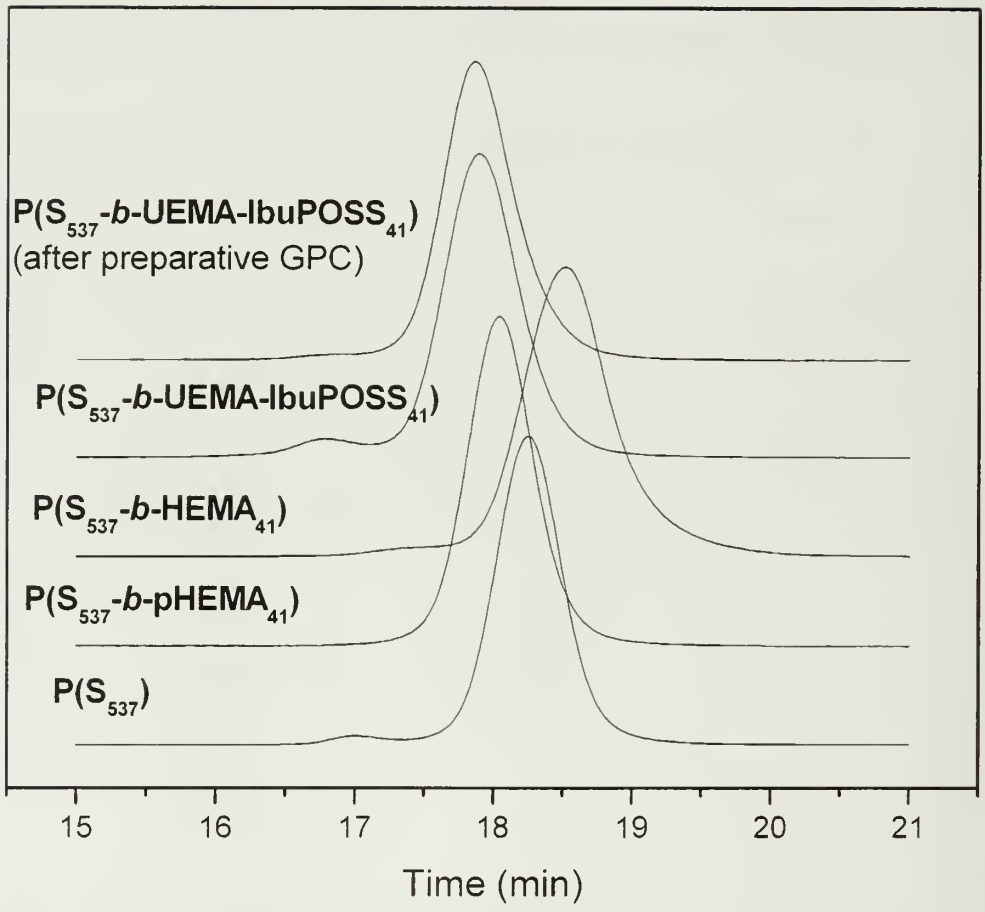

Figure 4.4 GPC Traces of P(S_{537}-*b*-UEMA-$POSS_{41}$) and its Diblock Copolymer Precursors.

Several polystyrene precursors with different molecular weights were synthesized to study the influence of the first block on the overall diblock morphology. The highest molecular weight of polystyrene was 56,000 g/mol, a molecular weight roughly equal to three times the entanglement molecular weight of styrene. This molecular weight is high enough to promote mechanical integrity to the sample while enabling diffusion of the polymer chains in bulk upon annealing. Blocks of polystyrene of 40,000 g/mol and 25,000 g/mol were also used as first block. The degree of

polymerization of the second block was calculated by ^{1}H NMR and was found to be between 7 and 41. Eight diblock copolymer precursors were synthesized followed by the removal of the trimethylsilyl protecting group from the second block and the urethane formation between the pendant alcohol of the HEMA block and the isocyanate of the POSS cube. Varying the degree of polymerization of HEMA is a convenient way of changing the amount of POSS incorporated into the hybrid organic-inorganic copolymer. This strategy was successfully used to vary the volume fraction of each block, resulting in a variety of morphologies, as will be described later in this chapter.

4.4.2 Removal of the Trimethylsilyl Protecting Group From the pHEMA Block and POSS Addition (Figure 4.5)

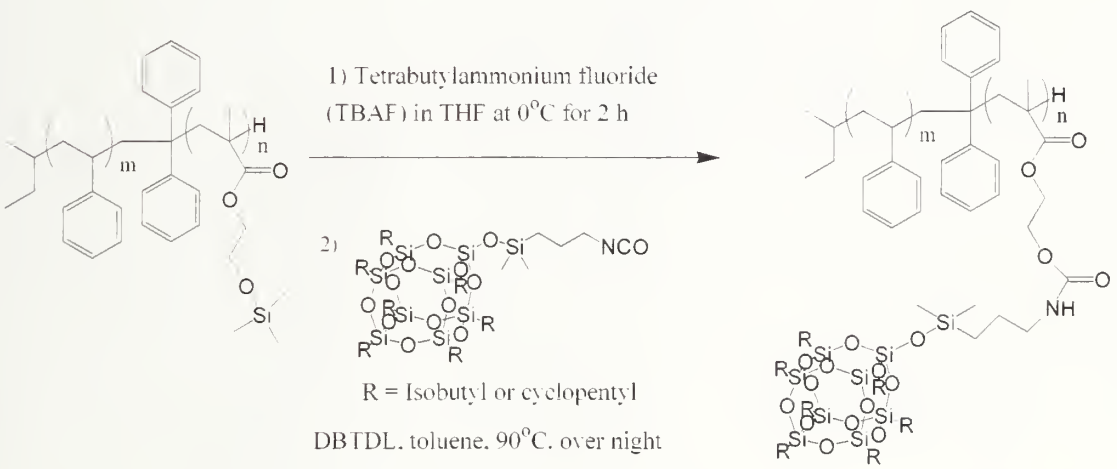

Figure 4.5 Deprotection of the Hydroxyl Group of the (Trimethylsilyloxy) Ethyl Methacrylate Block. Condensation of POSS on the Methacrylate Block by the Formation of a Urethane Linkage.

Deprotection of poly(2-(trimethylsilyloxy) ethyl methacrylate) has been reported several times in the literature.[33, 34] Common methods consist of precipitating the polymer in acidic methanol, reacting the polymer with HCl in THF, or use of *tert*-butyl ammonium fluoride (TBAF) as a source of fluorine atom to form the energetically favored Si-F bond. Deprotection by all these methods resulted in the formation of the

desired product along with a small polymer fraction having a molecular weight twice the molecular weight of the desired product. It was speculated that a transesterification between the pendant alcohol and the ester linkage of the second block was occurring, however, it was not possible to confirm this hypothesis by any characterization method since the amount of coupling between two polymeric chains is less than a few percent. Deprotection using a 5 to 10 fold excess of TBAF with respect to the amount of trimethylsilyl groups in THF at 0°C for an hour enabled a quantitative deprotection while limiting the amount of coupling. The disappearance of the singlet corresponding to TMS protons at 0.163 ppm in ^{1}H NMR confirmed a quantitative deprotection.

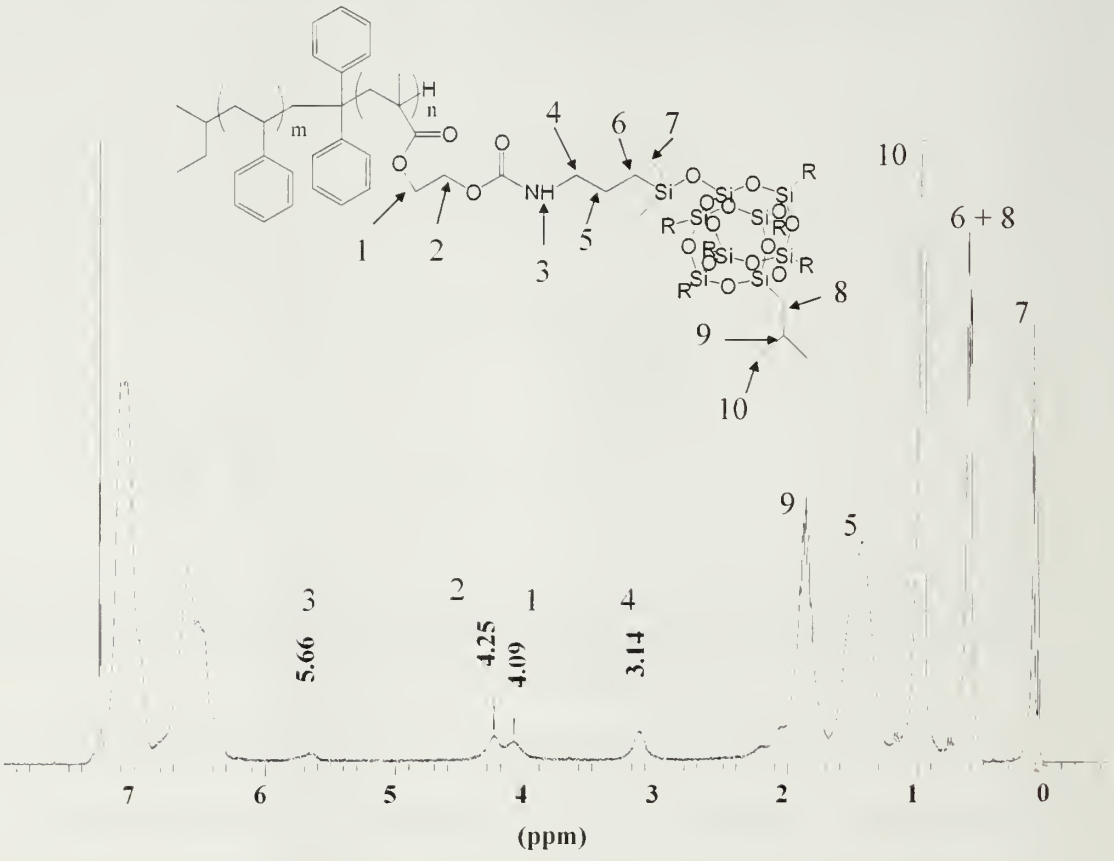

Figure 4.6 ^{1}H NMR of P(S_{537}-*b*-UEMA-IbuPOSS$_{13}$)

The POSS cube bearing one reactive isocyanate group was then condensed with the pendant alcohol of the HEMA block following a protocol previously reported.[26] The reaction proceeded smoothly as confirmed by ^{1}H and ^{13}C NMR, GPC and FT-IR. The methylene protons α to the nitrogen shifted downfield from δ 3.86 ppm to δ 4.09 ppm while the methylene α to the isocyanate shifted upfield from δ 3.28 ppm to δ 3.14 ppm upon urethane formation (Figure 4.6). Moreover, no residual unreacted POSS monomer is seen in ^{1}H NMR as confirmed by the disappearance of the triplet from the methylene α to the isocyanate. The same conclusions can be drawn from ^{13}C NMR (Figure 4.7).

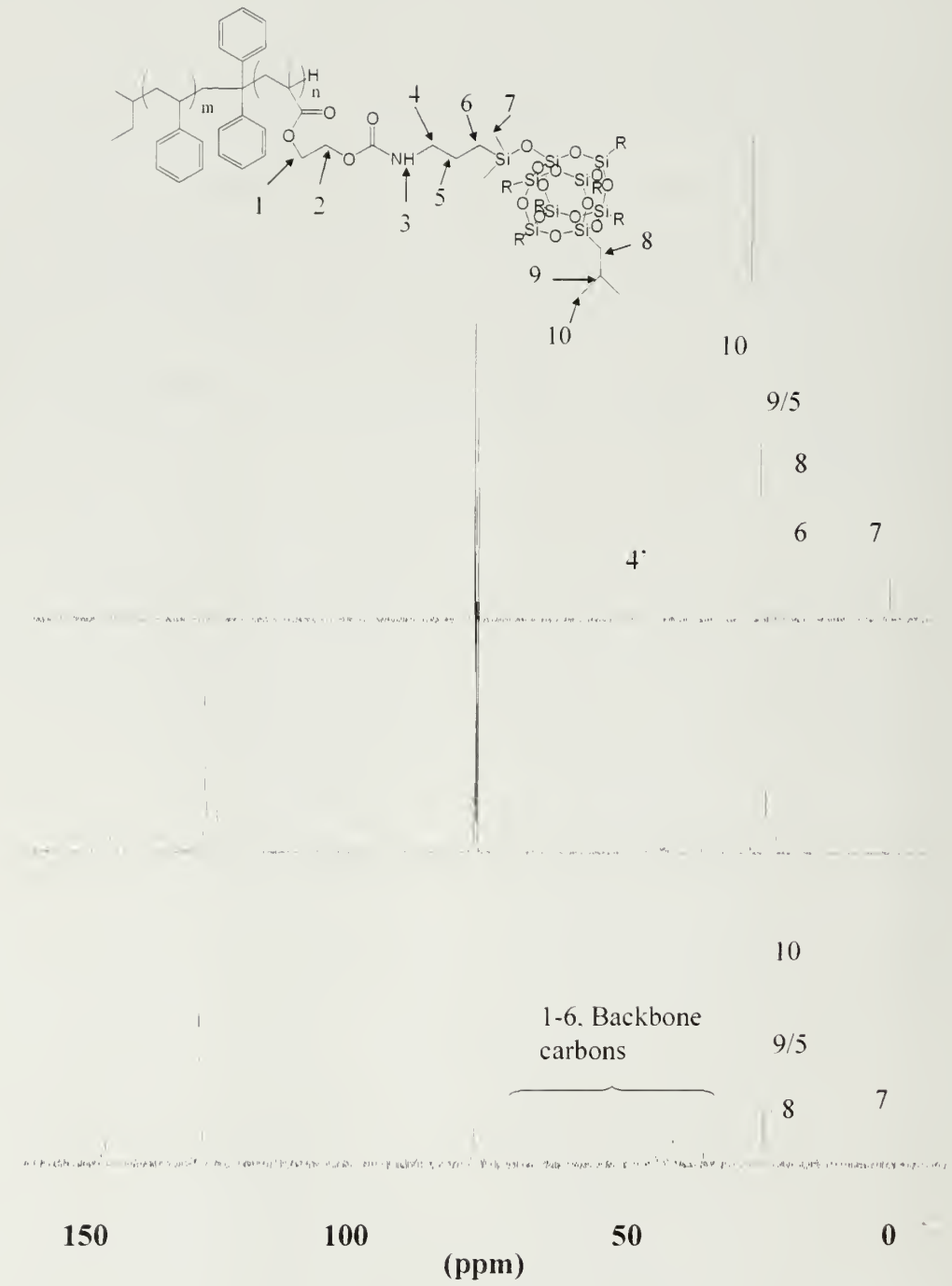

Figure 4.7 ^{13}**C NMR of P(S$_{537}$-*b*-UEMA-IbuPOSS$_{13}$)**

The FT-IR spectrum (Figure 4.8) confirms the appearance of the urethane linkage as shown by the carbonyl stretching absorption band at 1728 cm^{-1}. The isocyanate group absorption band at 2400 cm^{-1} of the POSS monomer has disappeared. Also, the Si-O vibration band at 1100 cm^{-1} can be observed in the final hybrid copolymer.

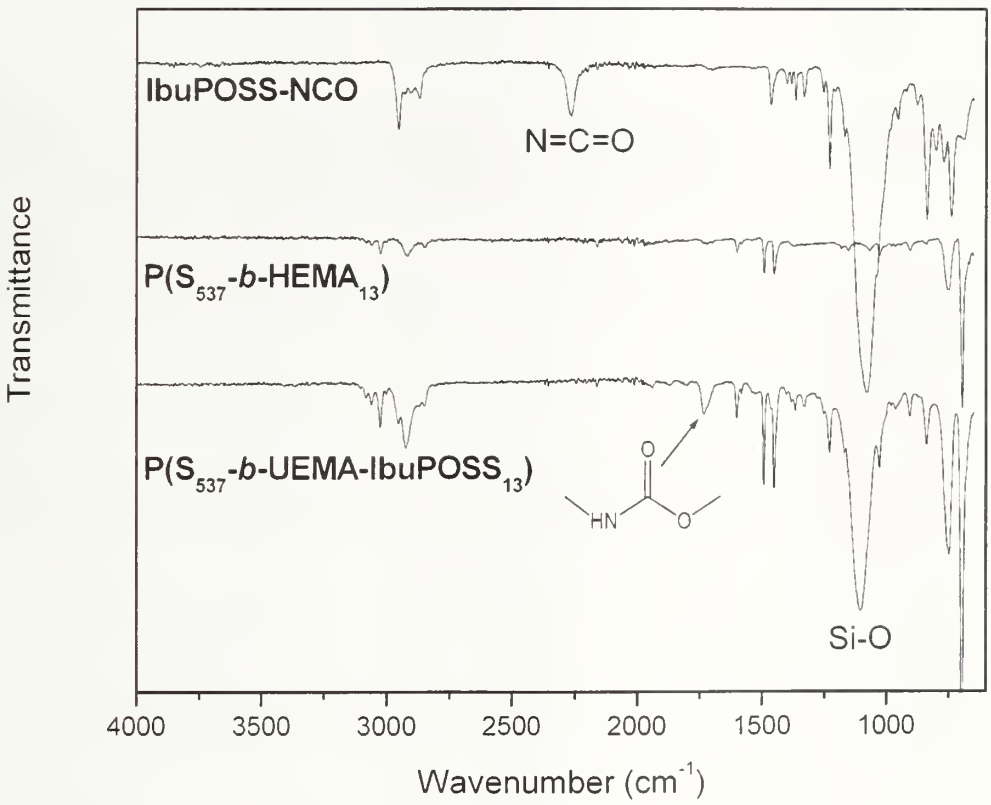

Figure 4.8 FT-IR of IbuPOSS-NCO (Top), P(S_{53}--*b*-$HEMA_{13}$) (Middle), P(S_{53}--*b*-UEMA-$IbuPOSS_{13}$) (Bottom)

A minute amount of dimeric product (a few % by volume) can still be found for polymers having ten HEMA repeat units or more. It is possible to remove this dimeric product using a preparative GPC system as shown in Figure 4.4. Although the

purification is efficient (i.e. a perfectly monodisperse polymer is obtained), yields of approximately 60% by weight are obtained. As will be seen in the following section, the dimeric product does not affect the overall morphology of the polymer. The same urethane formation protocol was successfully applied to the 8 diblock copolymers precursors. The degree of polymerization, the volume fraction and the molecular weight (M_n, g/mol) of the 8 samples is reported in Table 4.1. The morphology obtained from SAXS and correlated with TEM is given as well.

Table 4.1 Molecular Weight Characteristics of Poly(styrene-*b*-POSS) Diblock Copolymers. [1] From THF GPC Against Polystyrene Standards. [2] By Integration From ^{1}H NMR. [3] d (P(IbuPOSS-UEMA)) = 1.06 g/cm^3.

Sample ID	$N_{(styrene)}$ [1]	$N_{(POSS)}$ [2]	$f_{(polystyrene)}$	$f_{(polyPOSS)}$ [3]	M_n (PS) (g/mol) $(PDI)^2$	M_n P(S-*b*-POSS) (g/mol) $(PDI)^2$	Morphology
P(S_{537}-*b*-UEMA-IbuPOSS$_{41}$)	537	41	0.56	0.44	55,800 (1.03)	67,680 (1.03)	Lamellae
P(S_{537}-*b*-UEMA-IbuPOSS$_{13}$)	537	13	0.80	0.2	55,800 (1.03)	59,240 (1.03)	Cylinder
P(S_{537}-*b*-UEMA-IbuPOSS$_{6}$)	537	6	0.90	0.1	55,800 (1.03)	56,280 (1.03)	Cylinder
P(S_{389}-*b*-UEMA-IbuPOSS$_{29}$)	389	29	0.56	0.44	40,500 (1.03)	59,900 (1.04)	Lamellae
P(S_{389}-*b*-UEMA-IbuPOSS$_{15}$)	389	15	0.71	0.29	40,500 (1.03)	49,400 (1.04)	Lamellae
P(S_{385}-*b*-UEMA-IbuPOSS$_{10}$)	385	10	0.79	0.21	40,000 (1.03)	47,960 (1.03)	Cylinder
P(S_{240}-*b*-UEMA-IbuPOSS$_{7}$)	240	7	0.77	0.23	25,000 (1.03)	28,860 (1.03)	Lamellae
P(S_{240}-*b*-UEMA-CpPOSS$_{7}$)	240	7	0.77	0.23	25,000 (1.03)	27,270 (1.03)	Lamellae

4.4.3 Thermal Characterization of the Hybrid Organic-Inorganic Block Copolymers (Table 4.2)

4.4.3.1 TGA

IbuPOSS-NCO and **CpPOSS-NCO** have a degradation temperature (at 5 wt% loss) of 200 °C and 300 °C respectively. **P(S_{53}-*b*-pHEMA$_{13}$)** exhibits a decomposition temperature of 340°C which decreases to 300 °C upon POSS addition. This can be

understood by considering the fact that upon POSS addition, a thermally weak urethane linkage is introduced in the polymer chain. The general trend is that the decomposition temperature is inversely proportional to the molar mass of the POSS block. Nonetheless, the final polymers can withstand annealing temperature of up to 200 °C. **CpPOSS-NCO** has a char yield of 53% while **IbuPOSS-NCO** has a char yield of 12.3%. Similarly, **P(S_{240}-*b*-UEMA-CpPOSS-)** exhibit a higher char yield (2%) than **P(S_{240}-*b*-UEMA-IbuPOSS-)** (0%). Although not understood, the thermal degradation mechanisms are different in those two cases.

Table 4.2 Thermal Characterization of the Poly(styrene-*b*-UEMA-xPOSS) and its Precursors. $T_{g,1}$ Corresponds to the T_g of the POSS Block. $T_{g,2}$ Corresponds to the T_g of the PS Block. T_m is the Melting Temperature of POSS Crystals and T_{dec} is the Degradation Temperature at 5% Weight Loss.

Sample ID	$T_{g,1}$ (°C)	$T_{g,2}$ (°C)	T_m(°C)	T_{dec}(°C)
P(S_{537}-*b*-UEMA-IbuPOSS$_{41}$)	55	94	-	294
P(S_{537}-*b*-UEMA-IbuPOSS$_{13}$)	56	99	-	284
P(S_{537}-*b*-UEMA-IbuPOSS$_{6}$)	-	96	-	314
P(S_{389}-*b*-UEMA-IbuPOSS$_{29}$)	-	93	-	294
P(S_{389}-*b*-UEMA-IbuPOSS$_{15}$)	-	99	-	264
P(S_{385}-*b*-UEMA-IbuPOSS$_{10}$)	-	100	-	282
P(S_{240}-*b*-UEMA-IbuPOSS$_{7}$)	-	92	-	262
P(S_{240}-*b*-UEMA-CpPOSS$_{7}$)	-	100	238	297
P(S_{537}-*b*-HEMA$_{13}$)	-	94	-	334
IbuPOSS-Propanol	-	-	130	334
CpPOSS-NCO	-	-	290	206
P(IbuPOSS-Propanol)	54	-	122	305

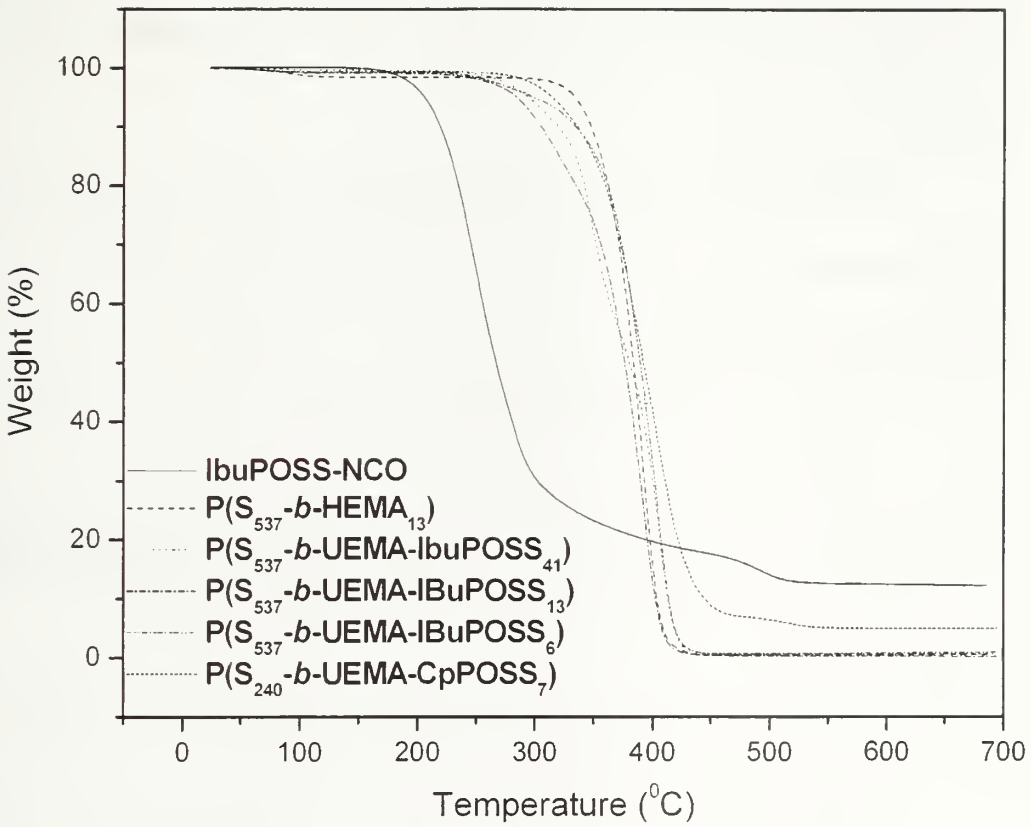

Figure 4.9 TGA Under Nitrogen of a Series of Poly(styrene-*b*-POSS) Block Copolymers

4.4.3.2 DSC

CpPOSS-NCO has a melting point of 290 °C (melting/degradation) while **IbuPOSS-NCO** has a melting point of 130°C. **IbuPOSS-NCO** was preferred to **CpPOSS-NCO** because of its lower melting point allowing annealing of block copolymers containing **IbuPOSS-NCO**. Noteworthy is the fact that **P(S_{240}-*b*-CpPOSS-)** exhibits a melting point at 238 °C, which is most likely due to POSS crystals melting. The confinement of POSS particle in a polymer matrix decreased the melting point of the crystal by 50 °C. A transition at 100 °C is observed on all the samples. It

corresponds to the glass transition temperature (T_g) of polystyrene, which is unaltered by the presence of the second inorganic block. This is an indication that the material is microphase separated.

IbuPOSS-NCO was reacted with propanol to be used as a model compound with a urethane linkage. A melting point of 98°C was found. Thermal analysis of **P(IbuPOSS-UEMA)** showed a T_g of 54°C and a T_m of 122°C. For the polymers with 13 and 41 repeat units of **IbuPOSS-UEMA**, a transition can be seen around 50°C, corresponding to the T_g of the POSS amorphous domain. This transition is not seen on for the polymers having 7 repeat units of **IbuPOSS-UEMA** or **CpPOSS-UEMA**, most likely due to a more efficient crystallization of the POSS segments.

4.4.4 Morphology Study of the Hybrid Organic-Inorganic Block Copolymers

Morphology of the hybrid organic-inorganic block copolymers was studied by SAXS and TEM. The volume fractions of each block calculated from the measured density of **P(IbuPOSS-UEMA)** (1.06) is in good agreement with the morphologies observed. No staining was needed for any of these polymers as POSS provides enough mass contrast, therefore, on the TEM pictures, the black domains correspond to POSS region while the white domains correspond to polystyrene. Figures 4.10, 4.11, 4.12 show the change in morphology as a function of POSS volume fraction. The **P(S_{537}-*b*-UEMA-IbuPOSS$_x$)** and the **P(S_{385}-*b*-UEMA-IbuPOSS$_x$)** series are shown on Figure 4.13 and Figure 4.14 respectively.

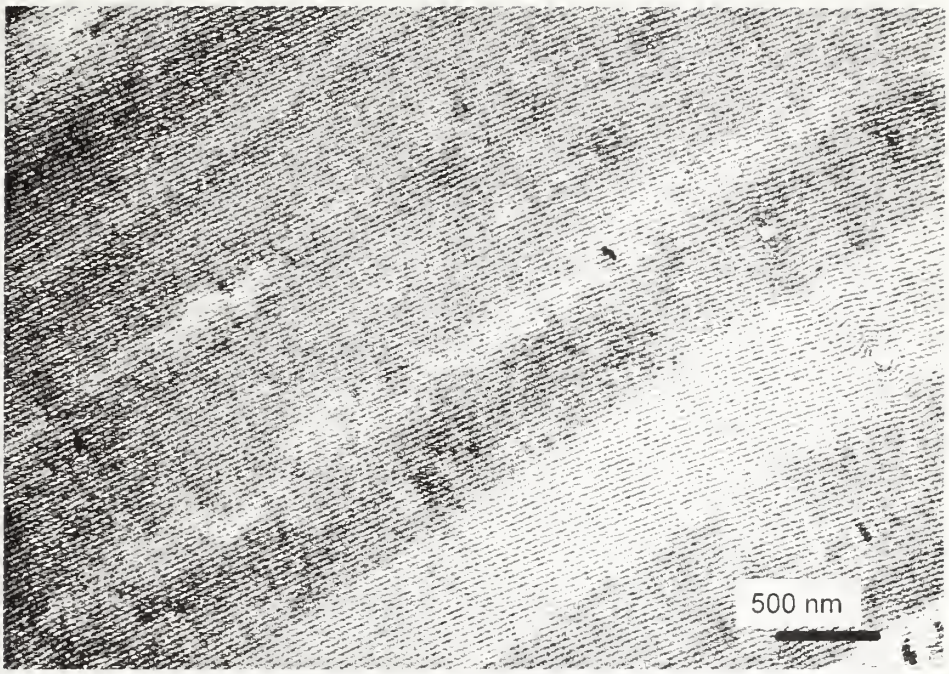

Figure 4.10 TEM of P(S_{53}-*b*-UEMA-IbuPOSS$_{41}$) after Preparative GPC, Natural Contrast

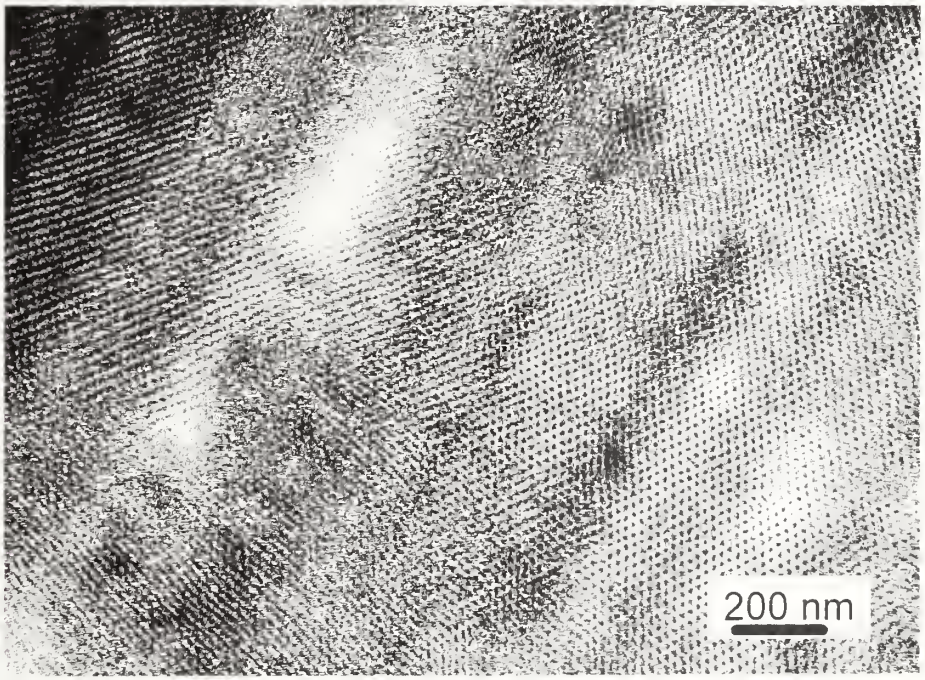

Figure 4.11 TEM of P(S_{53}-*b*-UEMA-IbuPOSS$_{13}$), Natural Contrast.

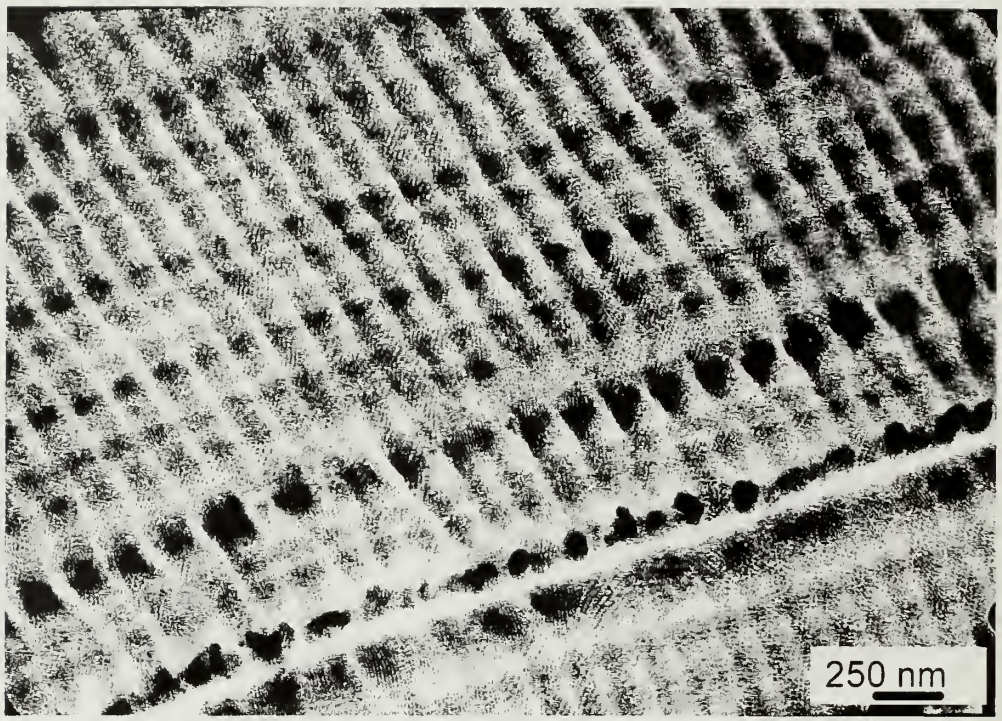

Figure 4.12 TEM of P(S_{537}-*b*-UEMA-IbuPOSS$_7$), Natural Contrast.

P(S_{537}-*b*-UEMA-IbuPOSS$_{41}$), P(S_{385}-*b*-HEMA-IbuPOSS$_{29}$) and **P(S_{240}-*b*-UEMA-CpPOSS$_7$)** show a lamellae structure with a long period D of 30.5 nm, 28.4 nm and 19.6 nm respectively (Figures 4.15, 4.16 and 4.17). D can therefore be changed by varying the molecular weight of polystyrene. Long-range order was obtained on all those samples as confirmed by the 3rd or 4th order diffraction peak observed on the three diffraction patterns. Orientation of the lamellae is seen from the 2D diffraction patterns (Figures 10.13 and 10.14) consistent with lamellae oriented parallel to the film surface. It demonstrates that the solvent-casting technique is capable of inducing macroscopically aligned samples for the present hybrid organic-inorganic block copolymer.[35, 36] As it can be seen on Figure 4.10, a lamellar structure was confirmed by TEM. Oriented, defect-free lamellae could be seen on area as large as several μm^2. The

lamellae thickness for POSS and polystyrene domains can be approximated to 10 nm and 50 nm from the image.

Annealing of the samples did not change the morphology. It is possible that POSS acts as an anchor within the material and annealing above the T_g of polystyrene does not provide enough mobility to the sample to show any change in the SAXS pattern.

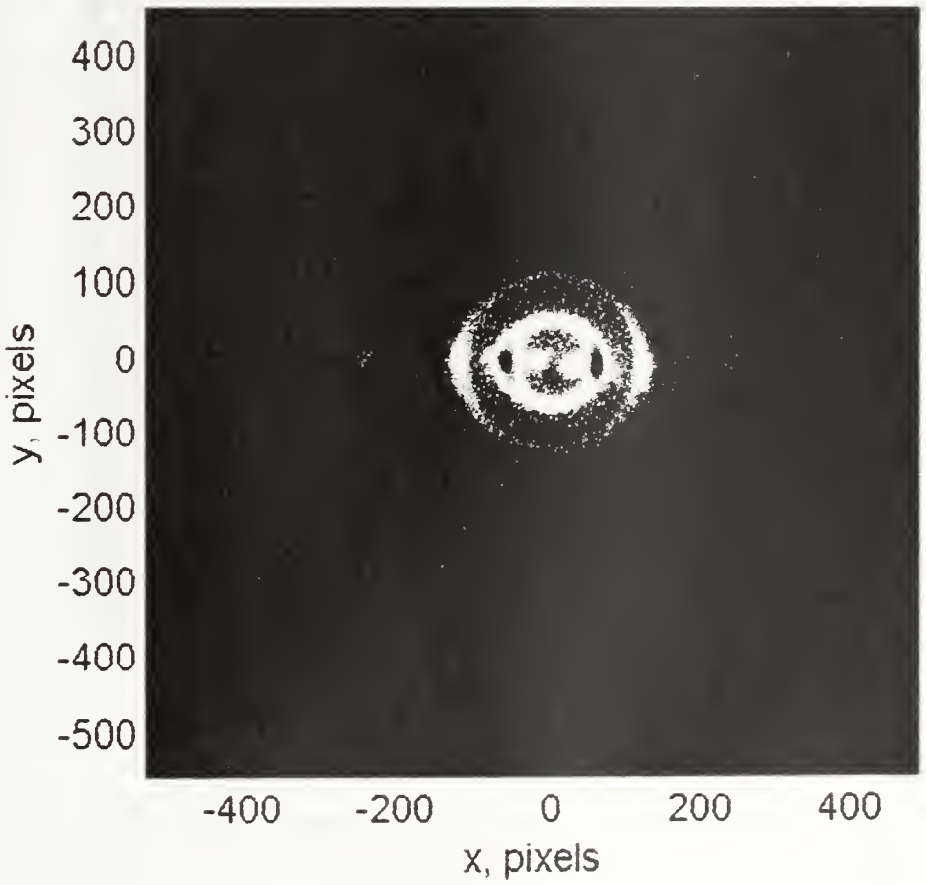

Figure 4.13 2D SAXS of P(S_{53}-*b*-UEMA-IbuPOSS$_{41}$) After Preparative GPC

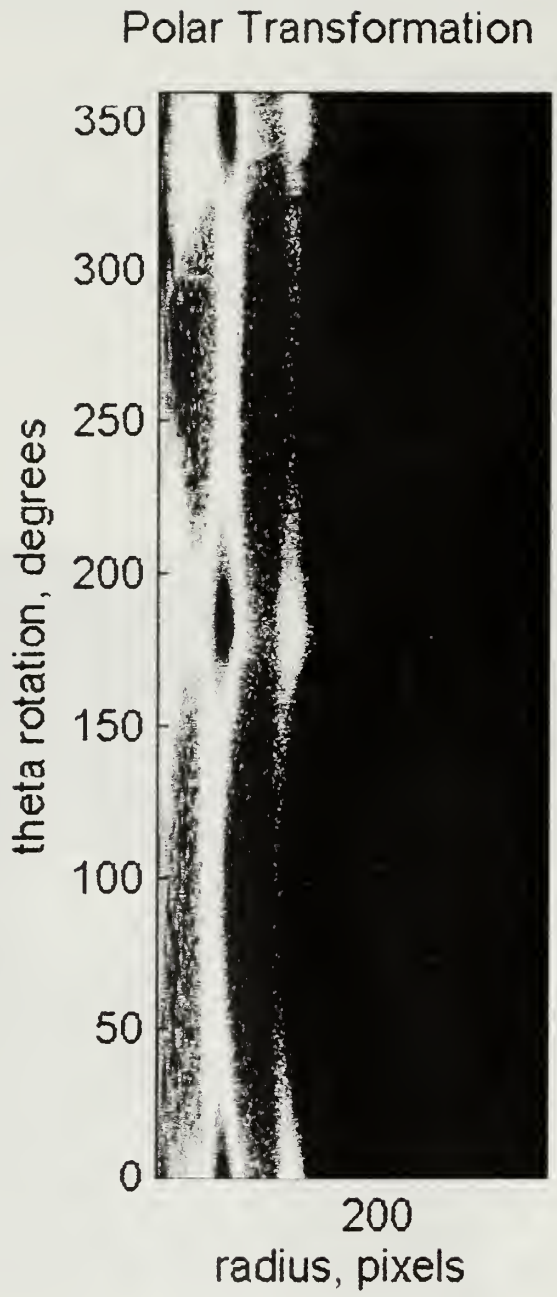

Figure 4.14 Polar Transformation of 2D SAXS of P(S_{53}-*b*-UEMA-IbuPOSS$_{41}$) After Preparative GPC

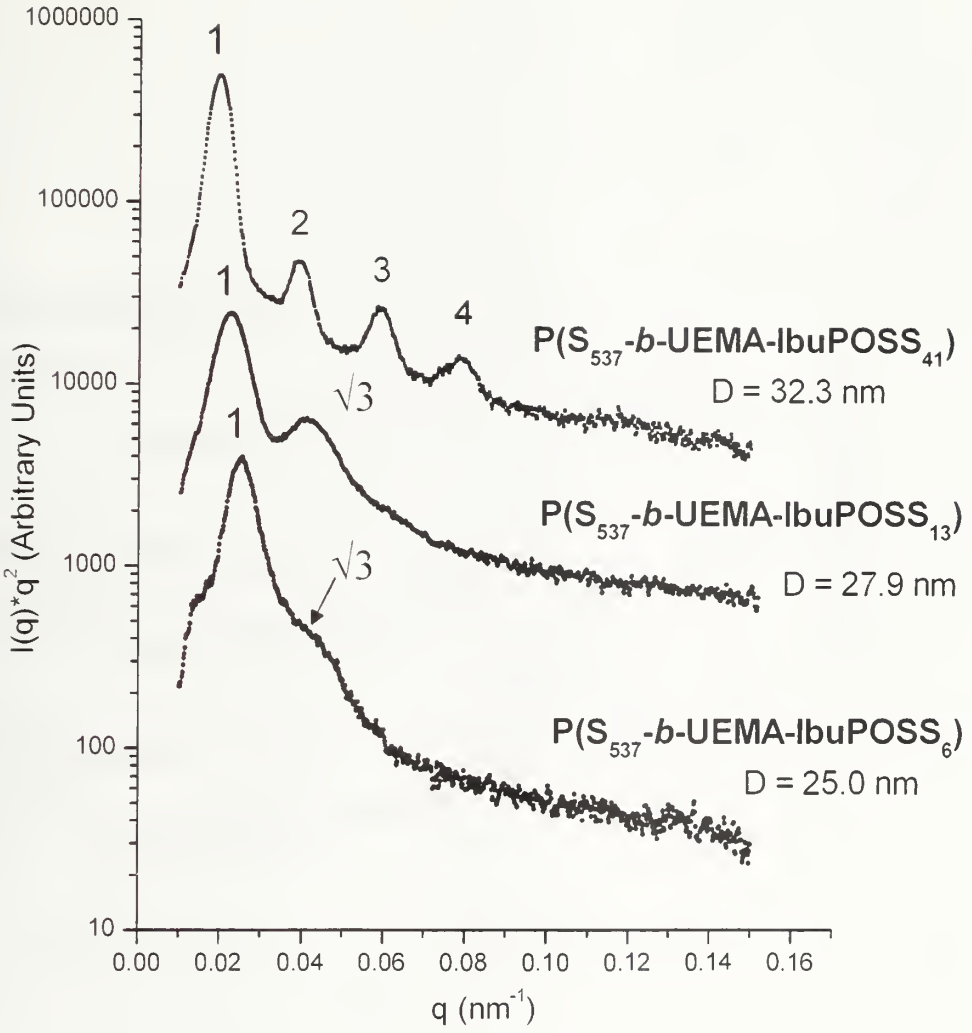

Figure 4.15 SAXS of the P(S_{537}-*b*-UHEMA-IbuPOSS$_x$) Series

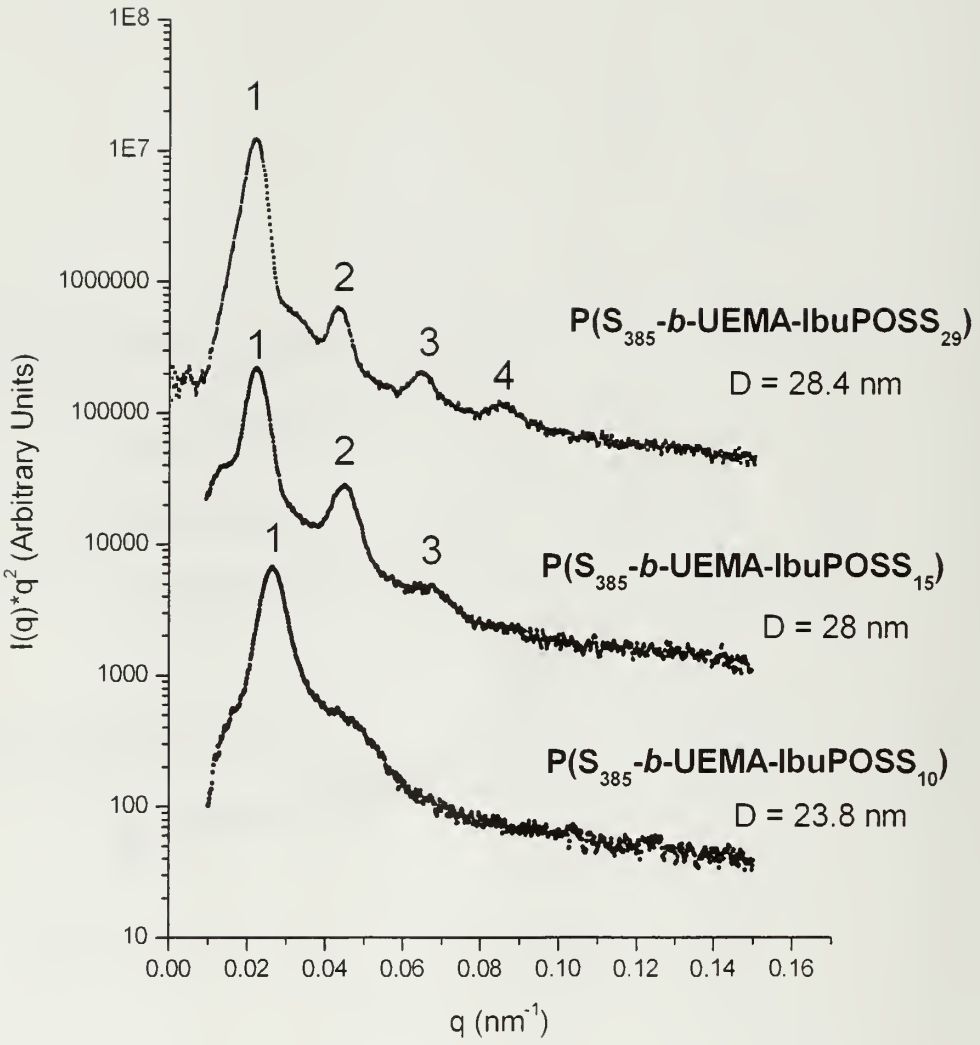

Figure 4.16 SAXS of the P(S_{385}-*b*-UEMA-IbuPOSS$_x$) Series

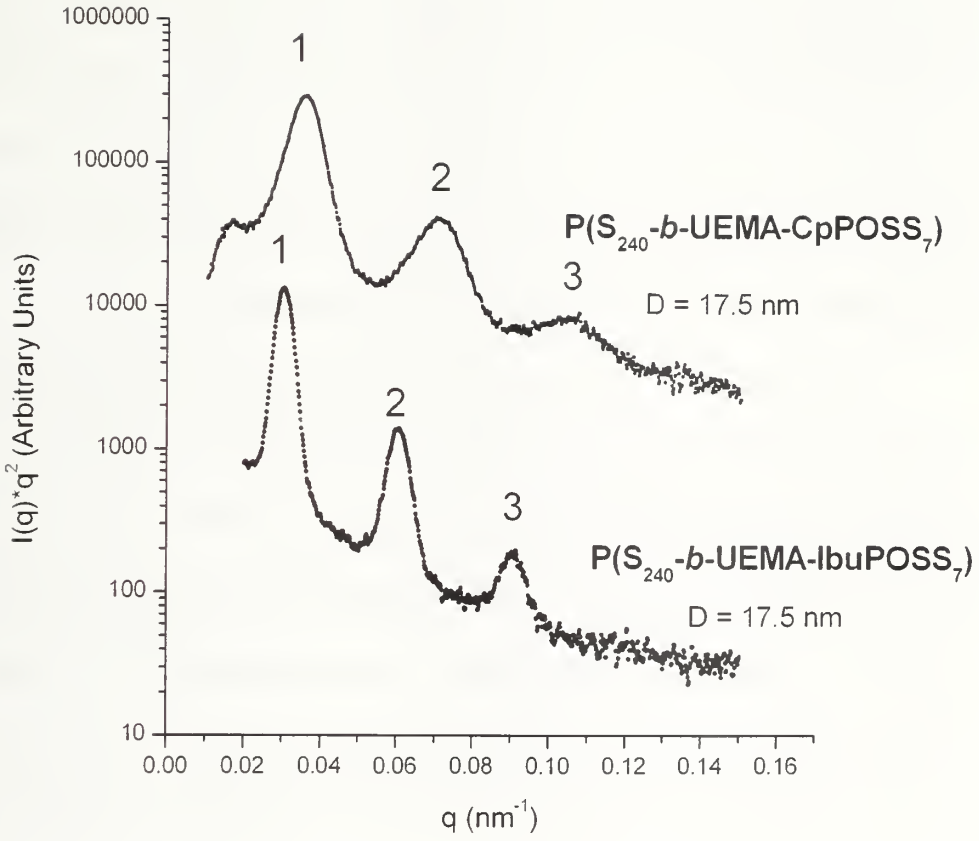

Figure 4.17 SAXS of P(S_{240}-*b*-UEMA-CpPOSS-$_7$) and P(S_{240}-*b*-UEMA-IbuPOSS-)

By varying the degree of polymerization of the second block and therefore the POSS volume fraction, cylinders could be obtained. **P(S_{53}-*b*-UEMA-IbuPOSS$_{13}$)**, **P(S_{53}-*b*-UEMA-IbuPOSS$_6$)** and **P(S_{385}-*b*-UEMA-IbuPOSS$_{10}$)** display a cylindrical morphology. For both **P(S_{53}-*b*-UEMA-IbuPOSS$_{13}$)** and **P(S_{385}-*b*-UEMAI-buPOSS$_{10}$)**, a second-order reflection at angular position of $\sqrt{3}$ of the first-order maximum is observed, indicating a possible cylindrical morphology. On the **P(S_{53}-*b*-UEMA-IbuPOSS$_6$)** diffractogram, the ratio between the second or third-order peak to the first-order one does not correspond to any known morphology. To further elucidate

the structure of these three samples, TEM study was carried out. Figures 4.11 and 4.12 show a cylindrical morphology for both **P(S_{537}-*b*-UEMA-IbuPOSS$_{13}$)** and **P(S_{537}-*b*-UEMA-IbuPOSS$_6$)**. Black cylinders containing POSS can be seen perpendicular and lying parallel to the surface of the microtomed section. From the TEM image, cylinder diameters of approximately 15 nm and 5 nm are observed for **P(S_{537}-*b*-UEMA-IbuPOSS$_{13}$)** and **P(S_{537}-*b*-UEMA-IbuPOSS$_6$)** respectively.

The only difference between **P(S_{240}-*b*-UEMA-IbuPOSS$_7$)** and **P(S_{240}-*b*-UEMA-CpPOSS$_7$)** is the alkyl periphery on the POSS cube (Figure 4.17). Interestingly enough, much sharper diffraction peaks can be observed in the case of an isobutyl versus a cyclopentyl periphery. A faster crystallization of CpPOSS versus IbuPOSS may be at the origin of this observation, preventing the material from reaching a state closer to equilibrium as the meta-stable morphology will get "frozen" when the POSS particles crystallize. Wider peaks in SAXS diffraction patterns would be obtained in that case.

4.5 Conclusion

A very efficient method to organize POSS particles at a microscopic level has been developed. A poly(styrene-*b*-HEMA) series was synthesized by sequential anionic polymerization, enabling a very precise control over the polydispersity and the degree of polymerization of each block. This method enables accurate control over the quantity of POSS incorporated into the hybrid organic-inorganic polymer. POSS-NCO was incorporated quantitatively into a poly(styrene-*b*-HEMA) block copolymer via condensation between the isocyanate of the POSS particles and the pendant alcohol of the HEMA block. This reaction proceeds to completion. Morphological studies by TEM and SAXS revealed long-range ordering of the material into lamellae or cylinders depending on the volume fraction of each block. Long-range order is obtained just by solvent casting and is a unique and unusual feature of this particular hybrid organic-inorganic material. These materials are currently being studied as thin film on silica wafer in an effort to orient the POSS domains perpendicular to the surface.

4.6 References

(1) Gomez-Romero, P. *Advanced Materials* **2001,** 13, (3), 163-174.

(2) Judeinstein, P.; Sanchez, C. *J. Mater. Chem.* **1996,** 6, (4), 511-525.

(3) Nalwa, H. S., *Handbook of organic-inorganic hybrid materials and nanocomposites*. American Scientific Publishers: Stevenson Ranch, Calif., 2003; p 2 v.

(4) Schottner, G. *Chem. Mater.* **2001,** 13, (10), 3422-3435.

(5) Houbertz, R.; Domann, G.; Schulz, J.; Olsowski, B.; Frohlich, L.; Kim, W. S. *Appl. Phys. Lett.* **2004,** 84, (7), 1105-1107.

(6) Hagfeldt, A.; Gratzel, M. *Acc. Chem. Res.* **2000,** 33, (5), 269-277.

(7) Innocenzi, P.; Lebeau, B. *J. Mater. Chem.* **2005,** 15, (35-36), 3821-3831.

(8) Kickelbick, G. *Progress in Polymer Science* **2003,** 28, (1), 83-114.

(9) Zhang, X.; Chan, E. R.; Glotzer, S. C. *J. Chem. Phys.* **2005,** 123, (18).

(10) Lee, J. Y.; Balazs, A. C.; Thompson, R. B.; Hill, R. M. *Macromolecules* **2004,** 37, (10), 3536-3539.

(11) Thompson, R. B.; Ginzburg, V. V.; Matsen, M. W.; Balazs, A. C. *Science* **2001,** 292, (5526), 2469-2472.

(12) Kawasumi, M. *J. Polym. Sci., Part A: Polym. Chem.* **2004,** 42, (4), 819-824.

(13) Sanchez, C.; Soler-Illia, G.; Ribot, F.; Lalot, T.; Mayer, C. R.; Cabuil, V. *Chem. Mater.* **2001,** 13, (10), 3061-3083.

(14) Mercier, L.; Pinnavaia, T. J. *Advanced Materials* **1997,** 9, (6), 500-&.

(15) Soler-illia, G. J. D.; Sanchez, C.; Lebeau, B.; Patarin, J. *Chemical Reviews* **2002,** 102, (11), 4093-4138.

(16) Templin, M.; Franck, A.; DuChesne, A.; Leist, H.; Zhang, Y. M.; Ulrich, R.; Schadler, V.; Wiesner, U. *Science* **1997,** 278, (5344), 1795-1798.

(17) Pittman, C. U.; Li, G. Z.; Ni, H. L. *Macromolecular Symposia* **2003,** 196, 301-325.

(18) Waddon, A. J.; Coughlin, E. B. *Chem. Mater.* **2003,** 15, (24), 4555-4561.

(19) Joshi, M.; Butola, B. S. *Journal of Macromolecular Science-Polymer Reviews* **2004,** C44, (4), 389-410.

(20) Haddad, T. S.; Lichtenhan, J. D. *Macromolecules* **1996,** 29, (22), 7302-7304.

(21) Bharadwaj, R. K.; Berry, R. J.; Farmer, B. L. *Polymer* **2000,** 41, (19), 7209-7221.

(22) Tsuchida, A.; Bolln, C.; Sernetz, F. G.; Frey, H.; Mulhaupt, R. *Macromolecules* **1997,** 30, (10), 2818-2824.

(23) Abad, M. J.; Barral, L.; Fasce, D. P.; Williams, R. J. J. *Macromolecules* **2003,** 36, (9), 3128-3135.

(24) Wright, M. E.; Schorzman, D. A.; Feher, F. J.; Jin, R. Z. *Chem. Mater.* **2003,** 15, (1), 264-268.

(25) Laine, R. M. *J. Mater. Chem.* **2005,** 15, (35-36), 3725-3744.

(26) Cardoen, G.; Coughlin, E. B. *Macromolecules* **2004,** 37, (13), 5123-5126.

(27) Pyun, J.; Xia, J. H.; Matyjaszewski, K. *Synthesis and Properties of Silicones and Silicone-Modified Materials* **2003,** 838, 273-284.

(28) Intasanta, N.; Russell, T. P.; Coughlin, E. B. In *Ultrathin films of self-assembled organic-inorganic hybrid nanoparticle block copolymers*, Abstracts of Papers of the American Chemical Society, Anaheim, 2004; Anaheim, 2004.

(29) Morton, M. F., L.J. *Rubber Chem. Technol.* **1974,** 48, 359.

(30) Hadjichristidis, N.; Iatrou, H.; Pispas, S.; Pitsikalis, M. *J. Polym. Sci., Part A: Polym. Chem.* **2000,** 38, (18), 3211-3234.

(31) Uhrig, D.; Mays, J. W. *Journal of Polymer Science Part a-Polymer Chemistry* **2005,** 43, (24), 6179-6222.

(32) Hadjichristidis, N.; Pitsikalis, M.; Pispas, S.; Iatrou, H. *Chemical Reviews* **2001,** 101, (12), 3747-3792.

(33) Hirao, A.; Kato, H.; Yamaguchi, K.; Nakahama, S. *Macromolecules* **1986,** 19, (5), 1294-1299.

(34) Ishizone, T.; Han, S.; Okuyama, S.; Nakahama, S. *Macromolecules* **2003,** 36, (1), 42-49.

(35) Ehlich, D.; Takenaka, M.; Okamoto, S.; Hashimoto, T. *Macromolecules* **1993,** 26, (1), 189-197.

(36) Hashimot,T; Nagatosh,K; Todo, A.; Hasegawa, H.; Kawai, H. *Macromolecules* **1974,** 7, (3), 364-373.

APPENDIX

MANIFOLD ASSEMBLY FOR THE CONVENIENT POLYMERIZATION OF ETHYLENE OXIDE AND BUTADIENE

A.1 Introduction

Working with gaseous compounds presents technical challenges not commonly encountered when using solutions and solids. Due to their volatility and potential toxicity, special equipment needs to be designed for safe handling of gaseous chemicals. Ethylene oxide (EO) and butadiene (BD) are two examples of gaseous monomers at room temperature. Typically, these two gaseous monomers are handled in expensive high-pressure stainless steel reactors or under high-vacuum using custom-made glassware.[1] Both monomers can be polymerized by "living" anionic polymerization to afford polymer with predictable molecular weight and low polydispersity (< 1.1).[1, 2] Nevertheless, rigorous purification as well as quantitative measurement or molar amounts are required to make the polymerization truly controlled. Traditionally, anionic polymerization has been done using high vacuum techniques.[3, 4] These techniques require extensive glass blowing expertise and are time consuming. Another limitation of high vacuum technique is that only a few grams of sample can be synthesized per polymerization. To circumvent these issues, protocols based on Schlenk techniques have been used to perform living anionic polymerization.[5] It is possible to synthesize tens of grams of polymer using Schlenk techniques in a single day.

Safety Note: ***CAUTION!*** *Operating with 1,3-butadiene and ethylene oxide require great care as they boils at -4.41°C and 10.7°C respectively and are toxic and flammable. Efficient thermostating at the temperatures reported is necessary when keeping or treating the monomers in glass containers or when it is transferred into the glass reactor. Failure to observe these precautions can lead to explosions and fire.*

Ethylene oxide can be polymerized anionically to afford poly(ethylene oxide) (PEO) with controlled molecular weight and low polydispersity (below 1.1), and as a consequence has been widely used as a hydrophilic block in macromolecular amphiphiles because of its high polarity, ion transporting ability,[6, 7] and bio-compatibility.[8] 1,3-Butadiene is a major commodity chemical used in the manufacture of synthetic rubber and various plastics. For instance, the incorporation of poly(butadiene) in a material drastically modifies mechanical properties. 1,3-Butadiene can be polymerized by radical, ionic or metal-catalyzed polymerizations. Anionic polymerization enables excellent control over molecular weight and polydispersity. A typical application of the anionic polymerization of 1,3-butadiene is found in the synthesis of styrene-butadiene-styrene rubber.[9]

Poly(butadiene-*b*-ethylene oxide) and more generally poly(alkane-*b*-ethylene oxide) have found applications in the biology arena. It has recently been shown that it is possible to self-assemble amphiphilic block copolymers into micelles which structurally mimic vesicles.[10] These vesicles-forming block-copolymers are potential candidates for entrapping biologically active molecules.[11] Also, vesicle-forming polymers offer fundamental insight into the natural design principles for biomembranes.[12]

As of today, only a few reports describing handling of gaseous monomers can be found.[5, 13] Herein, we describe the construction of a stainless steel manifold for the

facile and safe handling and polymerization of ethylene oxide and 1-3-butadiene. Standard Schlenk glassware can be efficiently used as a reactor for the living polymerization of the two gaseous monomers, which makes the setup ideal for use in an academic laboratory. The gases are transferred by vacuum distillation and condensed at low temperature. Using this manifold, it is possible to run several experiments in a single day. The synthesis of a model poly(butadiene-*b*-ethylene oxide) by anionic polymerization will be described to illustrate a typical experimental protocol using the manifold.

A.2 Manifold Description

A.2.1 Equipment

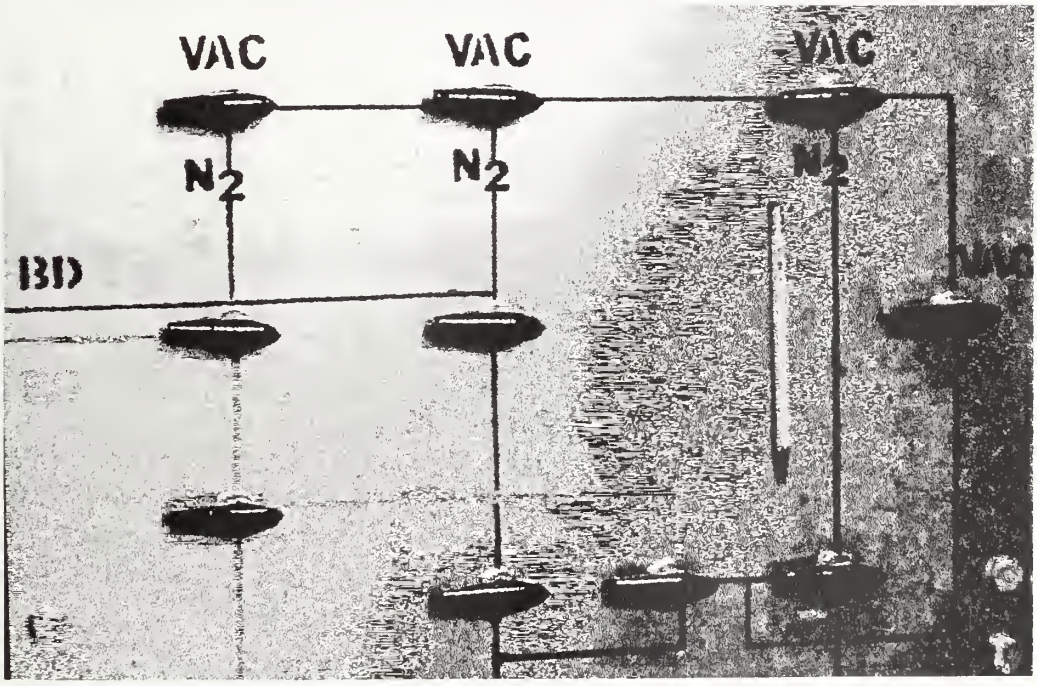

Figure A.1 Front of the Manifold

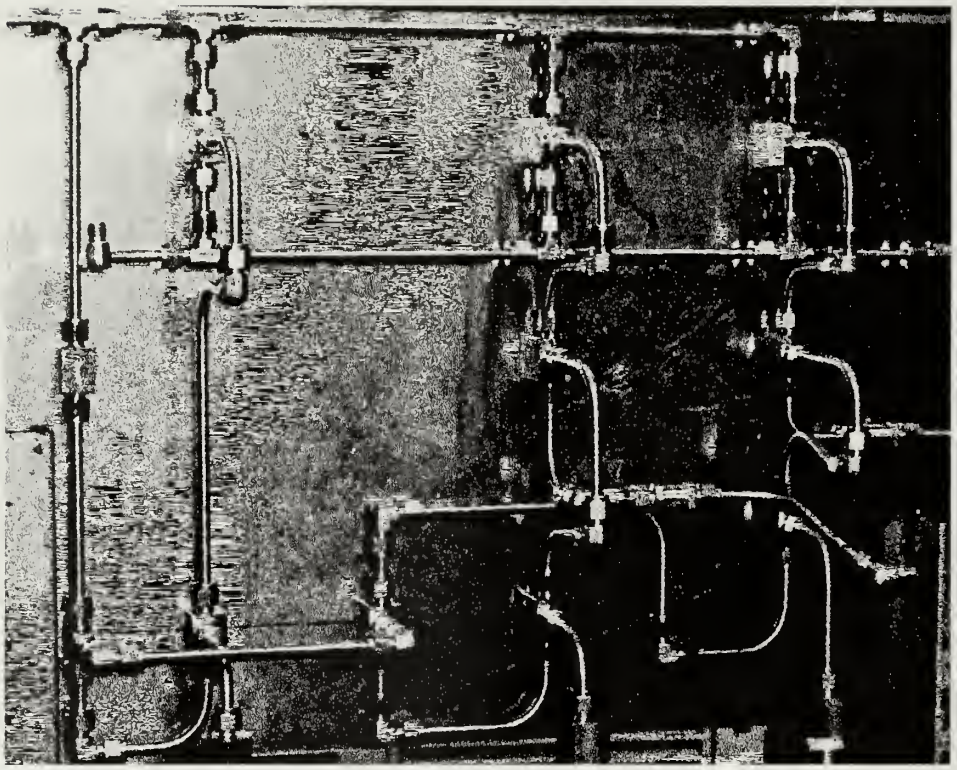

Figure A.2 Back of the Manifold

Pictures of the front and the back of the manifold can be seen on Figure 5.1 and Figure 5.2 respectively. On the front of the manifold, a pencil was attached to give a better idea of the size of the manifold, which can be conveniently set up inside a fume hood.

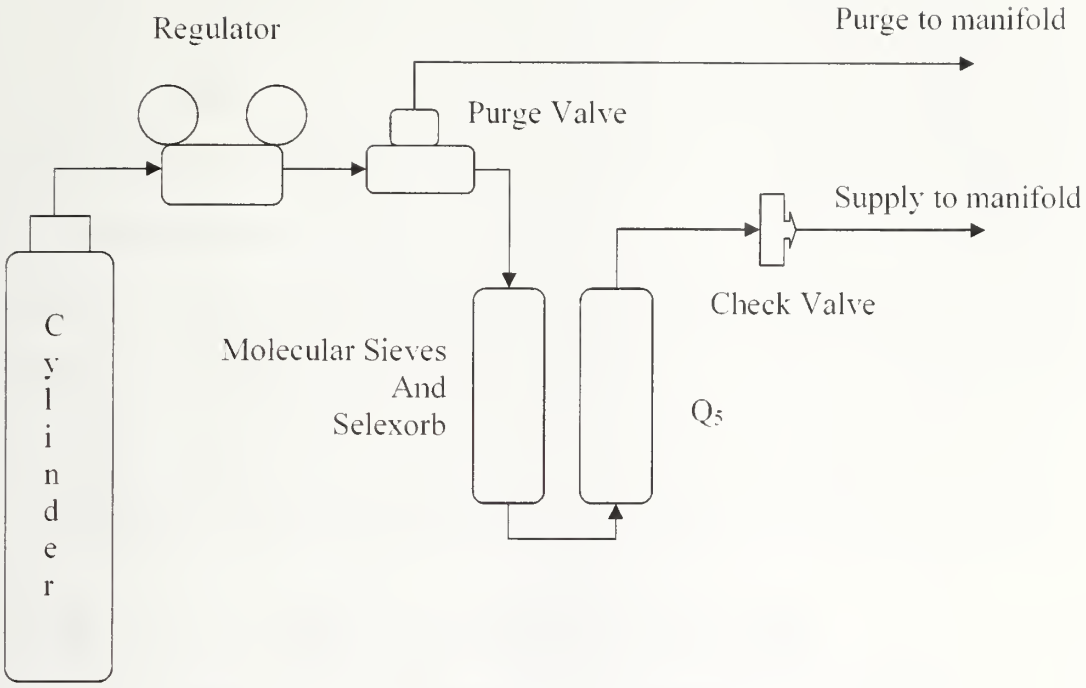

Figure A.3 Tank Farm Schematic for Butadiene and Nitrogen Supply Line. The Purification Train of the Ethylene Oxide Line Contains only Molecular Sieves.

A representative diagram for the monomer tank farm is shown in Figure 5.3. A detailed listing of the quantity, part numbers, and manufacturers for all materials needed to construct the manifold can be found in Table 5.1. The pressure regulators are connected to the gas cylinders of ethylene oxide, 1,3-butadiene, or nitrogen via flexible stainless steel tubing. A valve is placed after the regulator of each cylinder in order to shut off the supply line to the manifold and purge the regulator after replacing a cylinder. The nitrogen purification line is built identically to the butadiene purification line, columns of molecular sieves (3Å), Selexsorb® COS and copper (II) oxide on alumina (oxygen scavenger) are placed in line to remove residual water, carbon dioxide and oxygen impurities respectively. The copper (II) oxide on alumina is reduced to copper (0) by passing a mixture of nitrogen/hydrogen 95/5% though the column at 200 °C until no further water is generated. Argon may be used as an inert gas instead of

nitrogen. The purification column for the ethylene oxide line has only molecular sieves. It was observed that ethylene oxide will polymerize in contact with Selexorb and eventually clog the system. To maintain tank purity and laboratory safety, check valves are placed after the purification columns. Check valves with a relief pressure of 1/3 psig are used for the ethylene oxide and 1,3-butadiene supply while a check valve with a relief pressure of 10 psig is used for the nitrogen line. The lecture bottles of ethylene oxide and 1,3-butadiene are placed in a fume hood for safety purposes. All items have normal pipe thread (NPT) fittings and are connected with stainless steel tubing.

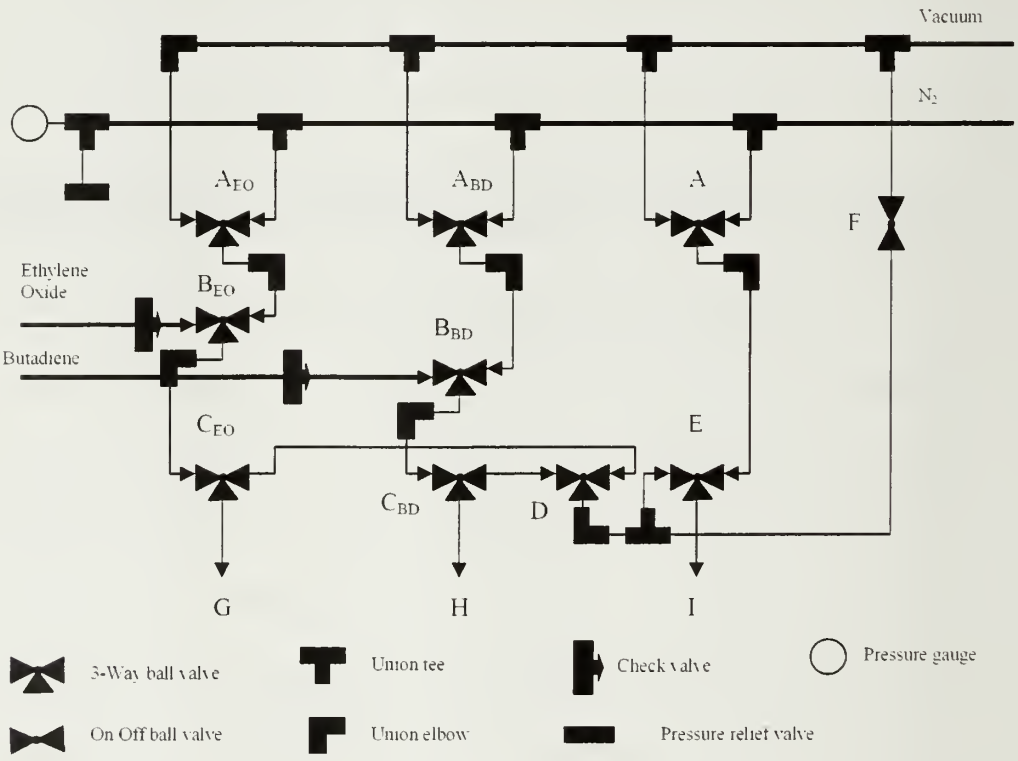

Figure A.4 Manifold schematic. Ball Valves and the Pressure Gauge are Mounted in the Faceplate with the Plumbing Behind the Plate. 3-Way Ball Valves are Drawn such that the Lower Triangle Represents the Back of the Valve.

A full diagram for the manifold is shown in Figure 5.4. The entire manifold is assembled on a 1.5 ft × 2 ft × $^1/_4$ in. sheet of rolled aluminum in which the ball valves

are mounted with the plumbing on the backside. Pressure gauges (0-15 psig) and pressure relief valves (set to 10 psi) are placed in the line with branch tees. Stainless steal tubing was bent, cut to length, and attached via Swagelok® fittings. After construction, the manifold was tested for leaks by pressurizing with N_2 (50 psig) and monitoring for a pressure drop over a 24 h period. The assembled manifold was then mounted in a fume hood via lab feet bolted on the corners and the middle of the faceplate. Additionally, the manifold was stabilized with horizontal legs attached directly behind the plate (1 in. unistrut). Outlets **G** and **H** (Figure 5.4) have standard taper 14/20 ground glass joints connected to ¼ in. glass tubing while outlet **I** has a standard taper 24/40 ground glass joint connected to ½ in. glass tubing. A glass-to-metal transition for the gas outlets **G**, **H** and **I** were made by using either an Ultra-Torr Swagelok Tube Fitting Union or a stainless steal union ($^1/_4$ in. for outlet **G** and **H**). In the later case, stainless steal ferrules were replaced by Teflon® ferrules to ensure a leak-free glass-to-metal transition. Outlet **I** was made with a reducing union (½ in. to ¼ in.) in conjunction with ½ in. Teflon® ferrule.

The vacuum line was custom-made but any commercial vacuum manifold with Teflon plugs would work.[5] A single-stage oil diffusion pump is used between the vacuum manifold and the mechanical pump for improved vacuum. Two vacuum traps, in series, prevent the diffusion pump oil and the mechanical pump oil from being contaminated. The working vacuum is found to be between 5 and 10 mTorr. One outlet of the vacuum manifold is connected to the stainless steal manifold via heavy wall rubber tubing. Another outlet of the vacuum manifold is used to purge the

ethylene oxide and 1,3-butadiene lines with nitrogen as described in the experimental procedure section.

Swagelock®	www.swagelock.com	
Part #	Description	Quantity
SS-43XS4	Switching 3-Way Valve	15
SS-83XTS4	Whitey Multi-Service Trunnion Ball Valve 3-way	3
SS-43S4	On-Off Valve	2
SS-400-3	Union Tee	8
SS-400-9	Union Elbow	20
SS-4C-1/3	Check Valve	4
SS-4C-10	Check Valve	1
SS-4CPA4-3	Check Valve Adj. 1/4 FTP 3-50 Cracking Pressure	1
304L-HDF4-75	Kit, Cylinder	4
304L-HDF4-300	Kit, Cylinder	2
SS-T4-S-035	SS 1/4" .035 Wall Tubing	40 Feet
SS-400-6	Union 1/4T	2
SS-810-6-4	Reducing Union 1/2T * 1/4T	1
SS-4-UT-6-400	Ultra-Torr Swagelok Tube Fitting Union 1/4T	2
SS-FM4SL4PF4-25	Flexible Metal Hose 1/4"	2
PFA-424-1	Teflon Back Ferrule 1/4"	2
PFA-423-1	Teflon Front Ferrule 1/4"	2
PFA-824-1	Teflon Back Ferrule 1/2"	1
PFA-823-1	Teflon Front Ferrule 1/2"	1
Omega	www.omega.com	
DPG1000B-15G	DPG1000 Digital Pressure Gauges 0-15.00 psig battery powered digital pressure gauge	
Aldrich	www.aldrich.com	
Z14,850-4	Corrosive Lecture Bottle Regulator	2
41,797-1	Copper (II) oxide on alumina	500g
208574	Molecular sieves (3A)	1kg
Alcoa	www.alcoa.com	
Selexsorb® COS		500g

Table A.1 Parts lists for the manifold

A.2.2 Experimental Procedures

A.2.2.1 Materials

Sec-butyl lithium (1.6 M), *n*-butyl lithium (1.6 M), butadiene (99+%), ethylene oxide (99.5+%), styrene (99+%), tetrahydrofuran (THF, anhydrous, 99.9%), *N,N*-Dimethylacetamide (99+%,spectrophotometric grade) and potassium (chunks in mineral oil, 98%) were purchased from Aldrich and used as received. Triphenyl methane was purchased from Aldrich and sublimed (103 °C, 6 mTorr) prior to use. *Sec*-butyl lithium was titrated by the Gilman double titration method.[14] Benzene (99+%) and chloroform were purchased from Fisher. Benzene was first stirred over sulfuric acid (100 ml of acid for one liter of solvent) for 24 h, distilled over calcium hydride and stored in a Schlenk flask containing a solution of *n*-butyl lithium/styrene (5 ml of *n*-butyl lithium and 0.5 ml of styrene per liter of solvent). Tetrahydrofuran was purified by distillation from a sodium/benzophenone mixture.

Trityl potassium solution was prepared by mixing triphenyl methane (8g, 32.7 mmol) and potassium (3g, 76.73 mmol) in 100 ml of THF. After stirring overnight, the deep-red solution was filtered to remove to excess of potassium metal and stored under an inert atmosphere. The solution can be stored in an air-free flask for months without degradation.

A.2.2.2 Instrumentation

Gel permeation chromatography (GPC) measurements of PBD-OH were performed in tetrahydrofuran (THF) at 1.0 mL/min using a Knauer K-501 Pump with a K-2301 refractive index detector and K-2600 UV detector, and a column bank consisting of two Polymer Labs PLGel Mixed D columns and one PLGel 50 A column (1.5 x 30 cm) at

35°C. Molecular weights are reported relative to polystyrene standards (Polymer Labs. Inc.). GPC measurements of PBD-PEO were performed in a mixture of THF and *N,N*-Dimethylacetamide (DMAc) (90:10 by vol) at 1ml/min.[15] A pump (HP Series 1050) with a refractive index detector (HP 1047A) and two Polymer Labs ResiPore 3μm (300 x 7.5mm) columns were used. Molecular weights are reported relative to PEO standards (Polymer Labs. Inc). ^{1}H NMR spectra were performed in $CDCl_3$ at room temperature on a Bruker 300 MHz.

A.3 Results and Discussion

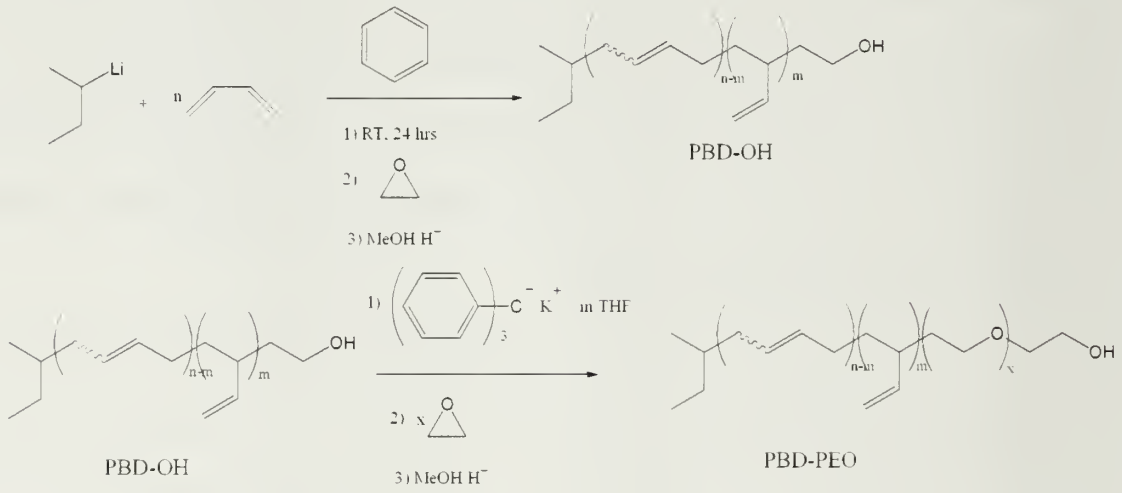

Figure A.5 Synthesis of Poly(butadiene-*b*-ethylene oxide) by Anionic Polymerization

The synthesis of a poly(butadiene-*b*-ethylene oxide) diblock copolymer by anionic polymerization is described to illustrate a typical experimental procedure using the manifold (Figure 5.5). The results obtained are summarized in Table 1. The description of the outlets and the various valves are referred to by a letter designation as shown in Figure 5.4. The manifold enables purification and measurement of a known

amount of gaseous monomer (outlets **G** and **H**). Then, the desired amount of monomer is transferred to the reaction flask (outlet **I**).

Table A.2 Summary of the Results of the Polymerization

Entry	Amount of monomer (vol at - 78°C, mol)	Amount of initiator (or macroinitiator) (vol or mass, mol)	$M_{n,theo}$ (calculated, g/mol)	$M_{n,obs}$[1] (PDI)
PBD polymerization	Butadiene (15 ml, 0.205 mol)	Sec-butyl lithium (0.92 ml, 1.29 mmol)	8,596	8660 (1.03)
PEO polymerization	Ethylene oxide (3.4ml, 77.2 mmol)	PBD-OH (4g, 0.462 mmol of OH	7,360	7260 (1.08)

[1] For polybutadiene. $M_{n,obs}$ (Number average molecular weight observed) was measured by THF GPC versus polystyrene standard. A coefficient of 1.86 was applied to calculate the real polybutadiene molecular weight (Mark-Houwink parameters). The observed molecular weight for PEO was calculated from ^{1}H NMR.

A.3.1 Synthesis of Hydroxy-Terminated Polybutadiene by Anionic Polymerization

The manifold is first evacuated by opening valves **A**, $\mathbf{A_{EO}}$, $\mathbf{A_{BD}}$, $\mathbf{B_{EO}}$ and valve $\mathbf{B_{BD}}$ to vacuum, and opening valve **F**. Valves $\mathbf{C_{EO}}$, $\mathbf{C_{BD}}$ and valve **E** are kept closed. Valve **D** allows switching from one gas to the other and should be open to the monomer used first, 1,3-butadiene in this case. Even after passing through the purification columns ethylene oxide and 1,3-butadiene are not pure enough to perform anionic polymerization. Additional purification steps are required. In a flame-dried 50 ml Schlenk flask, 3 ml of *n*-butyl lithium, 1.6 M, is added via syringe under inert atmosphere. Subsequently the flask is attached to outlet **H** and the hexanes are removed under vacuum by opening valve $\mathbf{C_{BD}}$. Subsequently, valve $\mathbf{A_{BD}}$ is closed and valve $\mathbf{B_{BD}}$

is opened to the 1.3-butadiene line. The evacuated Schlenk flask attached to outlet H is cooled to -78°C (acetone/dry ice mixture), and approximately 15 ml of 1.3-butadiene is condensed. This is then stirred at -10°C (salt/ice mixture) for one hour. Purified benzene (200 ml) is vacuum distilled into a flame-dried Schlenk flask containing a glass stir bar and 0.62 ml of *sec*-BuLi, 1.2 M. This Schlenk flask is connected to outlet **I** and is used as the reaction flask. Outlet **I** bears a side arm with a graduated cylinder attached as depicted in Figure 5.6. Once the reaction flask is connected to outlet **I**, valve **E** is opened to vacuum and the side arm is flame-dried while the reaction flask is kept closed. The density of butadiene is 0.74 g/ml at -78°C.[16] The purified 1.3-butadiene (15 ml, 0.205 mol) is then vacuum transferred into the side arm cooled to -78°C by closing valve **A** and valve **F** and turning valve $\mathbf{C_{BD}}$ the opposite way to connect the purified 1.3-butadiene to valve **D**. Finally, valve **E** is open to valve **D**. Finally, valve **A**, valve **E** and the Schlenk flask containing the initiator are open to nitrogen. The reactor is left under an inert atmosphere overnight. The 1.3-butadiene distills slowly into the reaction flask and is consumed by the living polymer chain-end. The pressure drop can be followed with the in-line pressure gauge.

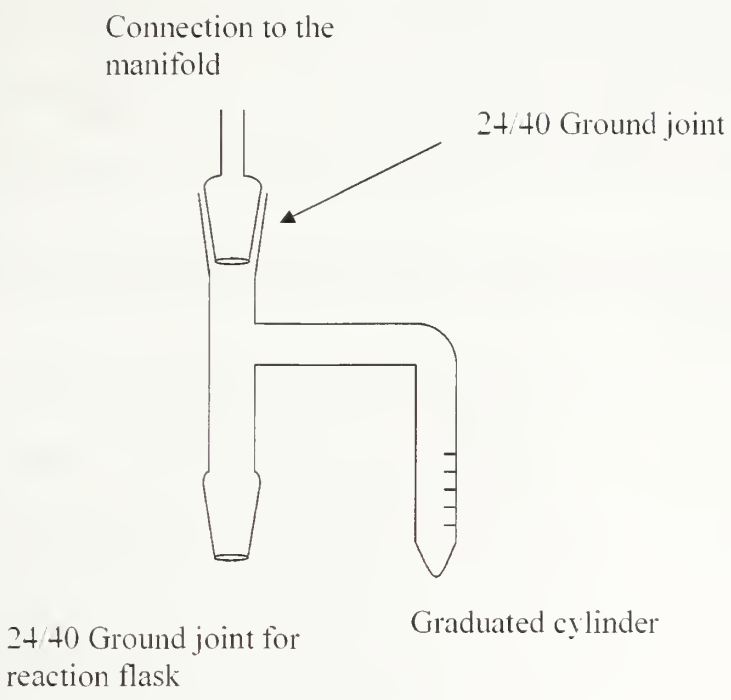

Figure A.6 Graduated Cylinder Connected to Outlet I

After 24 h, the reaction flask is closed and the side arm is evacuated again by opening valve **A** and valve **E** to vacuum. Ethylene oxide is also purified before being added to the reactor. Valve **F** is opened and then valve **E** is opened to ethylene oxide. In a flame-dried 25 ml Schlenk flask, 1 ml of *n*-butyl lithium (1.6M) was added by syringe, connected to outlet **G** and the hexane was distilled off by opening valves $\mathbf{A_{EO}}$, $\mathbf{B_{EO}}$ and $\mathbf{C_{EO}}$ to the vacuum. Ethylene oxide (2 ml, 0.045 mol) is condensed in the Schlenk flask at -78 °C by opening valve $\mathbf{B_{EO}}$ to the ethylene oxide line. Ethylene oxide is stirred over *n*-BuLi for 1 hour at 0 °C, and then 1ml of ethylene oxide (0.027mol), is subsequently condensed to a graduated cylinder connected to outlet **I** by opening valve $\mathbf{C_{EO}}$ to valve **D** and valve **E** to valve **D**. The ethylene oxide is subjected to three freeze-pump-thaw cycles, and valve **A**, valve **E** and the reaction flask are open to nitrogen. After one hour, the polymer (PBD-OLi) was precipitated in acidic methanol. A number

average molecular weight (M_n) of 16,110 g/mol was obtained for the resultant PBD-OH by GPC using a THF mobile phase. A correction according to the Mark-Houwink equation resulted in a M_n of 8660 g/mol with a polydispersity index of 1.03.

A.3.2 Synthesis of Poly(butadiene-*b*-ethylene oxide) (PBD-PEO) by Anionic Polymerization

PBD-OH (4g, 0.462 mmol) was first dried overnight in a vacuum oven at room temperature. Then, three consecutive azeotropic distillations from dried benzene at room temperature under reduced pressure (10mTorr) were performed and the polymer was left overnight under dynamic vacuum. Subsequently, 100ml of tetrahydrofuran was distilled into the reaction flask. The hydroxyl group of PBD-OH was titrated with trityl potassium to a 1:0.9 (hydroxyl group: trityl potassium) ratio. Titrating to the equivalent point is not necessary, as the proton exchange rate between the hydroxyl end-group of the polymer and the potassium alkoxide species generated by deprotonation proceeds at a much faster rate than the polymerization of ethylene oxide.[17]

The reaction flask containing PBD-OK is connected to outlet **I** and the manifold is evacuated by opening valves $\mathbf{A_{EO}}$, **A**, **F**, $\mathbf{B_{EO}}$, and valve **E** to vacuum. Valve **D** is opened to the ethylene oxide line. The same purification and transfer protocol that was used for the end-capping of the polybutadiene anion with ethylene oxide applies here. Ethylene oxide (3.4 ml, 77.2 mmol) was condensed in the graduated cylinder connected to outlet **I**. At this stage, ethylene oxide is slowly warmed to room temperature, enabling transfer to the reaction flask (Valve **A** is open to nitrogen and the reaction flask is also open). Alternatively, it is possible to condense ethylene oxide directly in

the reaction flask by cooling the THF solution in the reactor to 0°C. Once all the monomer has been condensed in the THF solution, the flask can be closed and disconnected from the line. The reaction flask was left for 3 days with stirring at room temperature. The living polymer was terminated by adding one drop of acidic methanol into the THF solution. To purify the resulting PBD-PEO, flash chromatography with silica gel (50 g) using chloroform as a solvent was used. The block copolymer adsorbs to the silica gel because of the PEO block. After washing the starting material away from the final polymer with 300 ml of chloroform, the polymer is recovered by flushing the silica gel with a 9:1 chloroform:methanol mixture. The solvent is removed and the polymer dried overnight. Analysis by GPC using the solvent mixture THF:Dimethylacetamide (90:10 v:v) gave M_n = 19.000 g/mol. PDI = 1.08. The M_n of PEO calculated from the ^{1}H NMR integrations was found to be equal to 7.260g/mol. An overlay of PBD-OH and PBD-PEO molecular weight traces obtained with the mixed solvent THF/DMAc GPC is shown in Figure 5.7.

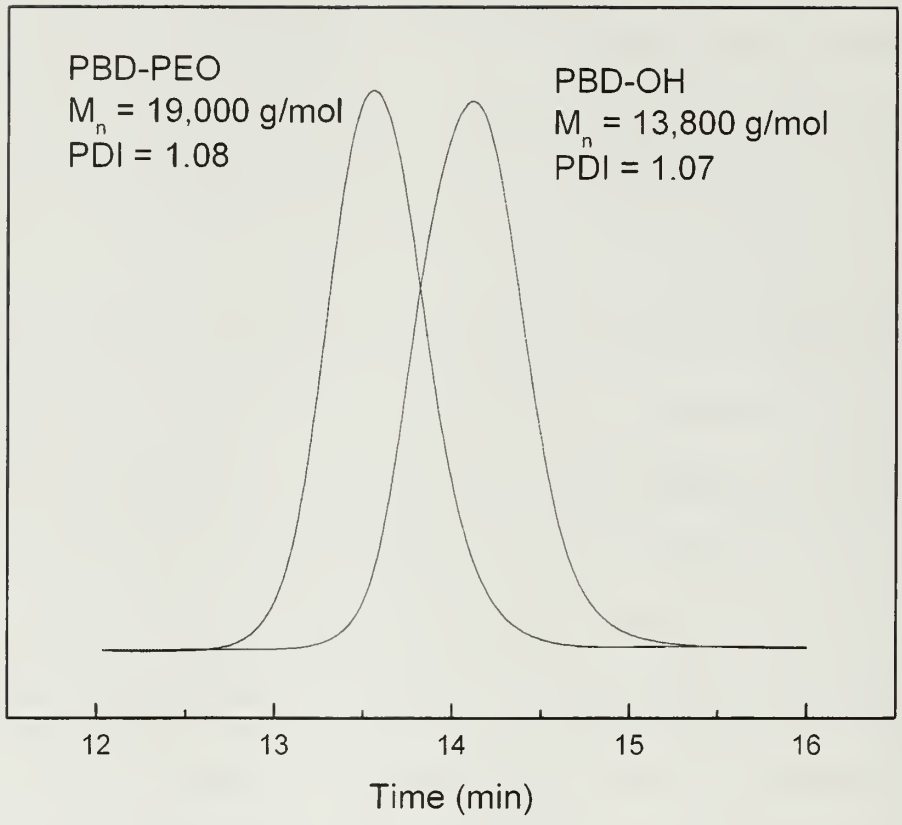

Figure A.7 Overlays of PBD-OH and PBD-PEO Traces Obtained with the THF/DMAc GPC.

A.4 Cleaning Procedure

It is important to maintain the system clean and free of impurities for the best results. After a monomer has been condensed and reacted, the corresponding purification columnss are evacuated and kept under vacuum. For 1,3-butadiene, a Schlenk tube with a side arm is connected to outlet **H**. Valve $\mathbf{B_{BD}}$ and $\mathbf{C_{BD}}$ are opened to the 1,3-butadiene purification train while vacuum is being pulled from the side arm of the Schlenk flask. A similar procedure is repeated for ethylene oxide.

A.5 Conclusion

In summary, we have developed a convenient and safe way to handle and polymerize 1,3-butadiene and ethylene oxide. Using a stainless steal manifold, it is possible to perform several reactions a day on a multi-gram scale. The gaseous monomers are pre-purified by passing through purification columns. It is possible to condense these gases at low temperature, enabling precise volume measurement of the monomers prior to addition into the reaction flask. Synthesis of a model poly(butadiene-*b*-ethylene oxide) was given as an example to illustrate the use of the manifold. It is possible to run polymerizations on a scale of several tens of grams by using the appropriate flasks and solvent quantities. The molecular characterization of the final diblock copolymer is in agreement with results obtained by living anionic polymerization, thus demonstrating the utility of Schlenk techniques to successfully perform anionic polymerizations.

A.6 References

(1) Hsieh, H. L.; Quirk, R. P., *Anionic Polymerization : Principles and Practical Applications*. Marcel Dekker: New York, 1996.

(2) Forster, S.; Kramer, E. *Macromolecules* **1999,** 32, (8), 2783-2785.

(3) Morton, M. F., L.J. *Rubber Chem. Technol.* **1974,** 48, 359.

(4) Hadjichristidis, N.; Iatrou, H.; Pispas, S.; Pitsikalis, M. *J. Polym. Sci., Part A: Polym. Chem.* **2000,** 38, (18), 3211-3234.

(5) Ndoni, S.; Papadakis, C. M.; Bates, F. S.; Almdal, K. *Rev. Sci. Instrum.* **1995,** 66, (2), 1090-1095.

(6) Ohtake, T.; Ogasawara, M.; Ito-Akita, K.; Nishina, N.; Ujiie, S.; Ohno, H.; Kato, T. *Chem. Mater.* **2000,** 12, (3), 782-789.

(7) Kishimoto, K.; Yoshio, M.; Mukai, T.; Yoshizawa, M.; Ohno, H.; Kato, T. *J. Am. Chem. Soc.* **2003,** 125, (11), 3196-3197.

(8) Gref, R.; Minamitake, Y.; Peracchia, M. T.; Trubetskoy, V.; Torchilin, V.; Langer, R. *Science* **1994,** 263, (5153), 1600-1603.

(9) Bhowmick, A. K.; Stephens, H. L., *Handbook of elastomers*. New York, 2001.

(10) Discher, B. M.; Won, Y. Y.; Ege, D. S.; Lee, J. C. M.; Bates, F. S.; Discher, D. E.; Hammer, D. A. *Science* **1999,** 284, (5417), 1143-1146.

(11) Discher, D. E.; Eisenberg, A. *Science* **2002,** 297, (5583), 967-973.

(12) Lee, J. C. M.; Santore, M.; Bates, F. S.; Discher, D. E. *Macromolecules* **2002,** 35, (2), 323-326.

(13) Constable, G. S.; Gonzalez-Ruiz, R. A.; Kasi, R. M.; Coughlin, E. B. *Macromolecules* **2002,** 35, (25), 9613-9616.

(14) Gilman, H.; Cartledge, F. K. *J. Organomet. Chem.* **1964,** 2, (6), 447-454.

(15) Allgaier, J.; Poppe, A.; Willner, L.; Richter, D. *Macromolecules* **1997,** 30, (6), 1582-1586.

(16) Reid, R. C.; Prausnitz, J. M.; Poling, B. E., *The properties of gases and liquids*. 4th ed.; McGraw-Hill: New York, 1987; p x, 741.

(17) Feng, X. S.; Taton, D.; Chaikof, E. L.; Gnanou, Y. *J. Am. Chem. Soc.* **2005,** 127, (31), 10956-10966.

BIBLIOGRAPHY

Lindsey, J. S. *New J. Chem.* **1991,** 15, (2-3), 153-180.

Sarikaya, M.; Tamerler, C.; Jen, A. K. Y.; Schulten, K.; Baneyx, F. *Nature Materials* **2003,** 2, (9), 577-585.

Whitesides, G. M.; Grzybowski, B. *Science* **2002,** 295, (5564), 2418-2421.

Whitesides, G. M.; Mathias, J. P.; Seto, C. T. *Science* **1991,** 254, (5036), 1312-1319.

Yurchenco, P. D.; Birk, D. E.; Mecham, R. P., *Extracellular matrix assembly and structure*. Academic Press: San Diego, 1994; p 468.

Glotzer, S. C. *Science* **2004,** 306, (5695), 419-420.

Jonas, U.; del Campo, A.; Kruger, C.; Glasser, G.; Boos, D. *Proc. Natl. Acad. Sci. U. S. A.* **2002,** 99, (8), 5034-5039.

Lehn, J. M. *Science* **2002,** 295, (5564), 2400-2403.

Rueckes, T.; Kim, K.; Joselevich, E.; Tseng, G. Y.; Cheung, C. L.; Lieber, C. M. *Science* **2000,** 289, (5476), 94-97.

McLeish, T. *Science* **1997,** 278, (5343), 1577-1578.

Penner, R. M.; Heben, M. J.; Longin, T. L.; Lewis, N. S. *Science* **1990,** 250, (4984), 1118-1121.

Corriu, R. J. P. *Angew. Chem., Int. Ed. Engl.* **2000,** 39, (8), 1376-1398.

Lai, W. Y.-C.; Pau, S.; López, O. D. In *Nanofabrication: technologies, devices, and applications*, 2004; SPIE--the International Society for Optical Engineering: 2004; p 450.

Loy, D. A. *MRS Bulletin* **2001,** 26, (5), 364-408.

Kawasumi, M. *J. Polym. Sci., Part A: Polym. Chem.* **2004,** 42, (4), 819-824.

Braun, T.; Schubert, A. P.; Kostoff, R. N. *Chem. Rev.* **2000,** 100, (6), 2475-2475.

Ajayan, P. M. *Chem. Rev.* **1999,** 99, (7), 1787-1799.

Alivisatos, A. P. *Science* **1996,** 271, (5251), 933-937.

Katsoulis, D. E. *Chem. Rev.* **1998,** 98, (1), 359-387.

Leites, L. A. *Chem. Rev.* **1992,** 92, (2), 279-323.

Li, G. Z.; Wang, L. C.; Ni, H. L.; Pittman, C. U. *Journal of Inorganic and Organometallic Polymers* **2001,** 11, (3), 123-154.

Scott, D. W. *J. Am. Chem. Soc.* **1946,** 68, (3), 356-358.

Brown, J. F.; Vogt, L. H. *J. Am. Chem. Soc.* **1965,** 87, (19), 4313-4317.

Feher, F. J.; Terroba, R.; Jin, R. J.; Wyndham, K. D.; Lucke, S.; Brutchey, R.; Nguyen, F. *Polym. Mater. Sci. Eng.* **2000,** 82, 301.

Loy, D. A.; Shea, K. J. *Chem. Rev.* **1995,** 95, (5), 1431-1442.

Baney, R. H.; Itoh, M.; Sakakibara, A.; Suzuki, T. *Chem. Rev.* **1995,** 95, (5), 1409-1430.

Waddon, A. J.; Coughlin, E. B. *Chem. Mater.* **2003,** 15, (24), 4555-4561.

Schwab, J. J.; Lichtenhan, J. D. *Applied Organometallic Chemistry* **1998,** 12, (10-11), 707-713.

Haddad, T. S.; Lichtenhan, J. D. *Macromolecules* **1996,** 29, (22), 7302-7304.

Bharadwaj, R. K.; Berry, R. J.; Farmer, B. L. *Polymer* **2000,** 41, (19), 7209-7221.

Mather, P. T.; Jeon, H. G.; Romo-Uribe, A.; Haddad, T. S.; Lichtenhan, J. D. *Macromolecules* **1999,** 32, (4), 1194-1203.

Tsuchida, A.; Bolln, C.; Sernetz, F. G.; Frey, H.; Mulhaupt, R. *Macromolecules* **1997,** 30, (10), 2818-2824.

Joshi, M.; Butola, B. S. *Journal of Macromolecular Science-Polymer Reviews* **2004,** C44, (4), 389-410.

Pan, Q. W.; Fan, X. H.; Chen, X. F.; Zhou, Q. F. *Progress in Chemistry* **2006,** 18, (5), 616-621.

Pu, K. Y.; Fan, Q.; Wang, L. H.; Huang, W. *Progress in Chemistry* **2006,** 18, (5), 609-615.

Epoxy Resins, Chemistry and Technology. Marcel Dekker: New York, 1988.

Abad, M. J.; Barral, L.; Fasce, D. P.; Williams, R. J. J. *Macromolecules* **2003,** 36, (9), 3128-3135.

Choi, J.; Harcup, J.; Yee, A. F.; Zhu, Q.; Laine, R. M. *J. Am. Chem. Soc.* **2001,** 123, (46), 11420-11430.

Matejka, L.; Strachota, A.; Plestil, J.; Whelan, P.; Steinhart, M.; Slouf, M. *Macromolecules* **2004,** 37, (25), 9449-9456.

Ni, Y.; Zheng, S. X.; Nie, K. M. *Polymer* **2004,** 45, (16), 5557-5568.

Tegou, E.; Bellas, V.; Gogolides, E.; Argitis, P. *Microelectron. Eng.* **2004,** 73-74, 238-243.

Tegou, E.; Bellas, V.; Gogolides, E.; Argitis, P.; Eon, D.; Cartry, G.; Cardinaud, C. *Chem. Mater.* **2004,** 16, (13), 2567-2577.

Eon, D.; Cartry, G.; Fernandez, V.; Cardinaud, C.; Tegou, E.; Bellas, V.; Argitis, P.; Gogolides, E. *Journal of Vacuum Science & Technology B* **2004,** 22, (5), 2526-2532.

Jakubek, V.; Liu, X. Q.; Vohra, V. R.; Douki, K.; Kwark, Y. J.; Ober, C. K.; Markley, T. J.; Robertson, E. A.; Carr, R. V. C.; Marsella, J. A.; Conley, W.; Miller, D.; Zimmerman, P. *Journal of Photopolymer Science and Technology* **2003,** 16, (4), 573-580.

Ali, M. A.; Gonsalves, K. E.; Agrawal, A.; Jeyakumar, A.; Henderson, C. L. *Microelectron. Eng.* **2003,** 70, (1), 19-29.

Wu, H. P.; Hu, Y. Q.; Gonsalves, K. E.; Yacaman, M. J. *Journal of Vacuum Science & Technology B* **2001,** 19, (3), 851-855.

Odian, G., Principles of Polymerization, Third Edition. In *Principles of Polymerization, Third Edition*, John Wiley & Sons, I., Ed. 1991; pp 158-162.

Lee, Y. J.; Huang, J. M.; Kuo, S. W.; Lu, J. S.; Chang, F. C. *Polymer* **2005,** 46, (1), 173-181.

Chen, Y. W.; Kang, E. T. *Mater. Lett.* **2004,** 58, (29), 3716-3719.

Huang, J. C.; Xiao, Y.; Mya, K. Y.; Liu, X. M.; He, C. B.; Dai, J.; Siow, Y. P. *J. Mater. Chem.* **2004,** 14, (19), 2858-2863.

Phillips, S. H.; Haddad, T. S.; Tomczak, S. J. *Current Opinion in Solid State & Materials Science* **2004,** 8, (1), 21-29.

Tamaki, R.; Choi, J. W.; Laine, R. M. *Chem. Mater.* **2003,** 15, (3), 793-797.

Leu, C. M.; Chang, Y. T.; Wei, K. H. *Chem. Mater.* **2003,** 15, (19), 3721-3727.

Leu, C. M.; Reddy, G. M.; Wei, K. H.; Shu, C. F. *Chem. Mater.* **2003,** 15, (11), 2261-2265.

Huang, J. C.; He, C. B.; Xiao, Y.; Mya, K. Y.; Dai, J.; Siow, Y. P. *Polymer* **2003,** 44, (16), 4491-4499.

Wright, M. E.; Schorzman, D. A.; Feher, F. J.; Jin, R. Z. *Chem. Mater.* **2003,** 15, (1), 264-268.

Gonzalez, R. I.; Phillips, S. H.; Hoflund, G. B. *Journal of Spacecraft and Rockets* **2000,** 37, (4), 463-467.

Joshi, A.; Butola, B. S. *Polymer* **2004,** 45, (14), 4953-4968.

Fu, B. X.; Gelfer, M. Y.; Hsiao, B. S.; Phillips, S.; Viers, B.; Blanski, R.; Ruth, P. *Polymer* **2003,** 44, (5), 1499-1506.

Zheng, L.; Farris, R. J.; Coughlin, E. B. *Abstracts of Papers of the American Chemical Society* **2000,** 220, U318-U318.

Zheng, L.; Kasi, R. M.; Farris, R. J.; Coughlin, E. B. *Abstracts of Papers of the American Chemical Society* **2001,** 221, U367-U367.

Zheng, L.; Farris, R. J.; Coughlin, E. B. *J. Polym. Sci., Part A: Polym. Chem.* **2001,** 39, (17), 2920-2928.

Zheng, L.; Waddon, A. J.; Farris, R. J.; Coughlin, E. B. *Macromolecules* **2002,** 35, (6), 2375-2379.

Grubbs, R. H., *Handbook of metathesis*. Weinheim [Germany] : Wiley-VCH: 2003.

Zheng, L.; Farris, R. J.; Coughlin, E. B. *Macromolecules* **2001,** 34, (23), 8034-8039.

Jeon, H. G.; Mather, P. T.; Haddad, T. S. *Polym. Int.* **2000,** 49, (5), 453-457.

Pyun, J.; Miller, P. J.; Matyjaszewski, K. *Abstracts of Papers of the American Chemical Society* **2000,** 219, U390-U390.

Pyun, J.; Matyjaszewski, K.; Wu, J.; Kim, G. M.; Chun, S. B.; Mather, P. T. *Polymer* **2003,** 44, (9), 2739-2750.

Pyun, J.; Xia, J. H.; Matyjaszewski, K. *Synthesis and Properties of Silicones and Silicone-Modified Materials* **2003,** 838, 273-284.

Drazkowski, D. B.; Lee, A.; Haddad, T. S.; Cookson, D. J. *Macromolecules* **2006,** 39, (5), 1854-1863.

Intasanta, N.; ; Russell, T. P.; ; Coughlin, E. B. In *Ultrathin films of self-assembled organic-inorganic hybrid nanoparticle block copolymers*. Abstracts of Papers of the American Chemical Society, Anaheim, 2004; Anaheim, 2004.

Carroll, J. B.; Frankamp, B. L.; Rotello, V. M. *Chemical Communications* **2002,** (17), 1892-1893.

Carroll, J. B.; Waddon, A. J.; Nakade, H.; Rotello, V. M. *Macromolecules* **2003,** 36, (17), 6289-6291.

Kennedy, J. P. *J. Polym. Sci., Part A: Polym. Chem.* **1999,** 37, (14), 2285-2293.

Patten, T. E.; Matyjaszewski, K. *Acc. Chem. Res.* **1999,** 32, (10), 895-903.

Hawker, C. J. *Acc. Chem. Res.* **1997,** 30, (9), 373-382.

Odian, G., *Principles of Polymerization, Third Edition*. John Wiley & Sons, Inc: 1991.

Szwarc, M. *Nature* **1956,** 178, (4543), 1168-1169.

Morton, M.; Fetters, L. J. *Rubber Chem. Technol.* **1974,** 48, 359.

Hadjichristidis, N.; Iatrou, H.; Pispas, S.; Pitsikalis, M. *J. Polym. Sci., Part A: Polym. Chem.* **2000,** 38, (18), 3211-3234.

Uhrig, D.; Mays, J. W. *J. Polym. Sci., Part A: Polym. Chem.* **2005,** 43, (24), 6179-6222.

Hamley, I. W., *The Physics of Block Copolymers*. Oxford University Press: New York, 1998.

Bates, F. S. *Science* **1991,** 251, (4996), 898-905.

Forster, S. *Colloid Chemistry 1* **2003,** 226, 1-28.

Ulrich, R.; Du Chesne, A.; Templin, M.; Wiesner, U. *Advanced Materials* **1999,** 11, (2), 141-146.

Thurn-Albrecht, T.; Schotter, J.; Kastle, C. A.; Emley, N.; Shibauchi, T.; Krusin-Elbaum, L.; Guarini, K.; Black, C. T.; Tuominen, M. T.; Russell, T. P. *Science* **2000,** 290, (5499), 2126-2129.

Tseng, G. Y.; Ellenbogen, J. C. *Science* **2001,** 294, (5545), 1293-1294.

Forster, S.; Plantenberg, T. *Angewandte Chemie-International Edition* **2002,** 41, (5), 689-714.

Ray, S. S.; Okamoto, M. *Progress in Polymer Science* **2003,** 28, (11), 1539-1641.

Giannelis, E. P. *Advanced Materials* **1996,** 8, (1), 29-&.

Godovski, D. Y. *Thermal and Electrical Conductivity of Polymer Materials* **1995,** 119, 79-122.

Nagata, K.; Kodama, S.; Kawasaki, H.; Deki, S.; Mizuhata, M. *J. Appl. Polym. Sci.* **1995,** 56, (10), 1313-1321.

Zhang, C. L.; Xu, T.; Butterfield, D.; Misner, M. J.; Ryu, D. Y.; Emrick, T.; Russell, T. P. *Nano Letters* **2005,** 5, (2), 357-361.

Bockstaller, M. R.; Lapetnikov, Y.; Margel, S.; Thomas, E. L. *J. Am. Chem. Soc.* **2003,** 125, (18), 5276-5277.

Thompson, R. B.; Ginzburg, V. V.; Matsen, M. W.; Balazs, A. C. *Science* **2001,** 292, (5526), 2469-2472.

Lamm, M. H.; Chen, T.; Glotzer, S. C. *Nano Lett.* **2003,** 3, (8), 989-994.

Lee, J. Y.; Balazs, A. C.; Thompson, R. B.; Hill, R. M. *Macromolecules* **2004,** 37, (10), 3536-3539.

Zhang, X.; Chan, E. R.; Glotzer, S. C. *J. Chem. Phys.* **2005,** 123, (18).

Kopesky, E. T.; Haddad, T. S.; Cohen, R. E.; McKinley, G. H. *Macromolecules* **2004,** 37, (24), 8992-9004.

Kulbaba, K.; Manners, I. *Macromolecular Rapid Communications* **2001,** 22, (10), 711-724.

Ni, Y. Z.; Rulkens, R.; Manners, I. *J. Am. Chem. Soc.* **1996,** 118, (17), 4102-4114.

Cheng, J. Y.; Ross, C. A.; Thomas, E. L.; Smith, H. I.; Vancso, G. J. *Advanced Materials* **2003,** 15, (19), 1599-+.

Cheng, J. Y.; Ross, C. A.; Thomas, E. L.; Smith, H. I.; Vancso, G. J. *Appl. Phys. Lett.* **2002,** 81, (19), 3657-3659.

Manners, I. *Science* **2001,** 294, (5547), 1664-1666.

Archer, R. D., *Inorganic and organometallic polymers*. Wiley-VCH: New York, 2001.

Manners, I. *Angew. Chem., Int. Ed. Engl.* **1996,** 35, (15), 1603-1621.

Kresge, C. T.; Leonowicz, M. E.; Roth, W. J.; Vartuli, J. C.; Beck, J. S. *Nature* **1992,** 359, (6397), 710-712.

Kickelbick, G. *Progress in Polymer Science* **2003,** 28, (1), 83-114.

Soler-Illia, G.; Crepaldi, E. L.; Grosso, D.; Sanchez, C. *Current Opinion in Colloid & Interface Science* **2003,** 8, (1), 109-126.

Sanchez, C.; Julian, B.; Belleville, P.; Popall, M. *J. Mater. Chem.* **2005,** 15, (35-36), 3559-3592.

Yang, P. D.; Deng, T.; Zhao, D. Y.; Feng, P. Y.; Pine, D.; Chmelka, B. F.; Whitesides, G. M.; Stucky, G. D. *Science* **1998,** 282, (5397), 2244-2246.

Yang, P. D.; Zhao, D. Y.; Margolese, D. I.; Chmelka, B. F.; Stucky, G. D. *Nature* **1998,** 396, (6707), 152-155.

Zhao, D. Y.; Feng, J. L.; Huo, Q. S.; Melosh, N.; Fredrickson, G. H.; Chmelka, B. F.; Stucky, G. D. *Science* **1998,** 279, (5350), 548-552.

Templin, M.; Franck, A.; DuChesne, A.; Leist, H.; Zhang, Y. M.; Ulrich, R.; Schadler, V.; Wiesner, U. *Science* **1997,** 278, (5344), 1795-1798.

Simon, P. F. W.; Ulrich, R.; Spiess, H. W.; Wiesner, U. *Chem. Mater.* **2001,** 13, (10), 3464-3486.

Whitesides, G. M.; Mathias, J. P.; Seto, C. T. *Science* **1991,** 254, (5036), 1312-1319.

Ikkala, O.; ten Brinke, G. *Science* **2002,** 295, (5564), 2407-2409.

Hartgerink, J. D.; Beniash, E.; Stupp, S. I. *Science* **2001,** 294, (5547), 1684-1688.

Matsen, M. W.; Bates, F. S. *Macromolecules* **1996,** 29, (4), 1091-1098.

Muthukumar, M.; Ober, C. K.; Thomas, E. L. *Science* **1997,** 277, (5330), 1225-1232.

Aksay, I. A.; Trau, M.; Manne, S.; Honma, I.; Yao, N.; Zhou, L.; Fenter, P.; Eisenberger, P. M.; Gruner, S. M. *Science* **1996,** 273, (5277), 892-898.

Yang, H.; Kuperman, A.; Coombs, N.; MamicheAfara, S.; Ozin, G. A. *Nature* **1996,** 379, (6567), 703-705.

Lu, Y. F.; Ganguli, R.; Drewien, C. A.; Anderson, M. T.; Brinker, C. J.; Gong, W. L.; Guo, Y. X.; Soyez, H.; Dunn, B.; Huang, M. H.; Zink, J. I. *Nature* **1997,** 389, (6649), 364-368.

Lichtenhan, J. D., Silsesquioxane-Based Polymers. In *Polymeric Materials Encyclopedia*, Salamone, J. C., Ed. CRC Press: Boca Raton: 1996; pp 7768-7777.

Choi, J.; Harcup, J.; Yee, A. F.; Zhu, Q.; Laine, R. M. *J. Am. Chem. Soc.* **2001,** 123, (46), 11420-11430.

Tamaki, R.; Tanaka, Y.; Asuncion, M. Z.; Choi, J.; Laine, R. M. *J. Am. Chem. Soc.* **2001,** 123, (49), 12416-12417.

Cassagneau, T.; Caruso, F. *J. Am. Chem. Soc.* **2002,** 124, (27), 8172-8180.

Tamaki, R.; Choi, J.; Laine, R. M. *Chem. Mater.* **2003,** 15, (3), 793-797.

Lichtenhan, J. D.; Vu, N. Q.; Carter, J. A.; Gilman, J. W.; Feher, F. J. *Macromolecules* **1993,** 26, (8), 2141-2142.

Lichtenhan, J. D.; Otonari, Y. A.; Carr, M. J. *Macromolecules* **1995,** 28, (24), 8435-8437.

Haddad, T. S.; Lichtenhan, J. D. *Macromolecules* **1996,** 29, (22), 7302-7304.

Tsuchida, A.; Bolln, C.; Sernetz, F. G.; Frey, H.; Mulhaupt, R. *Macromolecules* **1997,** 30, (10), 2818-2824.

Lee, A.; Lichtenhan, J. D. *Macromolecules* **1998,** 31, (15), 4970-4974.

Romo-Uribe, A.; Mather, P. T.; Haddad, T. S.; Lichtenhan, J. D. *J. Polym. Sci., Part B: Polym. Phys.* **1998,** 36, (11), 1857-1872.

Schwab, J. J.; Lichtenhan, J. D. *Appl. Organometal. Chem.* **1998,** 12, (10-11), 707-713.

Lee, A.; Lichtenhan, J. D. *J. Appl. Polym. Sci.* **1999,** 73, (10), 1993-2001.

Mather, P. T.; Jeon, H. G.; Romo-Uribe, A.; Haddad, T. S.; Lichtenhan, J. D. *Macromolecns* **1999,** 32, (4), 1194-1203.

Shockey, E. G.; Bolf, A. G.; Jones, P. F.; Schwab, J. J.; Chaffee, K. P.; Haddad, T. S.; Lichtenhan, J. D. *Appl. Organometal. Chem.* **1999,** 13, (4), 311-327.

Fu, B. X.; Zhang, W. H.; Hsiao, B. S.; Rafailovich, M.; Sokolov, J.; Johansson, G.; Sauer, B. B.; Phillips, S.; Balnski, R. *High Perform. Polym.* **2000,** 12, (4), 565-571.

Pyun, J.; Matyjaszewski, K. *Macromolecules* **2000,** 33, (1), 217-220.

Costa, R. O. R.; Vasconcelos, W. L.; Tamaki, R.; Laine, R. M. *Macromolecules* **2001,** 34, (16), 5398-5407.

Fu, B. X.; Hsiao, B. S.; Pagola, S.; Stephens, P.; White, H.; Rafailovich, M.; Sokolov, J.; Mather, P. T.; Jeon, H. G.; Phillips, S.; Lichtenhan, J.; Schwab, J. *Polymer* **2001,** 42, (2), 599-611.

Li, G. Z.; Wang, L. C.; Toghiani, H.; Daulton, T. L.; Koyama, K.; Pittman, C. U. *Macromolecules* **2001,** 34, (25), 8686-8693.

Li, G. Z.; Wang, L.; Toghiani, H.; Daulton, T. L.; Pittman, C. U. *Polymer* **2002,** 43, (15), 4167-4176.

Leu, C. M.; Chang, Y. T.; Wei, K. H. *Macromolecules* **2003,** 36, (24), 9122 - 9127.

Pittman, C. U.; Li, G. Z.; Ni, H. L. *Macromol. Symp.* **2003,** 196, 301-325.

Barry, A. J.; Daudt, W. H.; Domicone, J. J.; Gilkey, J. W. *J. Am. Chem. Soc.* **1955,** 77, 4248-4252.

Larsson, K. *Ark. Kemi* **1960,** 16, 203-28.

Larsson, K. *Ark. Kemi* **1960,** 16, 209-214.

Larsson, K. *Ark. Kemi* **1960,** 16, 215-219.

Auf der Heyde, T. P. E.; Burgi, H.-B.; Burgy, H.; Tornroos, K. W. *Chimia* **1991,** 45, 38-40.

Schwab, P.; Grubbs, R. H.; Ziller, J. W. *J. Am. Chem. Soc.* **1996,** 118, (1), 100-110.

Gonzalez, R. I.; Phillips, S. H.; Hoflund, G. B. *J. Spacecraft and Rockets.* **2000,** 37, 463-467.

Kojima, Y.; Usuki, A.; Kawasumi, M.; Okada, A.; Kurauchi, T.; Kamigaito, O. *J. Polym. Sci., Part A: Polym. Chem.* **1993,** 31, (4), 983-986.

Zhang, Z. L.; Horsch, M. A.; Lamm, M. H.; Glotzer, S. C. *Nano Letters* **2003,** 3, (10), 1341-1346.

Giannelis, E. P. *Adv. Mater.* **1996,** 8, (1), 29-35.

Pinnavaia, T. J.; Beal, G. W., *Polymer Clay Nanocomposites*, John Wiley & Sons: New York: 2001.

Kickelbick, G. *Prog. Polym. Sci.* **2003,** 28, (1), 83-114.

Gonsalves, K. E.; Merhari, L.; Wu, H. P.; Hu, Y. Q. *Adv. Mater.* **2001,** 13, (10), 703-714.

Barton, T. J.; Bull, L. M.; Klemperer, W. G.; Loy, D. A.; McEnaney, B.; Misono, M.; Monson, P. A.; Pez, G.; Scherer, G. W.; Vartuli, J. C.; Yaghi, O. M. *Chem. Mater.* **1999,** 11, (10), 2633-2656.

Pinnavaia, T. J.; Beal, G. W., *Polymer Clay Nanocomposites*, John Wiley & Son: New York, 2001.

Kojima, Y.; Usuki, A.; Kawasumi, M.; Okada, A.; Kurauchi, T.; Kamigaito, O. *J. Polym. Sci., Part A: Polym. Chem.* **1993,** 31, (4), 983-986.

Giannelis, E. P. *Adv. Mater.* **1996,** 8, (1), 29-35.

Corriu, R. J. P. *Angew. Chem., Int. Ed. Engl.* **2000,** 39, (8), 1376-1398.

Wen, J. Y.; Wilkes, G. L. *Chem. Mater.* **1996,** 8, (8), 1667-1681.

Pyun, J.; Matyjaszewski, K.; Wu, J.; Kim, G. M.; Chun, S. B.; Mather, P. T. *Polymer* **2003,** 44, (9), 2739-2750.

Pyun, J.; Matyjaseweski, K. *Macromolecules* **1999,** 33, 217-220.

Pyun, J.; Miller, P. J.; Matyjaszewski, K. *Abstracts of Papers of the American Chemical Society* **2000,** 219, U390-U390.

Kim, B. S.; Mather, P. T. *Macromolecules* **2002,** 35, (22), 8378-8384.

Riggs, J. E.; Guo, Z. X.; Carroll, D. L.; Sun, Y. P. *J. Am. Chem. Soc* **2000,** 122, (24), 5879-5880.

Song, T.; Dai, S.; Tam, K. C.; Lee, S. Y.; Goh, S. H. *Langmuir* **2003,** 19, (11), 4798-4803.

Song, T.; Dai, S.; Tam, K. C.; Lee, S. Y.; Goh, S. H. *Polymer* **2003,** 44, (8), 2529-2536.

Zhang, Z. L.; Horsch, M. A.; Lamm, M. H.; Glotzer, S. C. *Nano Lett.* **2003,** 3, (10), 1341-1346.

Thompson, R. B.; Ginzburg, V. V.; Matsen, M. W.; Balazs, A. C. *Science* **2001,** 292, (5526), 2469-2472.

Lamm, M. H.; Chen, T.; Glotzer, S. C. *Nano Lett.* **2003,** 3, (8), 989-994.

Hadjichristidis, N.; Pitsikalis, M.; Pispas, S.; Iatrou, H. *Chem. Rev.* **2001,** 101, (12), 3747-3792.

Brown, J. F.; Vogt, L. H. *J. Am. Chem. Soc.* **1965,** 87, 4313-4317.

Voronkov, M. G.; Lavrent'yev, V. I., Polyhedral Oligosilsesqioxanes and Their Homo Derivatives. In *Top. Curr. Chem.*, Boschke, F. L., Ed. Springer-Verlag: Berlin, 1982; Vol. 102, pp 199-236.

Lee, A.; Lichtenhan, J. D. *J. Appl. Polym. Sci.* **1999,** 73, (10), 1993-2001.

Shockey, E. G.; Bolf, A. G.; Jones, P. F.; Schwab, J. J.; Chaffee, K. P.; Haddad, T. S.; Lichtenhan, J. D. *Appl. Organometal. Chem.* **1999,** 13, (4), 311-327.

Lichtenhan, J. D.; Otonari, Y. A.; Carr, M. J. *Macromolecules* **1995,** 28, (24), 8435-8437.

Haddad, T. S.; Viers, B. D.; Phillips, S. H. *Journal of Inorganic and Organometallic Polymers* **2001,** 11, (3), 155-164.

Romo-Uribe, A.; Mather, P. T.; Haddad, T. S.; Lichtenhan, J. D. *J. Polym. Sci., Part B: Polym. Phys.* **1998,** 36, (11), 1857-1872.

Lee, A.; Lichtenhan, J. D. *Macromolecules* **1998,** 31, (15), 4970-4974.

Mather, P. T.; Jeon, H. G.; Romo-Uribe, A.; Haddad, T. S.; Lichtenhan, J. D. *Macromolecus* **1999,** 32, (4), 1194-1203.

Costa, R. O. R.; Vasconcelos, W. L.; Tamaki, R.; Laine, R. M. *Macromolecules* **2001,** 34, (16), 5398-5407.

Zheng, L.; Farris, R. J.; Coughlin, E. B. *J. Polym. Sci., Part A: Polym. Chem.* **2001,** 39, 2920-2928.

Zheng, L.; Kasi, R. M.; Farris, R. J.; Coughlin, E. B. *J. Polym. Sci., Part A: Polym. Chem.* **2002,** 40, (7), 885-891.

Liu, H. Z.; Zhang, W.; Zheng, S. X. *Polymer* **2005,** 46, (1), 157-165.

Xiao, S.; Nguyen, M.; Gong, X.; Cao, Y.; Wu, H. B.; Moses, D.; Heeger, A. J. *Advanced Functional Materials* **2003,** 13, (1), 25-29.

Miller, P. J.; Kickelbick, G.; Nakagawa, Y.; Diamanti, S.; Pacis, C.; Matyjaszewski, K. *Abstracts of Papers of the American Chemical Society* **1998,** 215, U394-U395.

Knischka, R.; Dietsche, F.; Hanselmann, R.; Frey, H.; Mulhaupt, R.; Lutz, P. J. *Langmuir* **1999,** 15, (14), 4752-4756.

Morton, M.; Fetters, L. J. *Rubber Chem. Technol.* **1974,** 48, 359.

Quirk, R. P.; Ma, J. J. *J. Polym. Sci., Part A: Polym. Chem.* **1988,** 26, (8), 2031-2037.

Hadjichristidis, N.; Iatrou, H.; Pispas, S.; Pitsikalis, M. *J. Polym. Sci., Part A: Polym. Chem.* **2000,** 38, (18), 3211-3234.

Ballard, D. G. H.; Wignall, G. D.; Schelten, J. *Eur. Polym. J.* **1973,** 9, (9), 965-969.

Wignall, G. D.; Ballard, D. G. H.; Schelten, J. *Eur. Polym. J.* **1974,** 10, (9), 861-865.

Gomez-Romero, P. *Advanced Materials* **2001,** 13, (3), 163-174.

Judeinstein, P.; Sanchez, C. *J. Mater. Chem.* **1996,** 6, (4), 511-525.

Nalwa, H. S., *Handbook of organic-inorganic hybrid materials and nanocomposites*. American Scientific Publishers: Stevenson Ranch, Calif., 2003; p 2 v.

Schottner, G. *Chem. Mater.* **2001,** 13, (10), 3422-3435.

Houbertz, R.; Domann, G.; Schulz, J.; Olsowski, B.; Frohlich, L.; Kim, W. S. *Appl. Phys. Lett.* **2004,** 84, (7), 1105-1107.

Hagfeldt, A.; Gratzel, M. *Acc. Chem. Res.* **2000,** 33, (5), 269-277.

Innocenzi, P.; Lebeau, B. *J. Mater. Chem.* **2005,** 15, (35-36), 3821-3831.

Kickelbick, G. *Progress in Polymer Science* **2003,** 28, (1), 83-114.

Zhang, X.; Chan, E. R.; Glotzer, S. C. *J. Chem. Phys.* **2005,** 123, (18).

Lee, J. Y.; Balazs, A. C.; Thompson, R. B.; Hill, R. M. *Macromolecules* **2004,** 37, (10), 3536-3539.

Thompson, R. B.; Ginzburg, V. V.; Matsen, M. W.; Balazs, A. C. *Science* **2001,** 292, (5526), 2469-2472.

Kawasumi, M. *J. Polym. Sci., Part A: Polym. Chem.* **2004,** 42, (4), 819-824.

Sanchez, C.; Soler-Illia, G.; Ribot, F.; Lalot, T.; Mayer, C. R.; Cabuil, V. *Chem. Mater.* **2001,** 13, (10), 3061-3083.

Mercier, L.; Pinnavaia, T. J. *Advanced Materials* **1997,** 9, (6), 500-&.

Soler-illia, G. J. D.; Sanchez, C.; Lebeau, B.; Patarin, J. *Chemical Reviews* **2002,** 102, (11), 4093-4138.

Templin, M.; Franck, A.; DuChesne, A.; Leist, H.; Zhang, Y. M.; Ulrich, R.; Schadler, V.; Wiesner, U. *Science* **1997,** 278, (5344), 1795-1798.

Pittman, C. U.; Li, G. Z.; Ni, H. L. *Macromolecular Symposia* **2003,** 196, 301-325.

Waddon, A. J.; Coughlin, E. B. *Chem. Mater.* **2003,** 15, (24), 4555-4561.

Joshi, M.; Butola, B. S. *Journal of Macromolecular Science-Polymer Reviews* **2004,** C44, (4), 389-410.

Haddad, T. S.; Lichtenhan, J. D. *Macromolecules* **1996,** 29, (22), 7302-7304.

Bharadwaj, R. K.; Berry, R. J.; Farmer, B. L. *Polymer* **2000,** 41, (19), 7209-7221.

Tsuchida, A.; Bolln, C.; Sernetz, F. G.; Frey, H.; Mulhaupt, R. *Macromolecules* **1997,** 30, (10), 2818-2824.

Abad, M. J.; Barral, L.; Fasce, D. P.; Williams, R. J. J. *Macromolecules* **2003,** 36, (9), 3128-3135.

Wright, M. E.; Schorzman, D. A.; Feher, F. J.; Jin, R. Z. *Chem. Mater.* **2003,** 15, (1), 264-268.

Laine, R. M. *J. Mater. Chem.* **2005,** 15, (35-36), 3725-3744.

Pyun, J.; Xia, J. H.; Matyjaszewski, K. *Synthesis and Properties of Silicones and Silicone-Modified Materials* **2003,** 838, 273-284.

Intasanta, N.; Russell, T. P.; Coughlin, E. B. In *Ultrathin films of self-assembled organic-inorganic hybrid nanoparticle block copolymers*. Abstracts of Papers of the American Chemical Society, Anaheim, 2004: Anaheim, 2004.

Morton, M. F., L.J. *Rubber Chem. Technol.* **1974,** 48, 359.

Hadjichristidis, N.; Iatrou, H.; Pispas, S.; Pitsikalis, M. *J. Polym. Sci., Part A: Polym. Chem.* **2000,** 38, (18), 3211-3234.

Uhrig, D.; Mays, J. W. *Journal of Polymer Science Part a-Polymer Chemistry* **2005,** 43, (24), 6179-6222.

Hadjichristidis, N.; Pitsikalis, M.; Pispas, S.; Iatrou, H. *Chemical Reviews* **2001,** 101, (12), 3747-3792.

Hirao, A.; Kato, H.; Yamaguchi, K.; Nakahama, S. *Macromolecules* **1986,** 19, (5), 1294-1299.

Ishizone, T.; Han, S.; Okuyama, S.; Nakahama, S. *Macromolecules* **2003,** 36, (1), 42-49.

Ehlich, D.; Takenaka, M.; Okamoto, S.; Hashimoto, T. *Macromolecules* **1993,** 26, (1), 189-197.

Hashimot.T; Nagatosh.K; Todo, A.; Hasegawa, H.; Kawai, H. *Macromolecules* **1974,** 7, (3), 364-373.

Hsieh, H. L.; Quirk, R. P., *Anionic Polymerization : Principles and Practical Applications*, Marcel Dekker: New York, 1996.

Forster, S.; Kramer, E. *Macromolecules* **1999,** 32, (8), 2783-2785.

Morton, M. F., L.J. *Rubber Chem. Technol.* **1974,** 48, 359.

Hadjichristidis, N.; Iatrou, H.; Pispas, S.; Pitsikalis, M. *J. Polym. Sci., Part A: Polym. Chem.* **2000,** 38, (18), 3211-3234.

Ndoni, S.; Papadakis, C. M.; Bates, F. S.; Almdal, K. *Rev. Sci. Instrum.* **1995,** 66, (2), 1090-1095.

Ohtake, T.; Ogasawara, M.; Ito-Akita, K.; Nishina, N.; Ujiie, S.; Ohno, H.; Kato, T. *Chem. Mater.* **2000,** 12, (3), 782-789.

Kishimoto, K.; Yoshio, M.; Mukai, T.; Yoshizawa, M.; Ohno, H.; Kato, T. *J. Am. Chem. Soc.* **2003,** 125, (11), 3196-3197.

Gref, R.; Minamitake, Y.; Peracchia, M. T.; Trubetskoy, V.; Torchilin, V.; Langer, R. *Science* **1994,** 263, (5153), 1600-1603.

Bhowmick, A. K.; Stephens, H. L., *Handbook of elastomers*, New York, 2001.

Discher, B. M.; Won, Y. Y.; Ege, D. S.; Lee, J. C. M.; Bates, F. S.; Discher, D. E.; Hammer, D. A. *Science* **1999,** 284, (5417), 1143-1146.

Discher, D. E.; Eisenberg, A. *Science* **2002,** 297, (5583), 967-973.

Lee, J. C. M.; Santore, M.; Bates, F. S.; Discher, D. E. *Macromolecules* **2002,** 35, (2), 323-326.

Constable, G. S.; Gonzalez-Ruiz, R. A.; Kasi, R. M.; Coughlin, E. B. *Macromolecules* **2002,** 35, (25), 9613-9616.

Gilman, H.; Cartledge, F. K. *J. Organomet. Chem.* **1964,** 2, (6), 447-454.

Allgaier, J.; Poppe, A.; Willner, L.; Richter, D. *Macromolecules* **1997,** 30, (6), 1582-1586.

Reid, R. C.; Prausnitz, J. M.; Poling, B. E., *The properties of gases and liquids*, 4th ed.; McGraw-Hill: New York, 1987; p x, 741.

Feng, X. S.; Taton, D.; Chaikof, E. L.; Gnanou, Y. *J. Am. Chem. Soc.* **2005,** 127, (31), 10956-10966.